Chapter–2

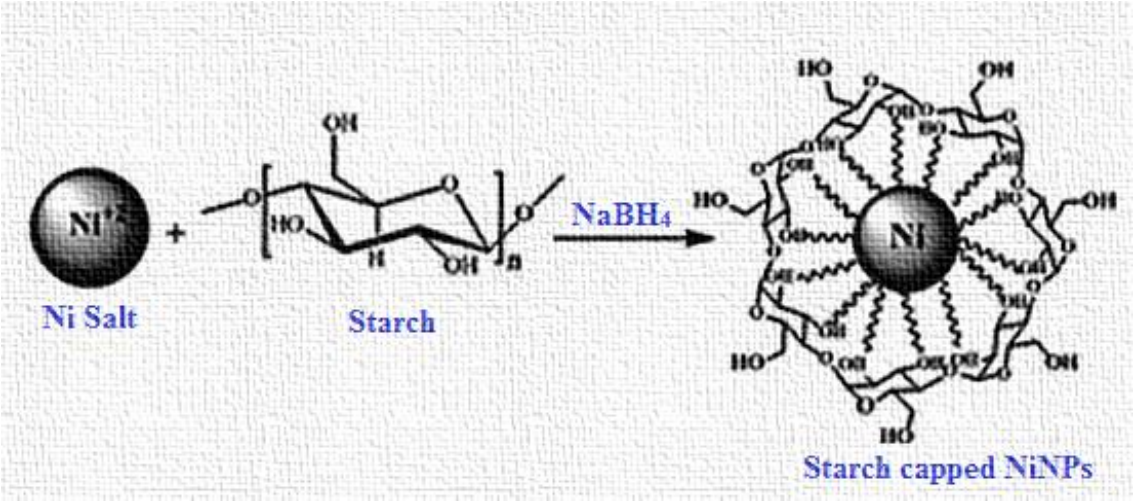

Nickel Nano–catalysts: Synthesis, characterisation and catalytic application

2.1 Introduction

The role of the nanometals as catalysts have been specifically discussed for understanding their technological applications in the field of catalysis.[1,2] Metal nanoparticles (NPs), in particular, being cheap, require only mild reaction conditions for high yields of products in short reaction times as compared to traditional catalysts. A significant change in reduction potential is observed for metal nanoparticles of different sizes in comparison to bulk metals as the Fermi potential of nanoparticles becomes more negative. This particular property allows them to act as catalysts in various electron transfer processes. There are various advantages like easy synthesis, tunable size and narrow size distribution with easy adjustment of synthesis parameters, stability in organic solvents, and reusability. Above all there is improved efficiency under mild and environmentally benign conditions in the context of green chemistry. Noble metal and transition- metal nanoparticles such as Cu, Ag, Pd, Pt, Rh, Ru, Au, and Ni have exhibited higher catalytic activity than conventional supported metal catalysts in many reactions like hydrogenation[3] and oxidation.[4]

Nanosized nickel has become one of the interesting materials in research communities due to the diverse promising applications in the field of catalysis.[5,6,7] Among the various kinds of metal nanoparticles, the preparation of some metal nanoparticles such as nickel, copper, and iron, are relatively difficult because they are easily oxidized. Nagashima et al.[8] first prepared nickel particles by a spray pyrolysis method of nickel precursors more than 14 years ago. Many techniques have been and are being developed for preparation of nanosized metallic materials. Therefore, different types of reducing agents and stabilizing compounds are employed to control particle size and shape. Size of NPs, itself is affected by several factors such as concentration of metal precursor, concentration of stabilizing agent, type of stabilizing agent, efficiency of stabilizing agent, stirring speed and method of synthesis. Generally, NiNPs can be prepared by a variety of methods, such as a wet chemical reduction in aqueous solution[5] or inorganic medium[9], microemulsion[10] and hydrothermal methods.[11] Among these preparation routes; wet chemical reduction is a versatile and economic method. Thus, the remarkable catalytic activity, easy synthesis, operational simplicity, ecofriendliness, and recycling efficiency encouraged us to utilize NiNPs as a catalyst for the synthesis and the electron transfer reaction.

The present study illustrates simple, green, convenient and technologically significant method for the synthesis of nickel nanoparticles in aqueous medium.

2.2 Objective and methodology of the present work

The efficient, controlled, and cost-effective design of catalysts is thus a goal of great importance. One area of catalysis that is growing at a rapid pace is metal nanocatalysis. Striking novel catalytic properties including greatly enhanced reactivities and selectivities have been reported for metal nanoparticle (NP) catalysts as compared to their bulk counterparts, for example, it is reported that nickel nanocatalysts were better than Raney Ni in terms of activity, selectivity and thermal stability in the hydrogenation reactions[12] so metal nanoparticles are better options in place of bulk metals in heterogeneous catalysis reactions.

Nickel nanoparticles (NiNPs) have been used effectively for various organic transformations.[6,13,14,15] A general problem of metal nanoparticles is their tendency to undergo agglomeration, which increases their particle size, and therefore, dramatically reduces the catalytic activity. Two general strategies to stabilize the particle size of the metal, are, supporting the metal nanoparticles on suitable solid surfaces or by using suitable ligands.[16] New possibilities for catalysis can be developed when the nanoparticles could be stabilized by encapsulating them in a structured host to combine the unique catalytic properties of nanoparticles with reaction shape-selectivity effects. Synthesis of NiNPs was carried out by using biopolymer starch as a stabilizing agent in aqueous medium (wet chemical reduction).

This chapter is devoted to the synthesis, characterization and catalytic application of nickel nanoparticles. The application part is divided into three subparts.

Part-1 Catalytic application of NiNPs in transesterification of primary esters

Part-2 Catalytic application of NiNPs in transesterification of *Aloe vera* seed oil and other oils

Part-3 Catalytic applications of NiNPs in electron transfer reactions

2.3 Experimental section

Nickel acetate ($Ni(CH_3COO)_2.4H_2O$), soluble starch, sodium borohydrides ($NaBH_4$), liquid ammonia and methanol etc. were purchased from Merck, Mumbai, India. All the solutions were prepared using double-distilled and demineralized water.

2.3.1 Synthesis of nickel nanoparticle (NiNPs)

NiNPs were synthesized through a wet chemical reduction process (**Scheme 2.1**) using a 1M solution of $Ni(CH_3COO)_2.4H_2O$ and soluble starch (1%, W/V) as a metal salt precursor and stabilizing agent respectively. $NaBH_4$ (10%, W/V) was used as reducing agent and liquid ammonia as complexing agent. In a typical process 10 ml of 1% starch solution and 0.4 ml of 1M $Ni(CH_3COO)_2.4H_2O$ were mixed together and stirred on a magnetic stirrer at RT (25 to 30 °C). The pH of the solution was adjusted to 10 by adding liquid ammonia whereby the initial green colour of solution changes in Prussian blue colour. Finally, 0.6 ml of 10% $NaBH_4$ solution was added dropwise with continuous stirring until black colour colloidal suspension was formed. These NPs were isolated by centrifugation process carried out at 10000 rpm for 10 minutes. The NPs were isolated by centrifugation and dried under vacuum at 50 °C.

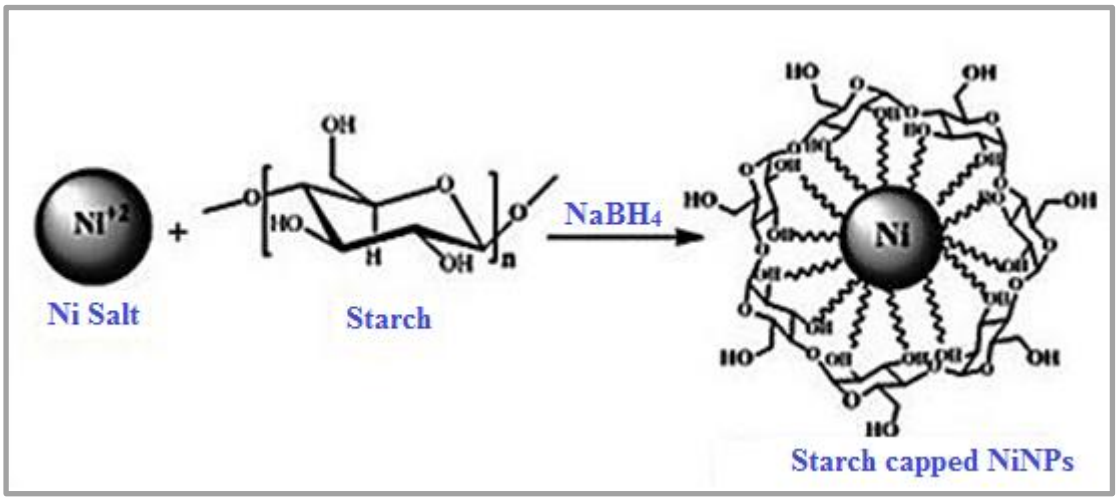

Scheme 2.1 Schematic presentation of the NiNPs synthesis

2.3.2 Characterizations methods

The starch capped NiNPs were characterized by X-ray diffraction (XRD) by using PANalytical 'X'PERT-PRO XRPD of Cu Kα radiation (λ= 0.15406 nm) with a scanning rate of 2°/min and 2θ ranging from 10 to 70°. Size and shape of the NiNPs in solution were determined by using TEM on a Philips, Holland Technai 20 model operating at 200 kV. The sample for transmission electron microscopy (TEM) was prepared by putting one drop of the suspension onto standard carbon-coated copper grids and then drying under an IR lamp for 30 min. Dynamic light scattering (DLS) was carried out on a 90 Plus DLS unit from Brookhaven (Holtsville, USA). Thermo gravimetric analysis (TGA) was recorded on TG-DTA 6300 INCARP EXSTAR 6000 in nitrogen atmosphere in a temperature range of 30 °C to 450 °C at a heating rate of 10 ºC/min. FT-IR spectra of NiNPs was recorded as KBr pellet on the Perkin Elmer RX1 model in the range of 4000-400 cm^{-1}. Energy dispersive X-ray (EDX) analysis of the vacuum dried NiNPs was recorded by the model-JSM-5610 LV attached to Scanning electron microscopy (SEM). Surface area and porosity of the samples were measured by a volumetric adsorption system (Micromeritics Instrument Corporation, USA, model ASAP 2010) using N_2 adsorption/desorption isotherms at 77 K up to 1 bar. Prior to the measurements, the samples were activated (degassed) by heating at the rate of 1K/min upto 383 K under vacuum. The temperature as well as vacuum was maintained for 7h prior to the measurements. The surface area was calculated by Brunauer-Emmet-Teller (BET) method while the porosity by Barrett-Joyner-Halenda (BJH) method.

2.4 Results and Discussion

2.4.1 Characterization of nickel nanoparticles (NiNPs)

XRD pattern of NiNPs in **Figure 2.1a** clearly shows NiNPs embedded in amorphous starch matrix. The peak due to Bragg's reflection is observed at 2θ value corresponding to 44.54° and 51. 2° representing b111N and b220N planes of fcc crystal structures of bulk nickel. The XRD pattern also does not show any peak at 37 deg due to formation of NiO. The Similar XRD pattern was obtained by Khanna *et al* [17] and Wang *et al*.[18] and the absence of oxide peak was attributed to the instant formation of metal NPs due to sodium borohydride. This, combined with stabilization

by starch, in the present case, prevents the formation of oxide on exposure to air. The pattern indicates that NiNPs are nanocrystalline in nature.[19] DLS analysis from **Figure 2.1b** it was observed that the particles are in the range of 70-95 nm in diameter with narrow size distribution. The average particle size was confirmed as 75±5 nm by TEM (**Figure 2.1c and d**). The NPs have a somewhat spherical shaped morphology and are monodispere in nature.

Energy Dispersive X-ray Analysis (EDX) indicates that the well-cleaned final product is mostly composed of Ni, with no other signal (**Figure 2.2a**). The FT-IR spectra (**Figure 2.2b**) of NiNPs and pure starch both display the typical profile of polysaccharides in the range 920–1100 cm^{-1} (characteristic peaks attributed to C-C/C-O bond stretching). The peaks at 1020–1100 cm^{-1} are characteristic of the anhydroglucose ring. The peaks at 1404–1420 cm^{-1} are due to C-H bending. Other peaks appeared at 1620 cm^{-1} due to the tightly bound water present in the starch. It is seen that the peak at 1620 cm^{-1} shifts to 1640 cm^{-1} in the NiNPs. The shifts observed in the spectra can be attributed to the interaction of NiNPs with starch. The band at

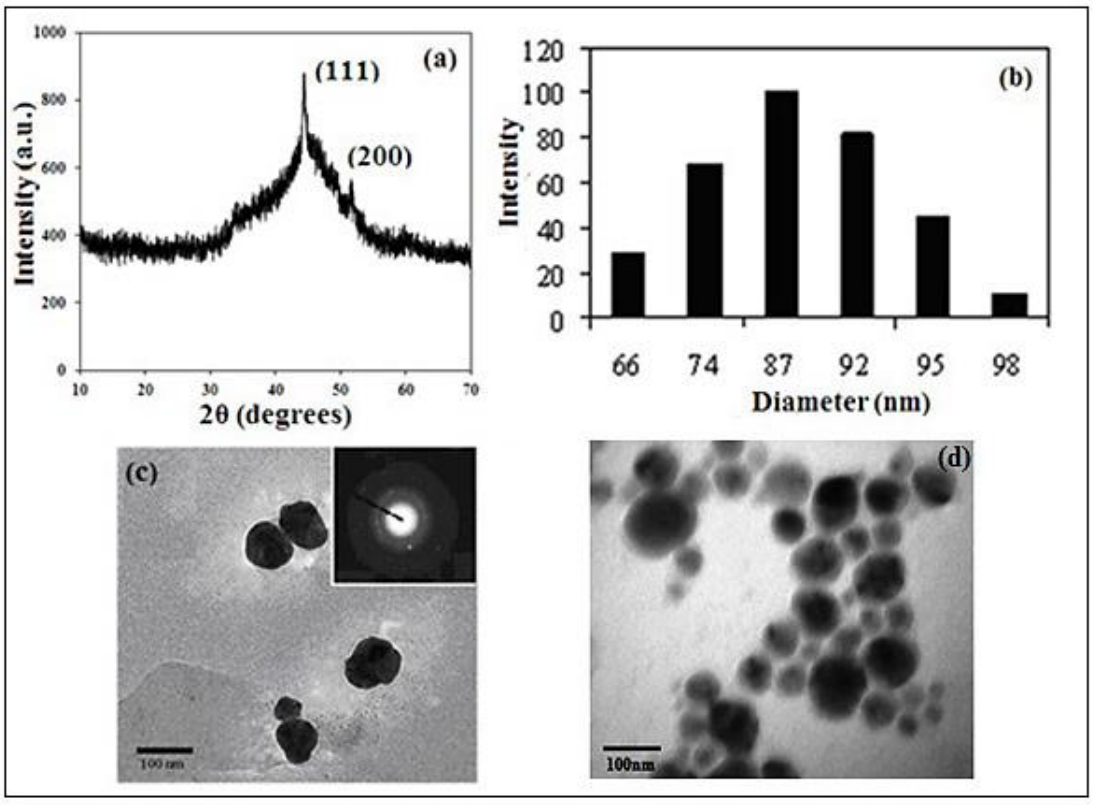

Figure 2.1 (a) XRD pattern, (b) DLS analysis, (c) and (d) TEM images of NiNPs

2910–2930 cm^{-1} is characteristic of C–H stretching. A broadband due to hydrogen bonded hydroxyl group (O–H) appeared at 3400–3420 cm^{-1} and is attributed to the complex vibrational stretching, associated with free, inter and intra molecular bound hydroxyl groups. The degradation pattern in TGA (**Figure 2.2c**) also supports the presence of organic matter on the surface of NiNPs.[20]

The Brunauer-Emmet-Teller (BET) surface area of a NiNPs sample was determined to be 17.07m^2/g (**Figure 2.3a**). NiNPs have high surface area which greatly differs from that obtained for NiNPs synthesised from the electric explosion of wire, the specific area of which was 4.4 m^2/g.[21] The pore size of the NPs was determined to be 12.37nm by the Barrett-Joyner-Halenda (BJH) analysis of the isotherms (**Figure 2.3b**). The total pore volumes were 0.05cm^3/g.

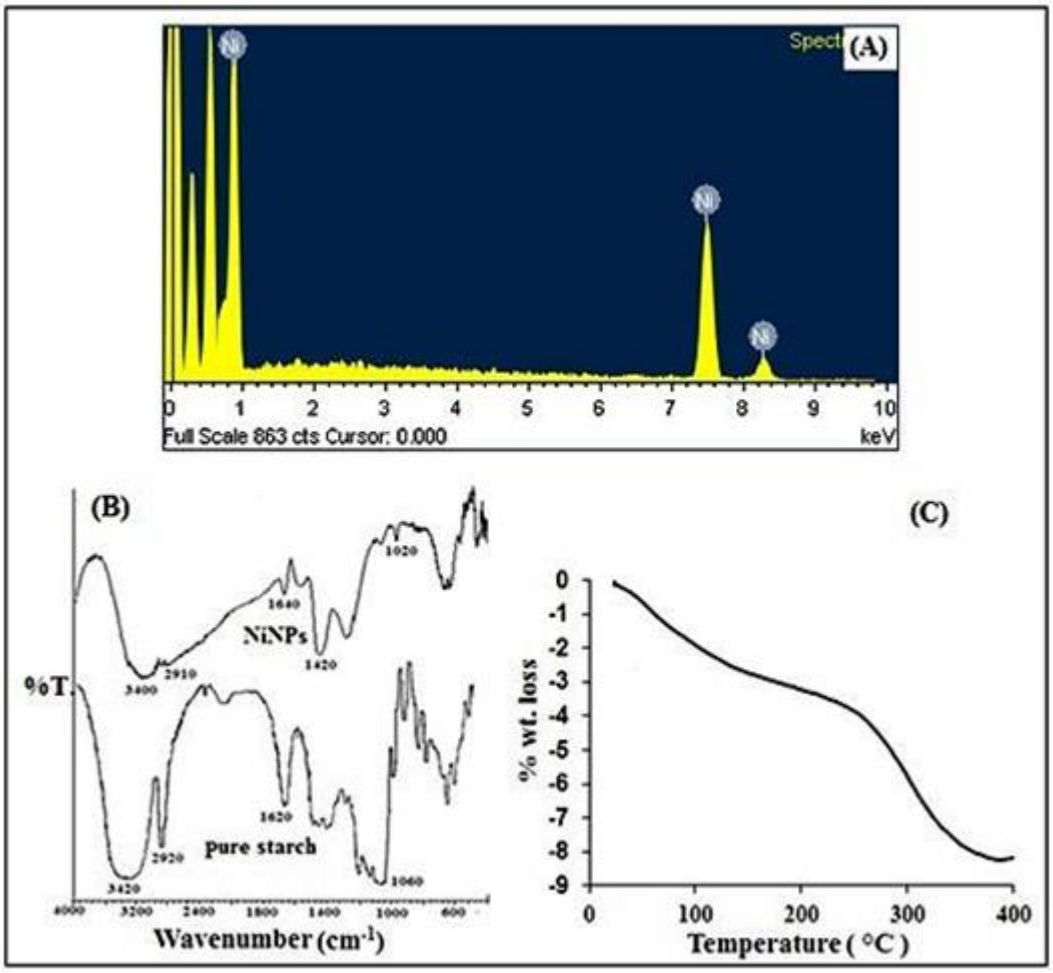

Figure 2.2 (A) EDX analysis, (B) FT-IR spectra and (C) TGA degradation curve of NiNPs.

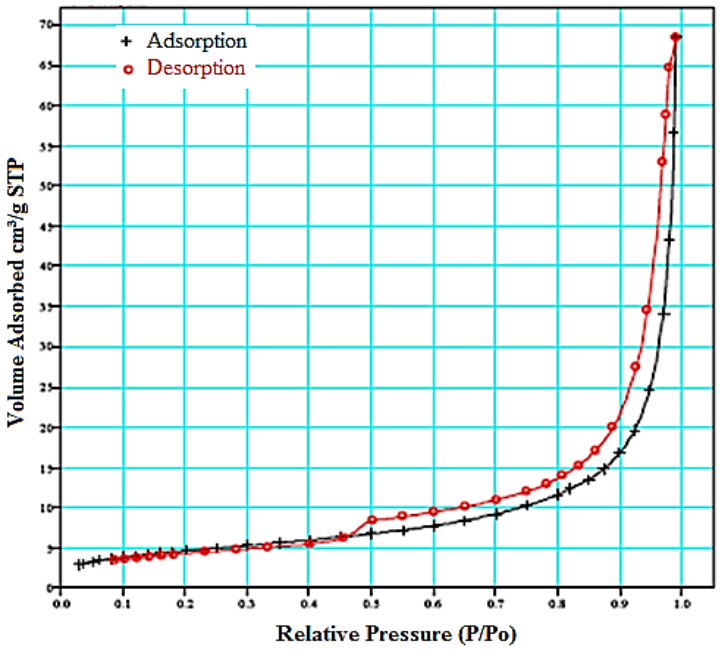

Figure 2.3a Nitrogen sorption isotherms for NiNPs

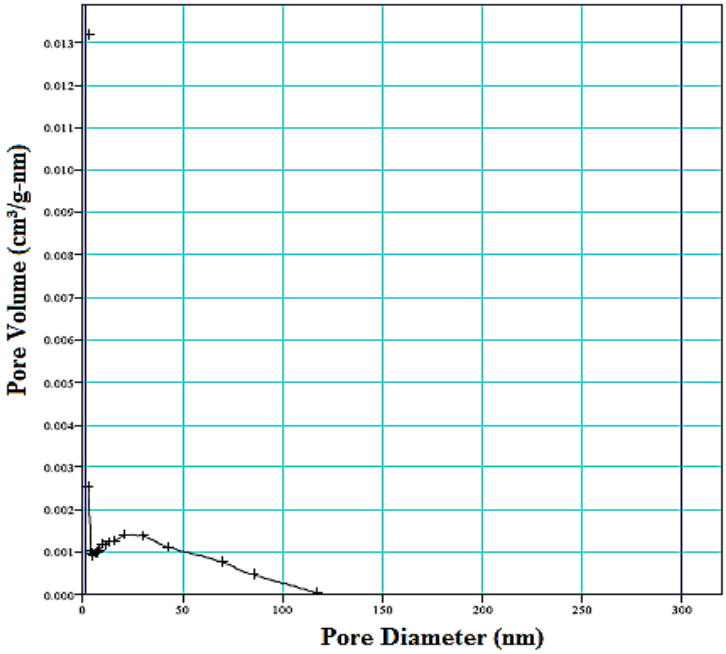

Figure 2.3b BJH Desorption dV/dD Pore Volume of NiNPs

2.5 References

1. C. J. Murphy, A. M. Gole, J. W. Stone, P. N. Sisco, A. M. Alkilany, E. C. Goldsmith and S. C. Baxter, *Acc. Chem. Res.*, 2008, **41**, 1721.

2. N. L. Rosi and C. A. Mirkin, *Chem. Rev.*, 2005, **105**, 1547.

3. M. M. Telkar, C.V. Rodea, R.V. Chaudhari, S.S. Joshi and A.M. Nalawade, *Appl. Catal. A: Gen.*, 2004, **27**, 11.

4. Z. Chen, C. D. Pina, E. Falletta, M. L. Faro, M. Pasta, M. Rossi and N. Santo, *J. Catal.* 2008, **259**,1.

5. M. L. Singla, A. Negi , V. Mahajan , K.C. Singh , D.V.S. Jain, *Appl. Catal. A: Gen*, 2007, **323**, 51.

6. A. Saxena, A. Kumar and S. J. Mozumdar, *Molecular Catal. A: Chem.*, 2007, **269**, 35.

7. R. Xu, T. Xie, Y. Zhao and Y. Li, *Nanotechnology,* 2007, **18**, 55602.

8. K. Nagashima, M. Wada and A. Kato, *J. Mater. Res.*, 1990, **5**, 2828.

9. G. G. Couto, J. J. Klein, W. H. Schreiner, D. H. Mosca, A .J. A. de Oliveira and A. J. G. Zarbin, *J. Colloid Interface Sci.*, 2007, **311**,461.

10. D. H. Chen and S.H.Wu, *Chem. Mater.*, 2000, **12**, 1354.

11. E. A. Abdel-Aal, S. M. Malekzadeh, M. M. Rashad, A. A. El-Midany and H. El-Shall, *Powder Technol.*, 2007, **171**, 63.

12. Y. Du, H. Chen, R. Chen and Xu, N. Aool., *Catal. A.*, 2004, **277**, 259.

13. M. Kidwai, N. K. Mishra, V. Bansal, A. Kumar and S. Mozumdar, *Catal. Commun.*, 2008, **9**, 612.

14. M. Kidwai, V. Bansal, A. Saxena, R. Shankar and S. Mozumdar, *Tetrahedron Lett.*, 2006, **47**, 4161.

15. F. Alonso, I. Osante and M. Yus, *Adv. Synth. Catal.*, 2006, **348**, 305.

16. S. Praharaj, S. K. Ghosh, S. Nath, S. Kundu, S. Panigrahi, S. Basu and T. Pal, J. *Phys. Chem. B*, 2005, **109**, 13166.

17. P. K. Khanna, P. V. More, J. P. Jawalkar and B. G. Bharate, *Mater.Lett.*, 2009, **63**, 1384.

18. J. Wang, A. Johnston-Peck and J. B. Tracy, *Chem. Mater.*, 2009, **21**, 4462.

19. Y. Chen, X. Luo, G. Yue, X. Luo and D. Peng, *Mater.Chem. and Phys* , 2009, **113**, 412.

20. M. Valodkar, A. Bhadoria, J. Pohnerkar, M. Mohan and S.Thakore, *Carbohydr. Res.*, 2010, **345**, 1767.

21. P. Song, D. Wen, Z. X. Guo and T. Korakianitis, *Phys Chem Chem Phys*, 2008, **10**, 5057.

Chapter–2

Part–1

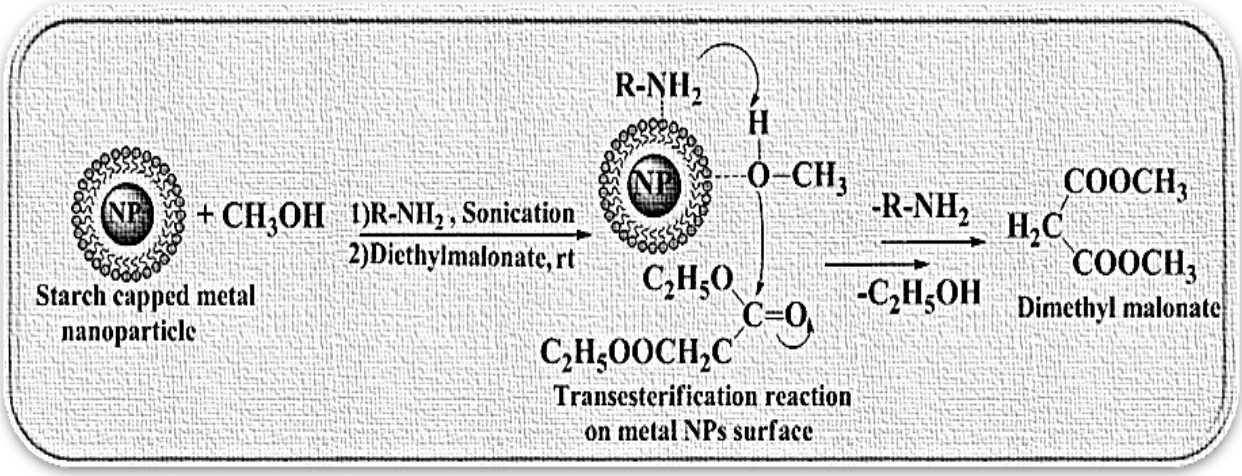

Catalytic application of Nickel Nanoparticles in Transesterification of primary esters

Published in *Journal of Molecular Catalysis A: Chemical*, 2013, 377, 129

2.1.1 Introduction

Catalytic transesterification of carboxylic esters with alcohols is an important organic synthesis[1] and an important tool in the synthesis of biologically active compounds and drugs.[1a,2,3] Esters play an important role in the multiple-step synthesis or as a protecting group of several natural products.[4] The large scale applications of transesterification are in polymerization processes,[5] paint industry [6] and in conversion of fats (triglycerides) into biodiesel.[7] Carboxylic acids are sparingly soluble in organic solvents, whereas esters are normally soluble in most of organic solvents.[8] Transesterification being an equilibrium reaction, high conversions are difficult to attain. Hence, reactions are catalyzed by acids [6b,9] and bases [10] under homogeneous as well as heterogeneous conditions.[11] However, acid catalysts [12] exhibit low substrate selectivity and can cleave sensitive functional groups. They may also lead to formation of side products.[13] A strongly basic catalyst leads to high conversions, but fail for base-sensitive substrates.[12] Therefore, with either acidic or basic conditions, such transesterification reactions do not prove to proceed efficiently under mild reaction conditions.[11c] A number of organic amines have shown good catalytic activity for transesterification.[14] Although the recovery process is simpler the process has narrow range of applicability due to longer reaction time and low conversions.

On the other hand, nanoparticles (NPs) are core base materials for implementing nanotechnology and have promising applications in organic synthesis.[15] It has been proved that Ni and CuNPs as catalysts offer great opportunities for a wide range of applications in organic synthesis.[16] The high efficiency of NPs system relies mainly on the approach to the metal core, size, and surface modification. Various functional groups can be introduced on the surface of the NPs by using appropriate capping agent. In order to identify an ideal catalyst for transesterification, we decided to study the catalytic activity of some organic amines in presence of metal NPs. In the past, we have synthesized metal NPs with various capping agents which were used for biological applications.[17] In this chapter, we report first protocol for metal NPs (nickel and copper) assisted amine catalyzed synthesis of higher to lower esters and vice-versa under ambient conditions. Initially diethylmalonate (DEM) was used as the model system to simplify the analysis and to accelerate the screening speed for suitable amine-NPs catalytic system. Consequently the optimized conditions were used for the synthesis of various esters.

2.1.2 Experimental section

2.1.2.1 Materials and Synthesis of metal nanoparticles

Triethylamine (TEA), diethylamine (DEA), ethylenediamine (EDA), methanol, ethanol, diethylmalonate (DEM) and other esters were purchased from Merck, Mumbai, India. GC was calibrated using standards of esters (purchased from Merck, Mumbai, India). Copper nanoparticles (CuNPs) were synthesized by using starch as stabilizing agent and ascorbic acid as reducing agent as reported earlier.[17a] The characterization of starch capped CuNPs is reported elsewhere.[17a]

2.1.2.2 Characterization methods

The progress of reactions was monitored by TLC (silica gel 60 F254, Merck, Mumbai, India). The solvent system consisted of hexane/ethyl acetate (75:25 v/v) for DEM. The spots were detected in iodine chamber. The product of DEM reaction was analyzed by gas chromatography on Perkin Elmerclarus 500 GC with the flame-ionization detector. The capillary column (RestekRtx®-5) used had a length of 30 m with an internal diameter of 0.25 mm. Nitrogen was used as the carrier gas at a constant flow rate. The column oven temperature was programmed from 80 to 280 °C (at the rate of 10 °C min^{-1}) with injector and detector temperatures at 240 and 280 °C, respectively. In case of transesterification phenyl benzoate / DEM / DMM with long chain alcohols, the column oven temperature was programmed from 100 to 320 °C (at a heating rate of 10 °C min^{-1}) with injector and detector temperatures at 270 and 280 °C, respectively. The products of triacetin reaction (methyl acetate or ethyl acetate) were analyzed by HPLC (Agilent 2000) with a C18 XDB column and diode array detector. The mobile phase was methanol–water (50:50) and was tested at 205 nm with a flow rate of 1.0 mL/min and a column temperature of 35 °C.

2.1.2.3 General procedure for room temperature transesterification

In a typical reaction methanol (20mmol), amines (0.12mmol) and starch capped nickel nanoparticles (NiNPs) (80 mg,) were initially sonicated at room temperature (rt) for 30 minutes in a round bottom flask (RBF) prior to addition of the substrate. After sonication diethylmalonate (1mmol) was added and the reaction mixture was stirred at rt (25-30 °C). In cases where the reaction did not proceed to completion the

mixture was gradually heated to reflux (at 70 °C) with an aim to achieve maximum conversion. Reaction monitoring was done by thin-layer chromatography (TLC) and gas chromatography (GC). After the completion of reaction, NPs were separated by centrifuge and alcohol (methanol or ethanol) and amines were distilled out. Isolated NPs were washed by acetone and they were dried at 60 ºC under vacuum and used for the next reaction.

The yield and purity of final products were analyzed by GC. Short- path silica gel chromatography (5:95, ethyl acetate in hexane v/v) was used to obtain an analytically pure dimethylmalonate (DMM). Finally, the product DMM was also analyzed by nuclear magnetic resonance (NMR) (BRUKER 400 MHz). Transesterification of other esters was carried out in a similar manner by using alcohol and esters molar ration 10:1. The products purified by short-path silica gel chromatography (0-25% ethyl acetate in hexane v/v) were analyzed by GC and NMR. All experiments have been repeated three times and the reproducibility confirmed.

2.1.3 Results and Discussion

2.1.3.1 Transesterification of diethylmalonate and other esters

In order to assess the efficiency of different amines as base catalyst the transesterification of diethylmalonate was carried out using each of the three amines (Triethylamine (TEA), Diethylamine (DEA), Ethylenediamine (EDA)) in the absence of NPs (**Table 2.1**).

It was observed that the reaction yields were very low (~ 50 to 55%) even after 72h at rt (**Table 2.1**, entries-3, 4, and 5 respectively) and after 48h under reflux (**Table 2.1**, entries-6, 7 and 8). The order of the catalytic activity of amines was observed to be EDA (pk_a-11.09 at 25°C)>DEA (pk_a-11.01 at 25°C) >TEA (pk_a-10.9 at 25°C) respectively which is the same as the order of basicity.

Hence for establishment of optimum conditions a preliminary study was carried out using EDA as the catalyst (**Table 2.2 to 2.4**). After several experiments with different concentrations of EDA, methanol and various quantities of NiNPs, the optimum conditions for transesterification of DEM to dimethylmalonate (DMM) were established (**Scheme 2.2**).

Interestingly, when the same reactions were carried in presence of NiNPs a significant enhancement in conversion was observed. The effect was more pronounced in EDA

and DEA catalyzed reactions, which were completed within 30min and 8h with 99% (entry-11) and 80% (entry-10) conversion respectively. On the other hand, TEA catalyzed reactions were less affected by NiNPs (entry-12).

Table 2.1 Transesterification of diethylmalonate[a]

Entry	Amines	Metal NPs	Temperature of reaction in °C	Reaction time (h)	GC yield (%±1)
1	-	-	Reflux	72	3
2	-	Cu / Ni	Reflux	72	8
3	TEA	-	Rt	72	42
4	DEA	-	Rt	72	47
5	EDA	-	Rt	72	50
6	TEA	-	Reflux	48	45
7	DEA	-	Reflux	48	49
8	EDA	-	Reflux	48	56
9	TEA	Ni	Rt	24	52
10	DEA	Ni	Rt	8.0	80
11	**EDA**	**Ni**	**Rt**	**0.5**	**99**
12	TEA	Ni	Reflux	8.0	56
13	DEA	Ni	Reflux	8.0	86
14	EDA	Ni	Reflux	0.25	99
15	EDA	Cu	Reflux	0.25	99
16	EDA	Cu	Rt	0.50	99

(a) Reaction condition: Substrate- diethylmalonate (1mmol), methanol (20mmol), amines (0.12mmol) (TEA/DEA/EDA) and NiNPs/CuNPs-80mg (60wt %)

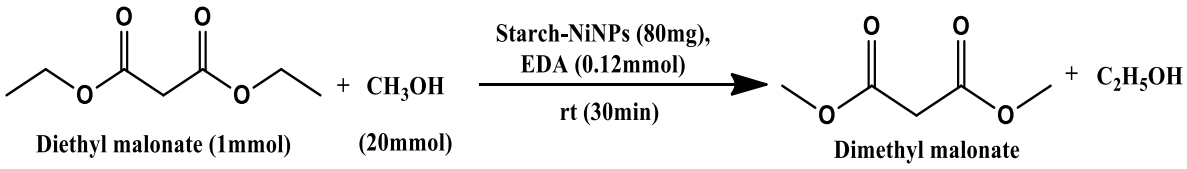

Scheme 2.2 Optimum conditions for transesterification of diethylmalonate.

Table 2.2 Transesterification of DEM at different DEM/methanol ratios.[a]

Entry	DEM/Methanol(mmol)	T (h)	Yield(±1,by GC)
1	1:1	24	76
2	1:2.5	12	95
3	1:5	12	99
4	1:10	3.0	99
5	1:15	1.5	99
6	**1:20**	**0.5**	**99**
7	1:25	0.5	99
8	1:30	0.5	99

(a) All reaction carried out at rt by using EDA (0.12mmol) and NiNPs (80mg).

Table 2.3 Transesterification of DEM at different DEM/NiNPs ratios.[a]

Entry	DEM/NiNPs(mg)	T (h)	Yield(±1, by GC)
1	1:0.0	72	49
2	1:10	5.0	98
3	1:20	4.0	99
4	1:40	3.0	99
5	1:60	1.0	99
6	**1:80**	**0.5**	**99**
7	1:100	0.5	99
8	1:120	0.5	99

(a) All reactions carried out at rt by using DEM (1mmol) EDA (0.12mmol) and Methanol (20mmol).

Table 2.4 Transesterification of DEM at different DEM/EDA ratios.[a]

Entry	DEM/EDA(mmol)	T (h)	Yield(±1, by GC)
1	1:0.0	72	8
2	1:0.03	72	85
3	1:0.06	5.0	98
4	**1:0.12**	**0.5**	**99**
5	1:0.16	0.5	99
6	1:0.20	0.5	99
7	1:0.25	0.5	99

(a) All reaction carried out at rt by using DEM (1mmol), NiNPs (80mg) and Methanol (20mmol).

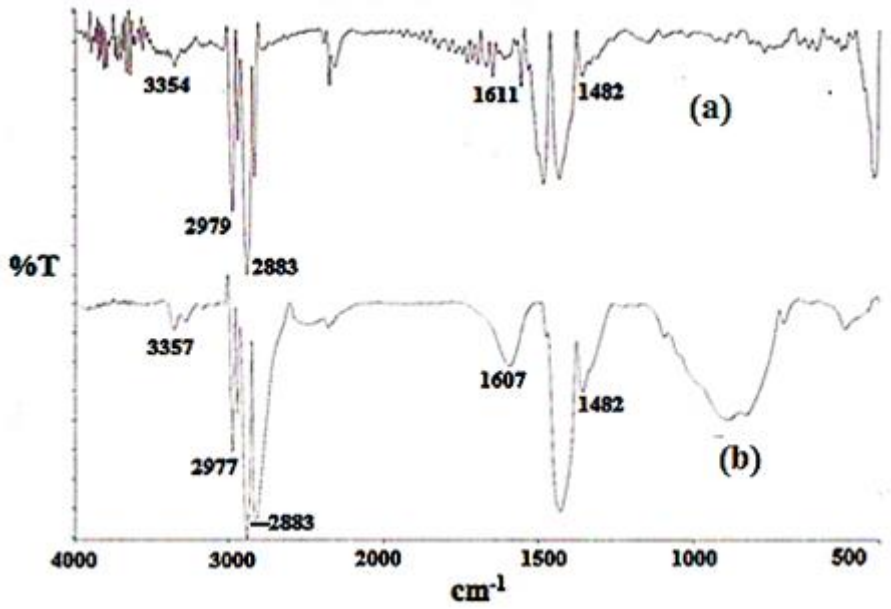

Figure 2.4 FT-IR spectra of (a) NiNPs recovered after 1st run showing traces of bound EDA (b) EDA alone.

To understand the role of metal, the reaction under optimized conditions was also carried out with copper nanoparticles (CuNPs) instead of NiNPs to yield similar results (**Table 2.1**, entry-15). Hence to get better insight into the mechanism of the reaction, the FT-IR spectrum (**Figure 2.4**) of the recovered NiNPs provided the evidence for surface-functionalization of NiNPs with EDA. The FT-IR spectrum of the NiNPs recovered (**Figure 2.4a**) after the first cycle of transesterification showed peaks at 3354 cm^{-1} and 1611 cm^{-1} which can be assigned to the N-H stretching and bending respectively. The peaks at 2979 and 2883 cm^{-1} are assigned to the C-H stretching vibrations and the one at 1482 cm^{-1} is due to C-H bending of alkanes. Based on these observations we propose that role of metal NPs is to provide surface binding sites for the reactants (methanol) and milder catalyst (amine) during sonication. This facilitates the generation of nucleophile, the methoxide ion, with the help of a weak base,[18] like EDA which then attacks DEM as shown in **Scheme 2.3**. The higher efficiency of metal NPs under mild conditions is due to their higher dispersion in solvent so that the reactant reaches the catalytic site by diffusion. EDA being a diamine gives highest catalytic activity because of greater basicity, followed by DEA. TEA being a tertiary amine was probably too weak to generate nucleophile due to steric hindrance.

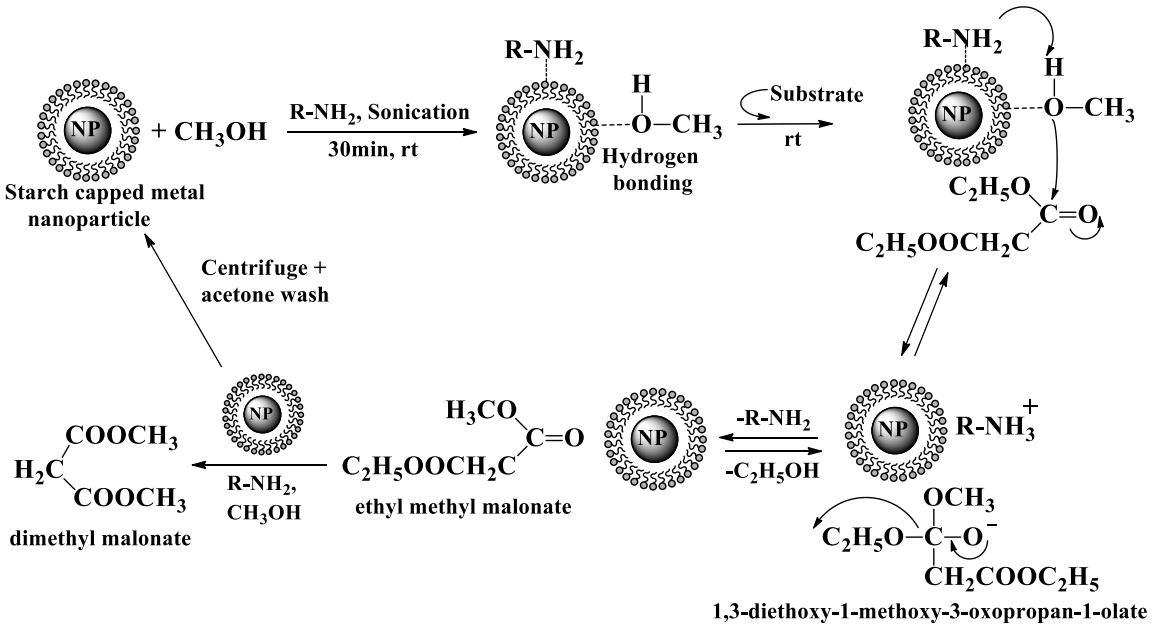

Scheme 2.3 A proposed reaction mechanism for Starch-NiNPs supported organic amine catalyzed transesterification of diethylmalonate systems.

Sequence of addition of reactants was also observed to be important. If substrate DEM is added before amine, the reaction slows down probably due to partial adsorption of DEM which affects the generation of nucleophile. Hence it is advantageous that amine and methanol come in contact with NiNPs before DEM. A similar observation has been reported by Liu et al.[19] for hydrotalcite based catalyst. At reflux temperature of the methanol, much better conversion was 99% and the reaction was complete within 15min (**Table 2.1**, entry - 14).

The NPs were recovered by centrifugation with insignificant loss and recycling experiments were carried out under optimized conditions. Interestingly, it was observed that the NPs could be reused directly without further purification for 24 consecutive runs as can be seen in **Table 2.5**. Upto seven cycles there was no loss in activity. After that, however, the reaction time increased in each successive recycling experiment reaching from 30min to 2h finally. This may be due to gradual loss of the catalytic activity of NiNPs with number of runs which may be due to various reasons. One of the reasons may be surface modification due to deposition of matter during reaction.[20,21] The IR spectra of the NiNPs recorded after 24th run displays a number of peaks of deposited matter as shown in **Figure 2.5**. Nevertheless, the reaction does proceed to completion at the same temperature at the end of 24 cycles giving the same yield. Further the used NiNPs were also characterized by XRD in order to confirm the metallic state of nickel or the possibility of surface oxidation. The formation of oxide is less as evident as seen from the XRD analysis (**Figure 2.6**) which does not show any peak corresponding to NiO at 37 deg. This can be attributed to the presence of starch coating which makes the NPs stable to water and air and maintains their metallic state.[17a,22] This increases their utility and enhances recycling efficiency. Further, it is also possible that hydrogen-bonding between hydroxyl groups of capping agent starch and methanol also assists the generation of methoxide ion on the surface of NiNPs.[23] Thus the metal surface, capping agent and amine simultaneously make the amine-NiNPs system an effective catalyst. Starch capped CuNPs were observed to be much less stable and more prone to oxidation than NiNPs. Hence there was considerable loss due to leaching out and recycling experiments were difficult to perform.

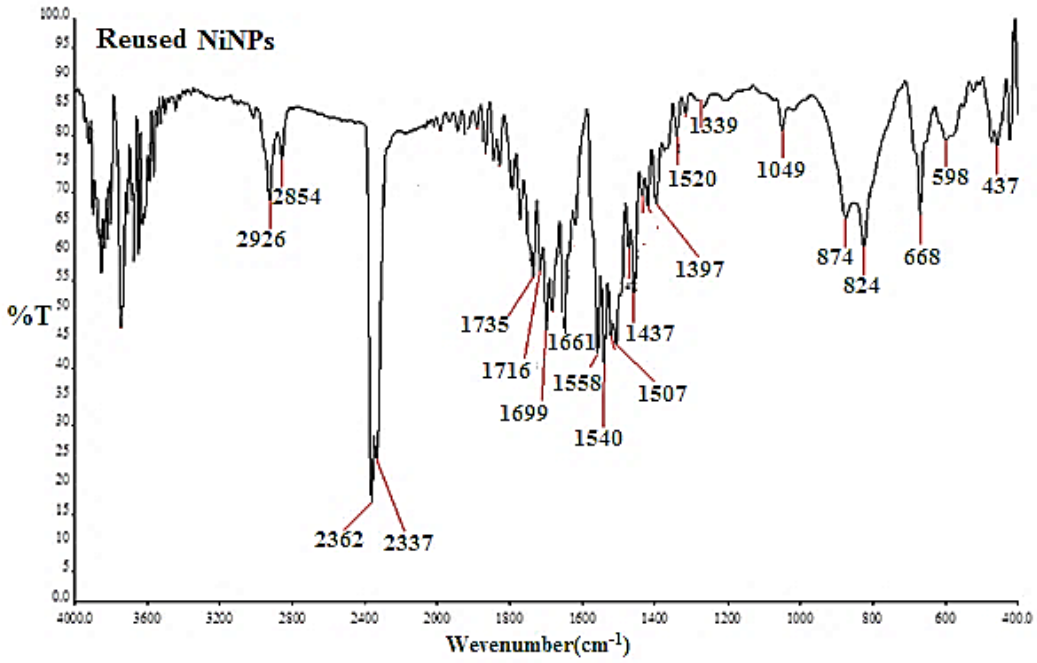

Figure 2.5 FT-IR spectra of the reused NiNPs after 24th run

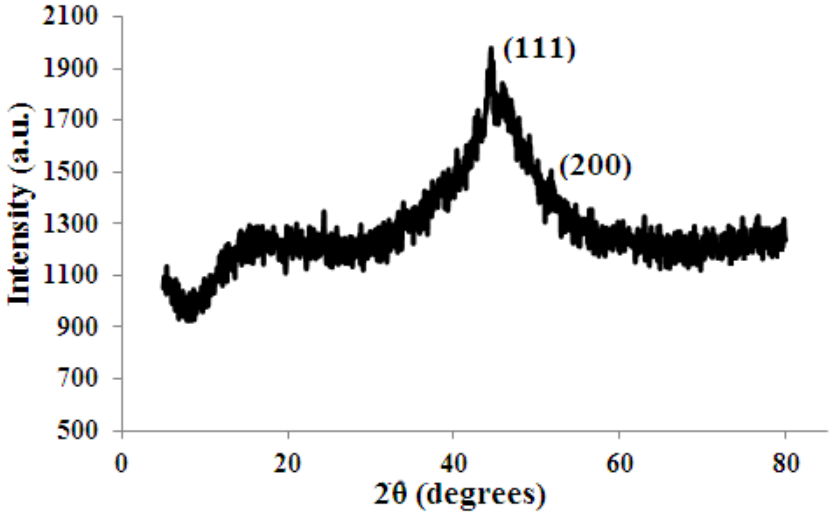

Figure 2.6 XRD pattern of NiNPs recovered after 24th run

Table 2.5 Transesterification of diethylmalonate at rt (25-30°C) with methanol using NiNPs and EDA (Recycling experiments)

Cycle	Time(min)	Yield[a](%)	IY[b](%)	Cycle	Time(min)	Yield[a](%)	IY[b](%)
1	30	99	96	13	60	99	96
2	30	99	96	14	60	99	96
3	30	99	96	15	60	99	96
4	30	99	96	16	60	99	96
5	30	99	96	17	60	99	96
6	30	99	96	18	60	99	96
7	30	99	96	19	60	99	96
8	40	99	96	20	60	99	96
9	40	99	96	21	60	99	96
10	60	99	96	22	60	99	96
11	60	99	96	23	90	99	96
12	60	99	96	24	120	99	96

(a) GC yield, (b) Isolated yield

Under the optimized conditions, we investigated the scope of converting various methyl esters to ethyl esters and vice-versa by using ethanol and methanol respectively (**Scheme 2.4**). Both NiNPs and CuNPs were applied for all substrate and they almost gave same yield in similar reaction time (**Table 2.6**). The results were satisfactory for aliphatic, aromatic, and heterocyclic substrates. Conversion from ethyl to methyl esters and vice-versa occurs almost in comparable time. Reaction conversion time was less in aliphatic diesters (entry-4, 5, 15 & 16) compared to long chain monoesters (entry - 6, 17) but, reaction yield were comparable in both cases. Heterocyclic esters undergo smooth conversion as any other ester (entry - 9, 10 & 19). The transesterification of triglyceride like triacetin (entry-11 and 21) with ethanol resulted in 96-97% HPLC yield (data not shown) in 3h. This opens up new possibilities for eco-friendly synthesis biodiesel since organic amines can be recovered by distillation[24, 25] and the NPs can be recycled.

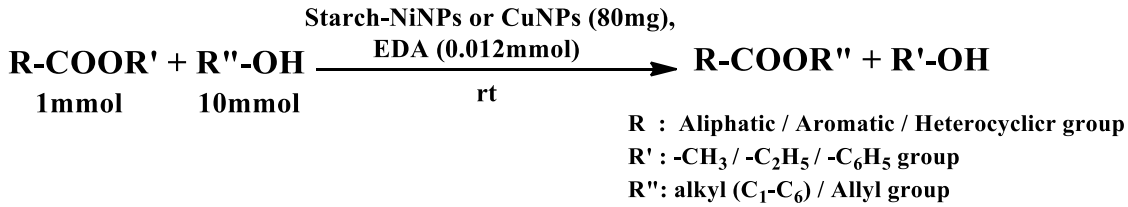

Scheme 2.4 General scheme for transesterification of various esters

Table 2.6 Transesterification of various esters at rt (25-30°C) with methanol/ ethanol using NPs and EDA

Entry	Substrate	Product	Time (h)	Yield[a] (±1%)		
				NiNPs	CuNPs	Without NPs[d]
1	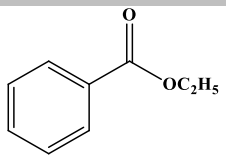	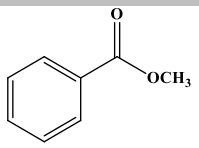	2.5(2.5)[b]	96	96	40
2	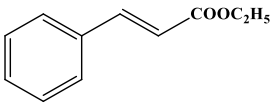	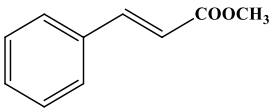	2.0(2.0)[b]	96	95	50
3	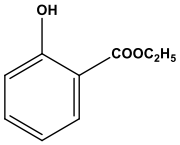	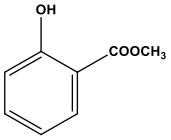	5.0(4.5)[b]	96.5	97	34
4	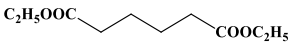	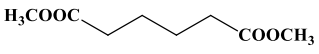	3.0(3.5)[b]	95	95	50
5	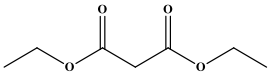	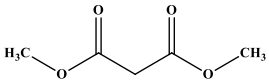	0.30(0.40)[b]	96	95	50
6	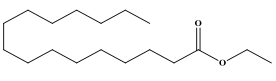	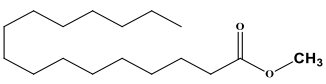	5.0(5.30)[b]	94	95	40
7	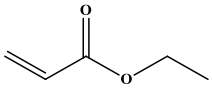	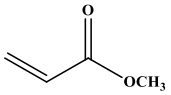	5.30(5.30)[b]	96	96	15

8	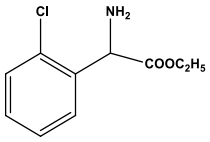	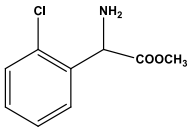	4.0(4.0)	95	95	23
9	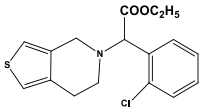	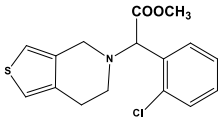	4.0(4.0)	95	95	20
10	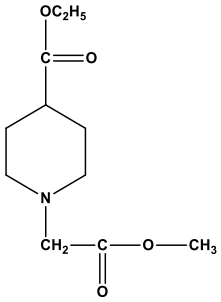	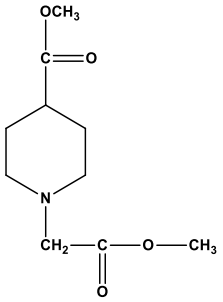	3.0 (3.0)	94	93	35
11	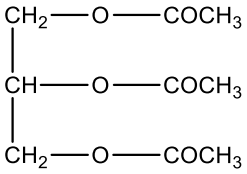	$3CH_3COOCH_3$	3.0 (3.0)[b]	97[c]	97[c]	45[c]
12	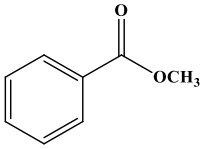	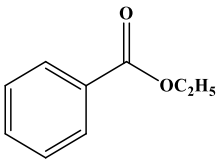	1.30 (1.0)[b]	92	93	10
13	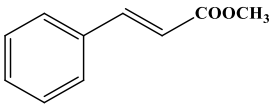	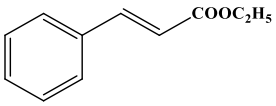	1.0 (1.0)[b]	96	95	20
14	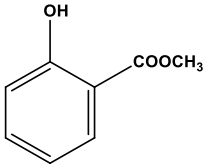	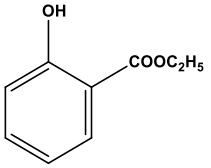	6.0 (5.0) [b]	90	91	30
15	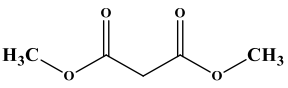	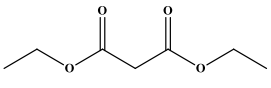	0.30 (0.30)[b]	95	96	40
16	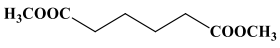	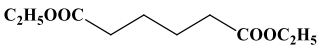	3.5 (3.5)[b]	80	81	2

17	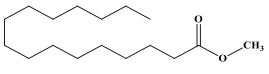	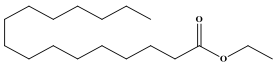	6.5 (7.0)[b]	96	96	20
18	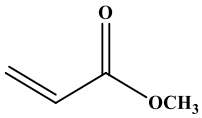	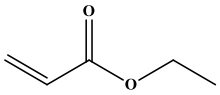	6.5 (6.5)[b]	90	92	5
19	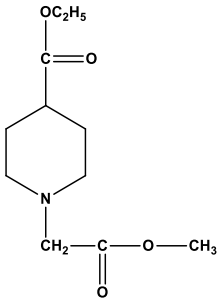	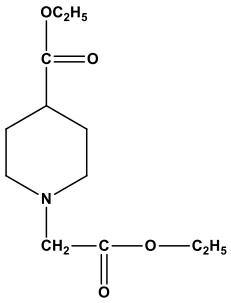	3.0 (3.5)[b]	95	95	40
20	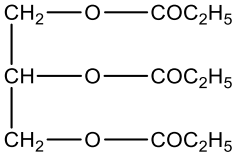	$3CH_3COOC_2H_5$	3.0 (3.0)[b]	96[c]	96[c]	40[c]

(a)Isolated yield after column chromatography, (b) Reaction time for CuNPs catalyzed reaction, (c) HPLC yield (data not shown) and (d) Reaction time after 24 h.

2.1.3.2 Transesterification with other alcohols

In order to validate the process further, the transesterification of DEM and DMM was attempted with other alcohols. The results in **Table 2.7** show that with primary alcohols (C3-C6) transesterification successfully occurred although a progressive decrease in yield was observed due to increasing steric hindrance. However with secondary, tertiary and benzylic alcohols as well as phenol the reaction either did not initiate or conversions were poor (data not shown). The reactions were also tried with a different substrate (**Table 2.7**, entry 5 to 11) having aromatic groups instead of ethyl/methyl side chains. But similar results were obtained.

Table 2.7 Transesterification with other alcohols using NPs and EDA at rt (25-30°C)

Entry	Substrate	Alcohol	Product	Yield[a] (±1%)		
				NiNPs	CuNPs	Without NPs
1	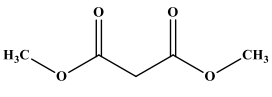	*n*-Propanol	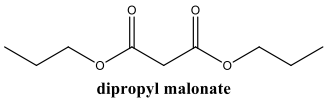 dipropyl malonate	94	94	23
2	„	*n*-Butanol	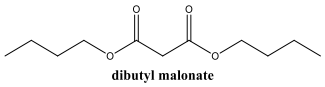 dibutyl malonate	89	91	15
3	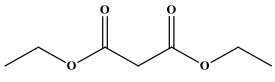	*n*-Propanol	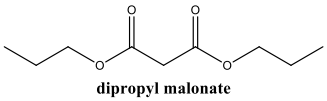 dipropyl malonate	94	93	24
4	„	*n*-Butanol	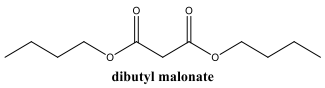 dibutyl malonate	88	90	10
5	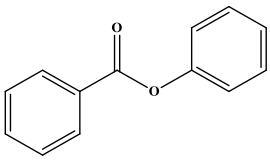 phenyl benzoate	Methanol	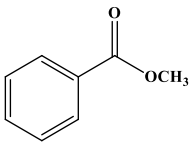	95	94	34
6	„	Ethanol	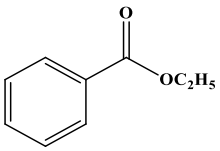	95	95	33
7	„	*n*-Propanol	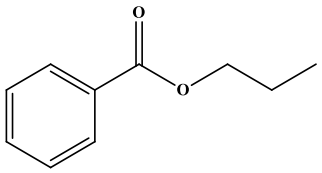 Propyl benzoate	92	93	30
8	„	*n*-Butanol	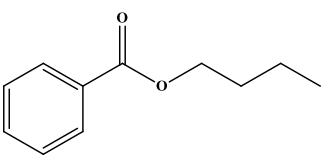 Butyl benzoate	92	91	15

9	”	*n*-Pentanol	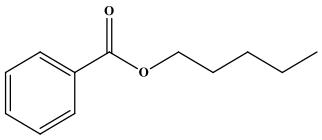 Pentyl benzoate	92	91	15
10	”	*n*-Hexanol	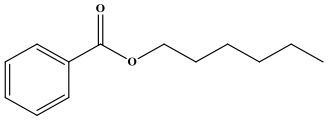 Hexyl benzoate	90	91	17
11	”	Allylalcohol	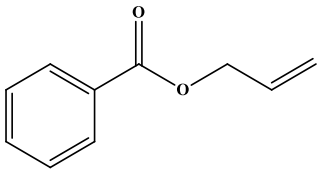 Allyl benzoate	93	93	32

(a) GC yield after 24 h.

2.1.4 Conclusion

The study leads to a conclusion that the present catalytic system of EDA–NiNPs, provides smooth transesterification over a wide range of structurally diverse esters without disturbing other functional groups. Catlyst exhibited excellent activity in the transesterification of higher to lower esters and vice-versa at room. The reaction proceeds to offer high yields under ambient conditions and starch capped NPs exhibited excellent recyclability. The entire system comprising metal core, capping agent and the amine works as effective catalyst. The scope of the procedure was successfully extended to aliphatic, heterocyclic and aromatic esters.

2.1.5 References

1. (a) J. Otera, Esterification; Wiley-VCH GmbH: Weinheim, Germany, 2003; (b) J. Otera, *Chem. Rev.* 1993, **93**, 1449; (c) G. A. Grasa, R. Singh and S. P. Nolan, *Synthesis*, 2004, **7**, 971; (d) D. Enders, O. Niemeier and A. Henseler, *Chem. Rev.*, 2007, **107**, 5606.
2. S. Wilson, S. Benetti, R. Romagnoli, C. De Risi, G. Spalluto and V. Zanirato, *Chem. Rev.*, 1995, **95**, 1065.
3. (a) R. Larock, In Comprehensive Organic Transformations, 2nd ed., Wiley-VCH New York, 1996. (b) J. Mulzer, B. M. Trost and I. Fleming, In Comprehensive Organic Synthesis Eds., Pergamon Press: New York, 1992.
4. T. W. Green and P. G. M. Wuts, In Protective Groups in Organic Synthesis, 3rd ed., Wiley New York, 1999.
5. W. Riemenschneider and H. M. Bolt, Esters, Organic Ullmann's Encyclopedia of Industrial Chemistry, Wiley-VCH, Weinheim 2005.
6. (a) V. Nair, S. Bindu and V. Sreekumar, *Angew. Chem., Int. Ed.*, 2004, **43**, 5130; (b) J. Otera, *Acc. Chem. Res.*, 2004, **37**, 288.
7. (a) M. Toda, A. Takagaki, M. Okamura, J. N. Kondo, S. Hayashi, K. Domen and M. Hara, *Nature*, 2005, **438**, 178; (b) G. Knothe, *Fuel Process. Technol.*, 2005, **86**, 1059; (c) E. Lotero, Y. Liu, D. E. Lopez, A. Suwannakaran, D. A. Bruce and J. G. Goodwin, *Ind. Eng. Chem. Res.*, 2005, **44**, 5353; (d) V. Reddy, R. Oshel and J. G. Verkade, *Energy Fuels*, 2006, **20**, 1310.
8. H. E. Hoydonckx, D. E. De Vos, S. A. Chavan and P. A. Jacobs, *Top. Catal.*, 2004, **27**, 83.
9. (a) H. Yazawa, K. Tanaka and K. Kariyone, *Tetrahedron Lett.*, 1974, **12**, 3995; (b) M. Brenner and W. Huber, *Helv. Chem. Acta* , 1953, **36**, 1109; (c) C. E. Rehberg and C. H. Fisher, *J. Am. Chem. Soc.*, 1944, **66**, 1203; (d) C. E. Rehberg, W. A. Faucette and C. H. Fisher, *J. Am. Chem. Soc.*, 1944, **66**, 1723; (f) C. E. Rehberg, In Organic Synthesis. Wiley, New York, 1955. (g) J. K. Haken, *J. Appl. Chem.*, 1963, **13**, 168.
10. (a) R. W. Taft, M. S. Newman and F. H. Verhoek, *J. Am. Chem. Soc.*, 1950, **72**, 4511; (b) J. H. Billman, W. T. Smith and J. L. Rendall, *J. Am. Chem. Soc.*, 1947, **69**, 2058; (c) L. Osipow, F. D. Snell, W. C. York and A. Finchler, *Ind. Eng. Chem.*, 1956, **48**, 1459; (d) L. Osipow, F. D. Snell and A. Finchler, *J.*

Am. Oil Chem. Soc., 1957, **34**, 185; (e) S. Komori, M. Okahara and K. Okamoto, *J. Am. Oil Chem. Soc.*, 1960, **37**, 468; (f) G. A. Grasa, T. Guveli, R. Singh and S. P. Nolan, *J. Org. Chem.*, 2003, **68,** 2812; (g) G. W. Nyce, J. A. Lamboy, E. F. Connor, R. M. Waymouth and J. L. Hedrick, *Org. Lett.*, 2002, **4**, 3587; (h) R. Singh, R. M. Kissling, M. A. Letellier and S. P. Nolan, *J. Org. Chem.*, 2004, **69**, 209; (i) G. A. Grasa, R. M. Kissling and S. P. Nolan, *Org. Lett.*, 2002, **4**, 3583.

11. (a) D. W. Yoo, J. H. Han, S. H. Nam, H. J. Kim, C. Kim and J. K. Lee, *Inorg. Chem. Commun.*, 2006, **9**, 654; (b) X. Hao, A. Yoshida and J. Nishikido, *Tetrahedron Lett.*, 2004, **45**, 781; (c) D. E. Ponde, V. H. Deshpande, V. J. Bulbule, A. Sudalai and A. S. Gajare, *J. Org. Chem.*, 1998, **63**, 1058; (d) B. M. Choudary, M. L. Kantam, C. Venkat Reddy, S. Aranganathan, P. L. Shanti and F. J. Figueras, *Mol. Catal. A: Chem.*, 2000, **159**, 411; (e) A. Solhy, J. H. Clark, R. Tahir, S. Sebtic and M. Larzek, *Green Chem.*, 2006, **8**, 871; (f) F. Bazi, H. E. Badaoui, S. Samira, S. Tamani, M. Hamza, S. Boulaajaj and S. Sebti, *Synth. Commun.*, 2006, **36**, 1585; (g) M. L. Kantam, V. Neeraja, B. Bharathi and C. V. Reddy, *Catal. Lett.*, 1999, **62**, 67.
12. M. G. Stanton and M. R. Gagne, *J. Org. Chem.*, 1997, **62**, 8240.
13. M. H. Lin and T. V. Rajanbabu, *Org. Lett.*, 2000, **2,** 997.
14. (a) J. J. Hans, R. W. Driver and S. D. Burke, *J. Org. Chem.*, 1999, **64**, 1430 ; (b) D. S. Tawfik, Z. Eshhar, A. Bentolila and B. S. Green, *Synthesis*, 1993, **256**, 968 ; (c) D. Seebach, A. Thaler, D. Blaser and S. Y. Ko, *Helv. Chim. Acta*, 1991, **74,** 1102 ; (d) M. Bodanszky and J. T. Sheehan, *Chem. Ind.*, 1966, **38**, 1597 ; (e) G. L. Reddy, E. Bikshapathy and R. Nagaraj, *Tetrahedron Lett.*, 1985, **26**, 4257 ; (f) M. A. Barton, R. U. Lemieux and J. Y. Savoie, *J. Am. Chem. Soc.*, 1973, **95,** 4501 ; (g) D. L. Holmes, E. M. Smith and J. S. Nowick, *J. Am. Chem. Soc.*, 1997, **119**, 7665.
15. (a) F. Alonso, P. Riente and M. Yus, *Acc. Chem. Res.*, 2011, **44**, 379; (b) F. Alonso and M. Yus, *Pure Appl. Chem.*, 2008, **80**, 1005; (c) N. Yan, C. Xiao and Y. Kou, *Coord. Chem. Rev.*, 2010, **254**, 1179; (d) S. Shylesh, V. Schnemann and W. R. Thiel, *Angew. Chem. Int. Ed.*, 2010, **49,** 3428; (e) V. Polshettiwar, R. Luque, A. Fihri, H. Zhu, M. Bouhrara and J-M. Basset, *Chem. Rev.*, 2011, **111**, 3036.

16. (a) A. Saxena, A. Kumar and S. Mozumdar, *J. Mol. Catal. A Chem.*, 2007, **269**, 35; (b) F. Alonso, P. Riente and M. Yus, *Synlett*. 2007, **12**, 1877; (c) F. Alonso, P. Riente and M. Yus, *Tetrahedron Lett.*, 2009, **50**, 3070; (d) F. Alonso, P. Riente and M. Yus, *Eur. J. Org. Chem.*, 2009, **34**, 6034; (e) F. Alonso, P. Riente and M. Yus, *Tetrahedron*, 2008, **64**, 1847; (f) F. Alonso, P. Riente and M. Yus, *Tetrahedron Lett.*, 2008, **49**, 1939; (g) A. Dhakshinamoorty and K. Pitchumani, *Tetrahedron Lett.*, 2008, **49**, 1818; (h) M. Kidwai, N. K. Mishra, V. Bansal, A. Kumar and S. Mozumdar, *Tetrahedron Lett.*, 2007, **48,** 8883; (i) M. Kidwai, S. Bhardwaj, N. K. Mishra, V. Bansal, A. Kumar and S. Mozumdar, *Catal. Commun.*, 2009, **10**, 1514; (j) M. Kidwai, V. Bansal, A. Saxena, S. Aerry and S. Mozumdar, *Tetrahedron Lett.***,** 2006, **47**, 4161; (k) P. Singh, A. Katyal, R. Kalra and R. Chandra, *Tetrahedron Lett.*, 2008, **49**, 727.
17. (a) M. Valodkar, P. S. Rathore, R. N. Jadeja, M. Thounaojam, R. V. Devkar and S. Thakore, *J. Hazar. Mater.*, 2012, **201-202,** 244; (b) M. Valodkar, A. Bhadoria, J. Pohnerkar, M. Mohan and S. Thakore, *Carbohydr. Res.*, 2010, **345**, 1767; (c) M. Valodkar, P. S. Nagar, R. N. Jadeja, M. C. Thounaojam, R. V. Devkar and S. Thakore, *Colloids Surf. A***,** 2011, **384,** 337; (d) M. Valodkar, R. N. Jadeja, M. C. Thounaojam, R. V. Devkar and S. Thakore, *Mater. Chem. Phys.*, 2011, **128**, 83; (e) M. Valodkar, S. Modi, A. Pal and S. Thakore, *Mater. Res. Bull.*, 2011, **46**, 384.
18. C. O. Dalaigh, S. A. Corr, Y. Gun'ko and S. J. Connon, *Angew. Chem. Int. Ed.*, 2007, **46**, 4329.
19. Y. Liu, E. Lotero, J. G. Goodwin and X. Mo, *Appl. Catal. A: Gen.*, 2007, **331**, 138.
20. J. J. Spivey, G. W. Roberts and B. H. Davies, Catalyst Deactivation, Elsevier, Amsterdam, 2001.
21. F. Alonso, P. Riente, J. A. Sirvent and M. Yus, *Appl. Catal. A: Gen.*, 2010, **378**, 42.
22. J. M. Yan, X. B. Zhang, S. Han, H. Shioyama and Q. Xu, *Inorg. Chem.*, 2009, **48**, 7389.
23. S. Banerjee, J. Das and S. Santra, *Tetrahedron Lett.*, 2009, **50**, 124.

24. J. Sun, J. X. Ju, L. Ji, L. X. Zhang and N. P. Xu, *Ind. Eng. Chem. Res.*, 2008, **47**, 1398.
25. L. Zhang, W. Guo, D. Liu, J. Yao, L. Ji, N. Xu and M. Min, *Energy Fuels*, 2008, **22,** 1353.

(Spectral Data)

^{1}HNMR of known compounds

^{1}HNMR (400 Hz) spectra were recorded in $CDCl_3$ and DMSO. All compounds described in Table 2.6 are known in the literature and were characterized by comparing their ^{1}H NMR spectra to the previously reported data. In all cases, the comparisons were very favorable. Previously known compounds for which spectral data were not published (Table 2.6 entries 8,9,10 and 19) were characterized by proton analysis as reported herein.

References for known compounds

www.sigma-aldrich.com (^{1}HNMR spectra available online)

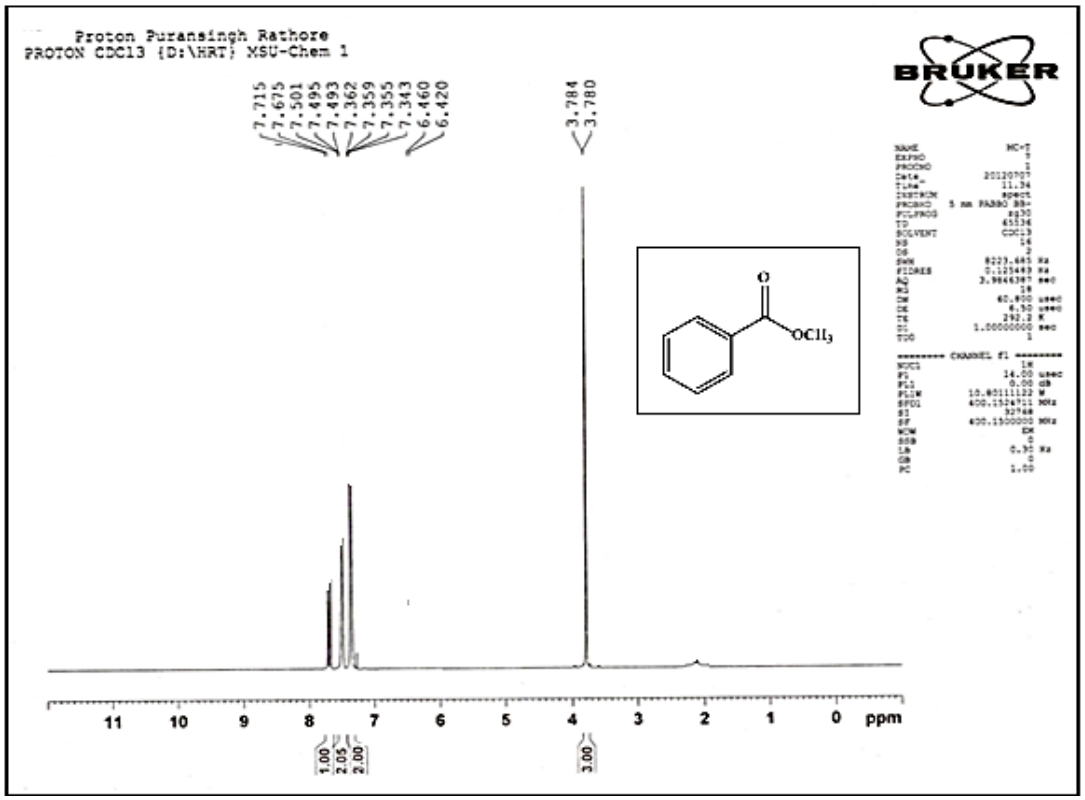

Figure S1 Proton NMR (400 MHz, $CDCl_3$) spectrum of methyl benzoate (Table 2.6, entry 1)

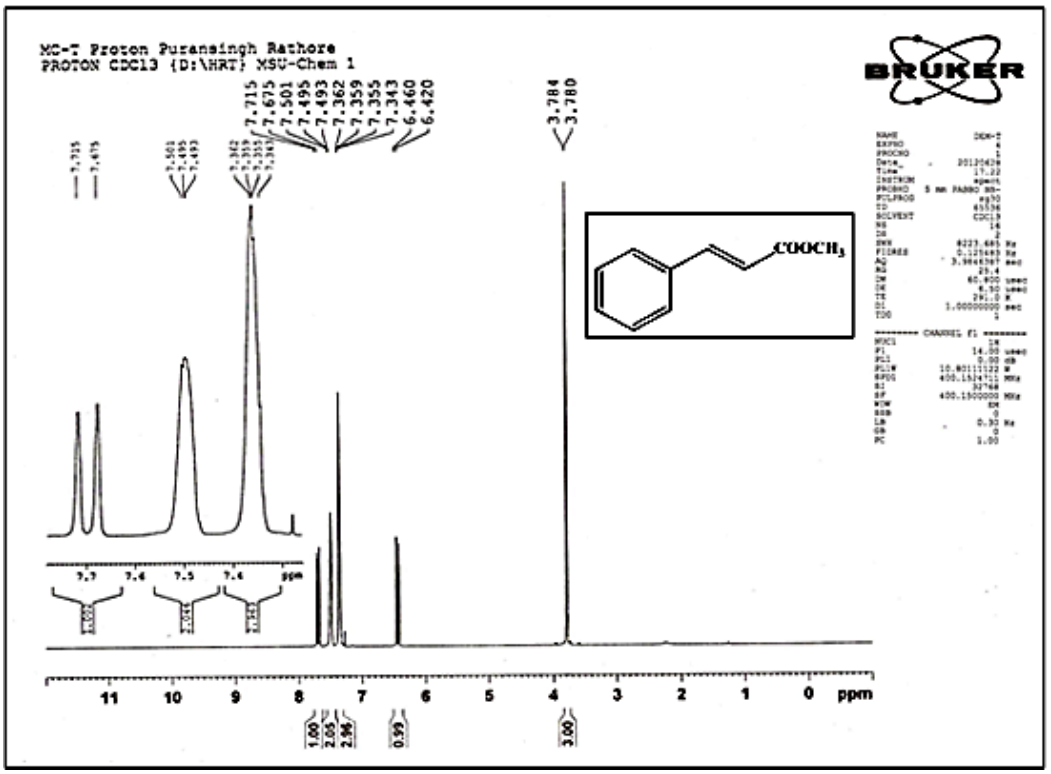

Figure S2 Proton NMR (400 MHz, $CDCl_3$) spectrum of methyl cinnamate (Table 2.6, entry 2)

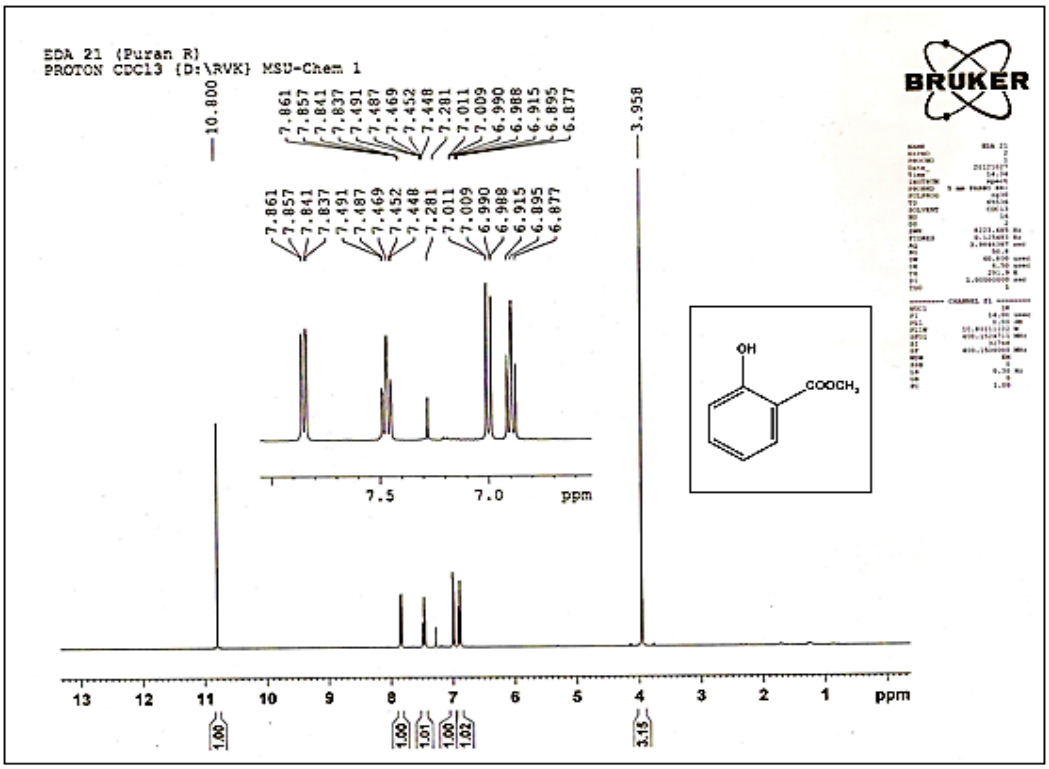

Figure S3 Proton NMR (300 MHz, $CDCl_3$) spectrum of methyl 2-hydroxybenzoate (Table 2.6, entry 3)

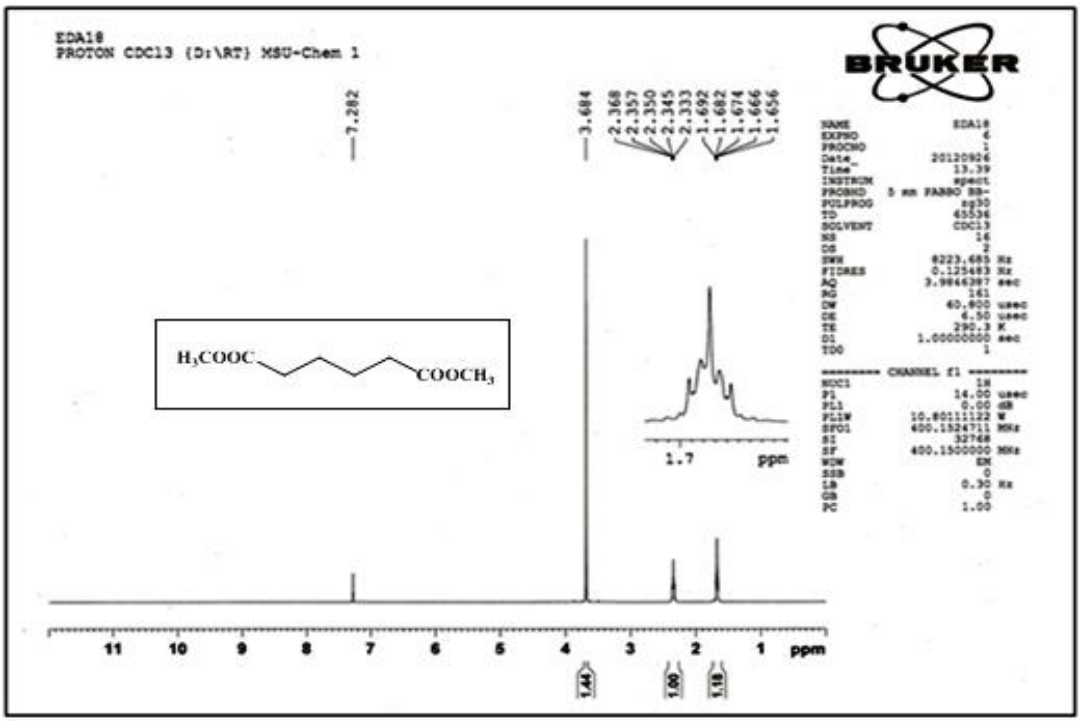

Figure S4 Proton NMR (400 MHz, $CDCl_3$) spectrum of dimethyl adipate (Table 2.6, entry 4)

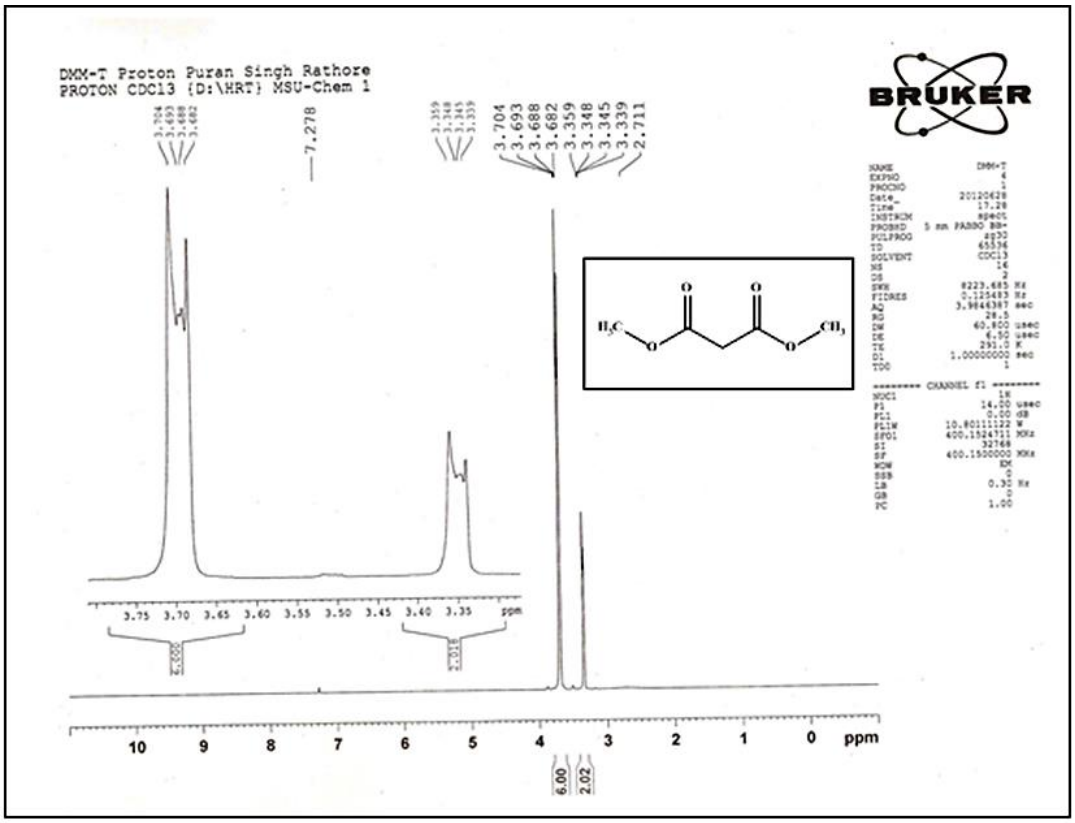

Figure S5 Proton NMR (400 MHz, $CDCl_3$) spectrum of dimethyl malonate (Table 2.6, entry 5)

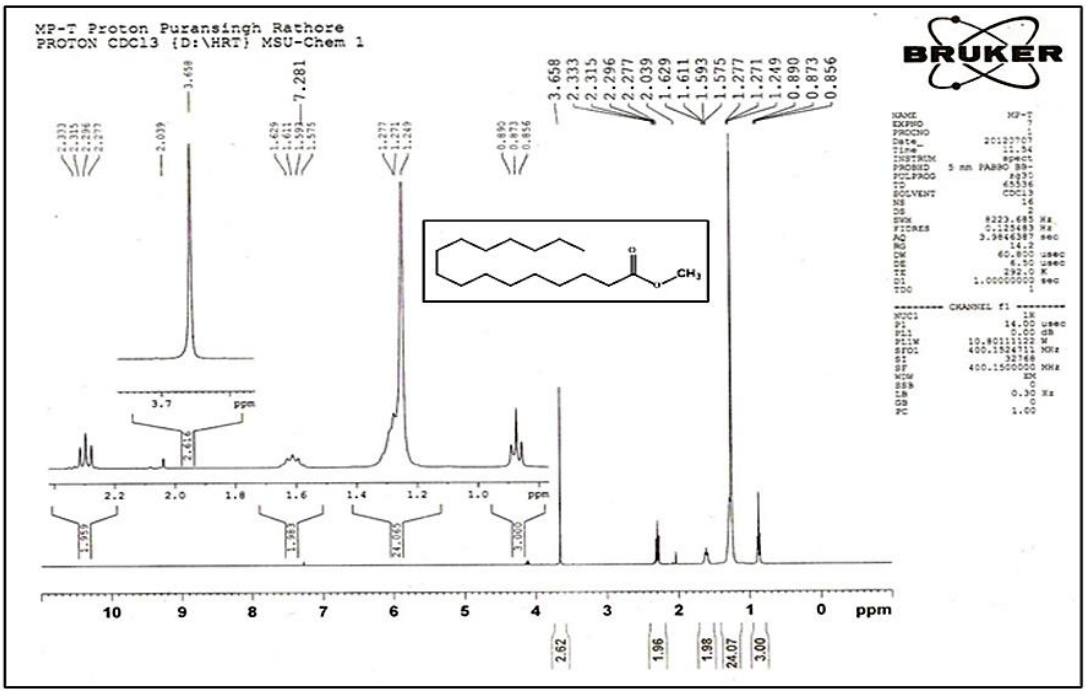

Figure S6 Proton NMR (400 MHz, $CDCl_3$) spectrum of methyl palmitate (Table 2.6, entry 6)

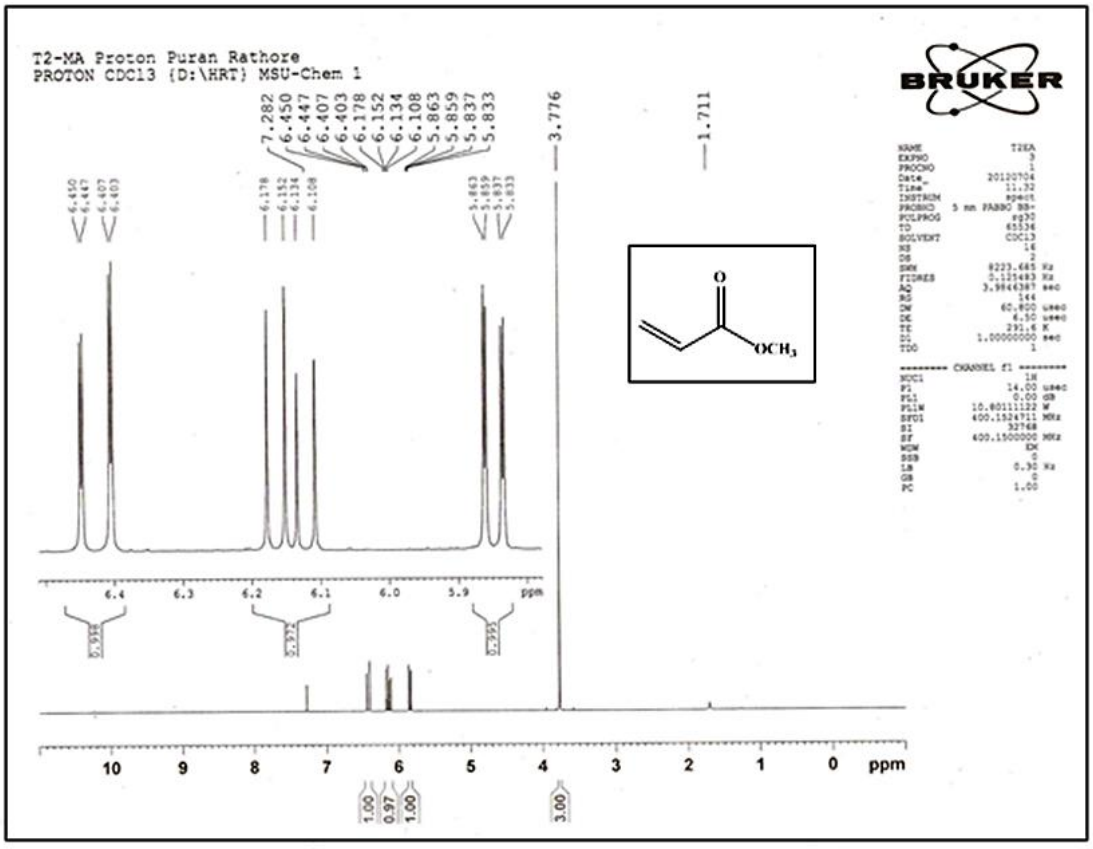

Figure S7 Proton NMR (400 MHz, $CDCl_3$) spectrum of methyl acrylate (Table 2.6, entry 7)

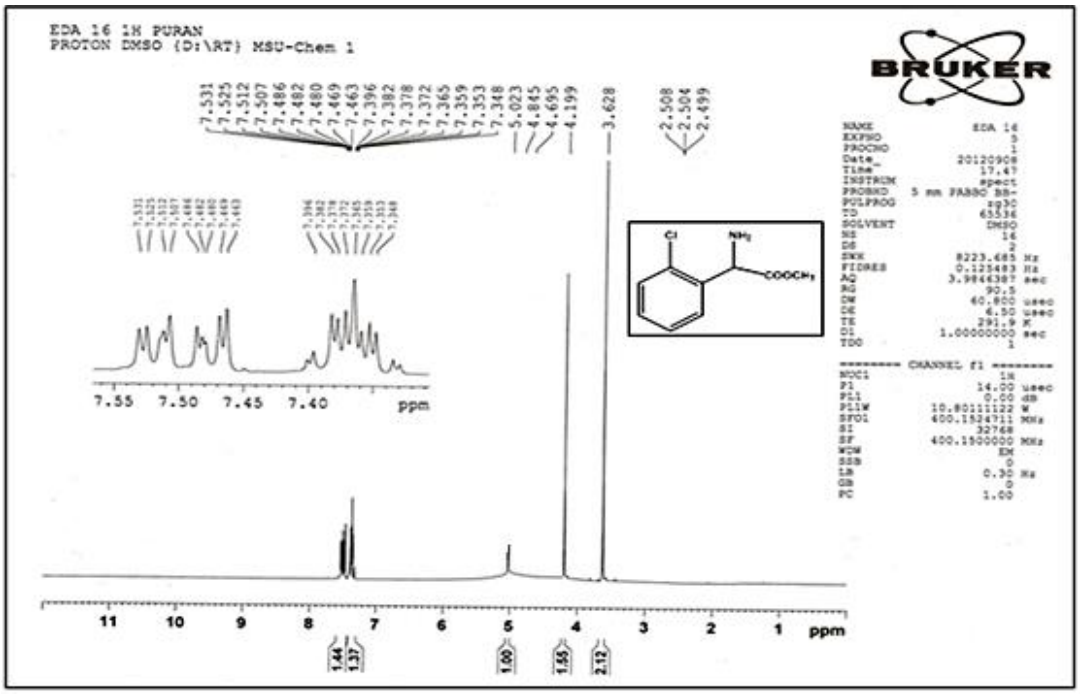

Figure S8 Proton NMR (400 MHz, DMSO) spectrum of methyl 2-amino-2-(2-chlorophenyl) acetate (Table 2.6, entry 8)

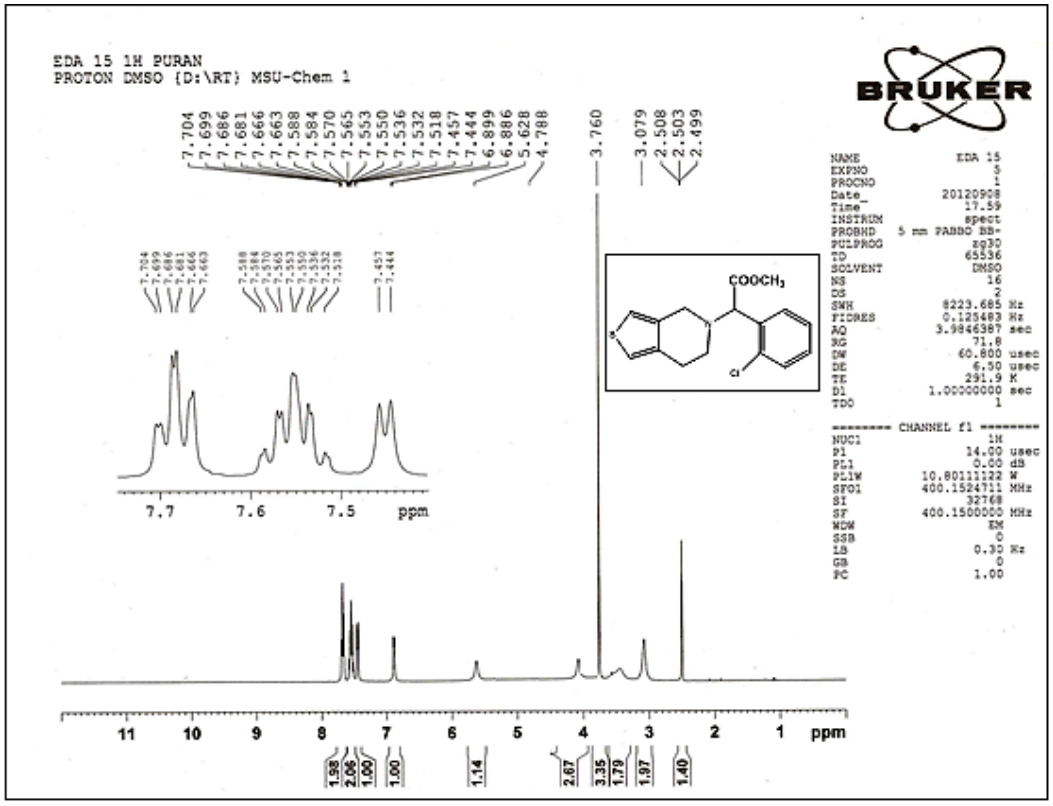

Figure S9 Proton NMR (400 MHz, DMSO) spectrum of methyl 2-(2-chlorophenyl)-2-(6,7-dihydrothieno[3,4-c]pyridin-5(4H)-yl) acetate (Table 2.6, entry 9)

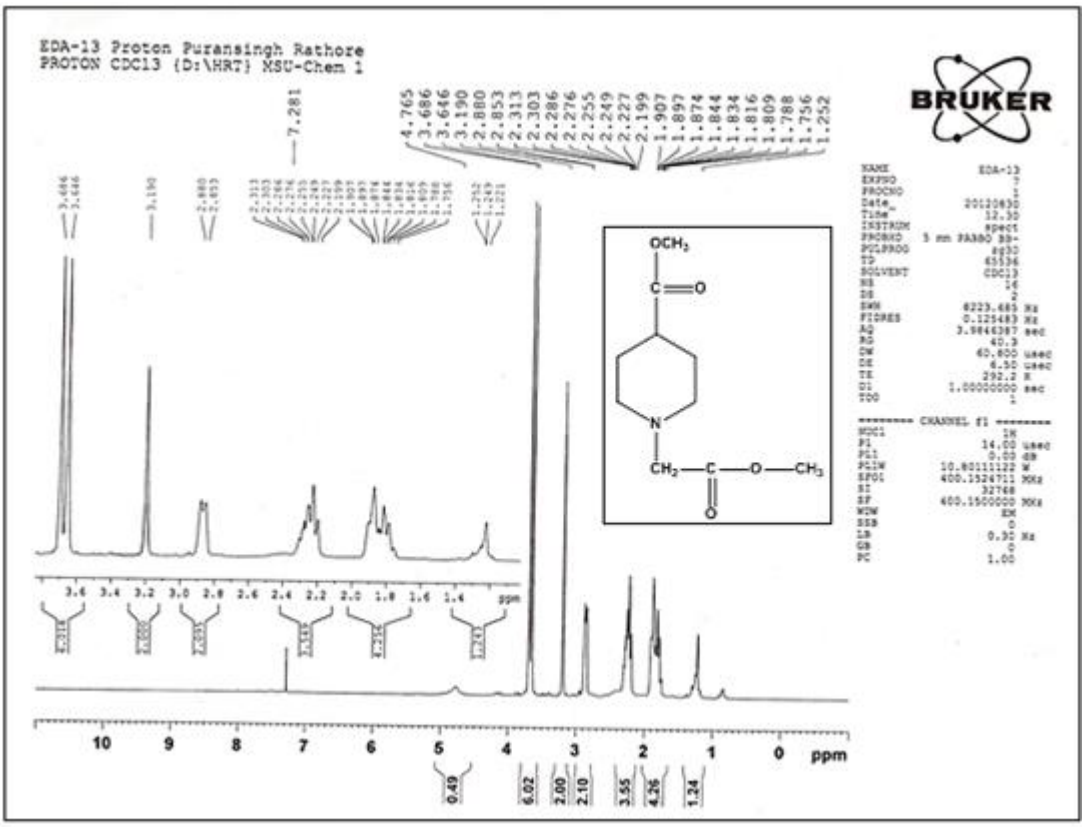

Figure S10 Proton NMR (400 MHz,$CDCl_3$) spectrum of methyl 1-(2-methoxy-2-oxoethyl) piperidine-4-carboxylate (Table 2.6, entry 10)

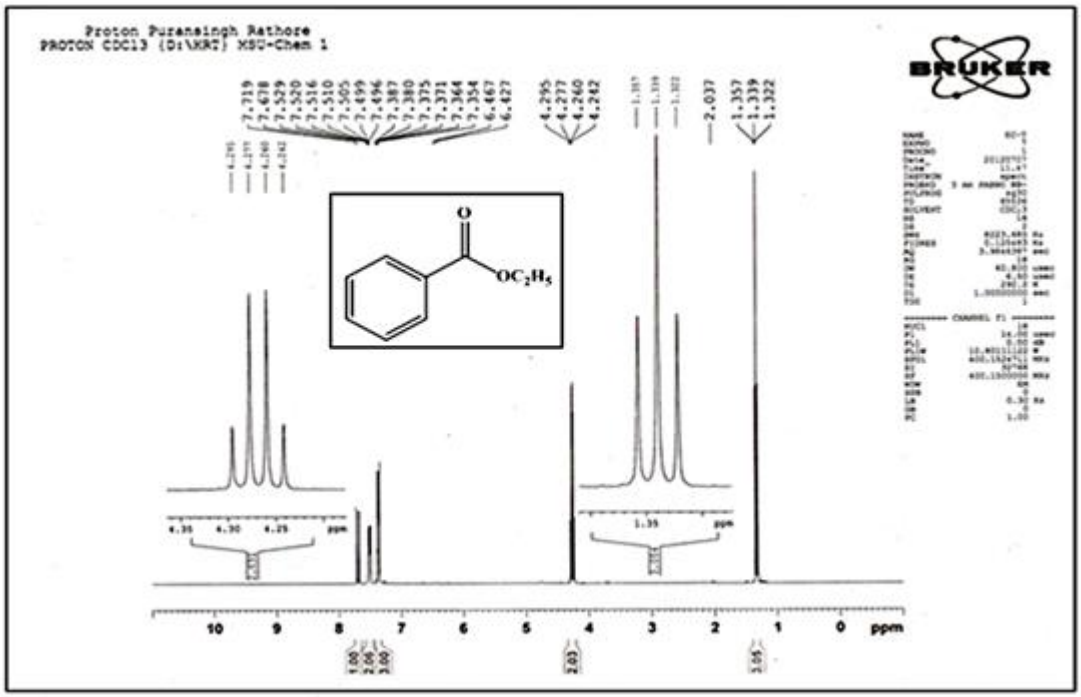

Figure S11 Proton NMR (400 MHz,$CDCl_3$) spectrum of ethyl benzoate (Table 2.6, entry 12)

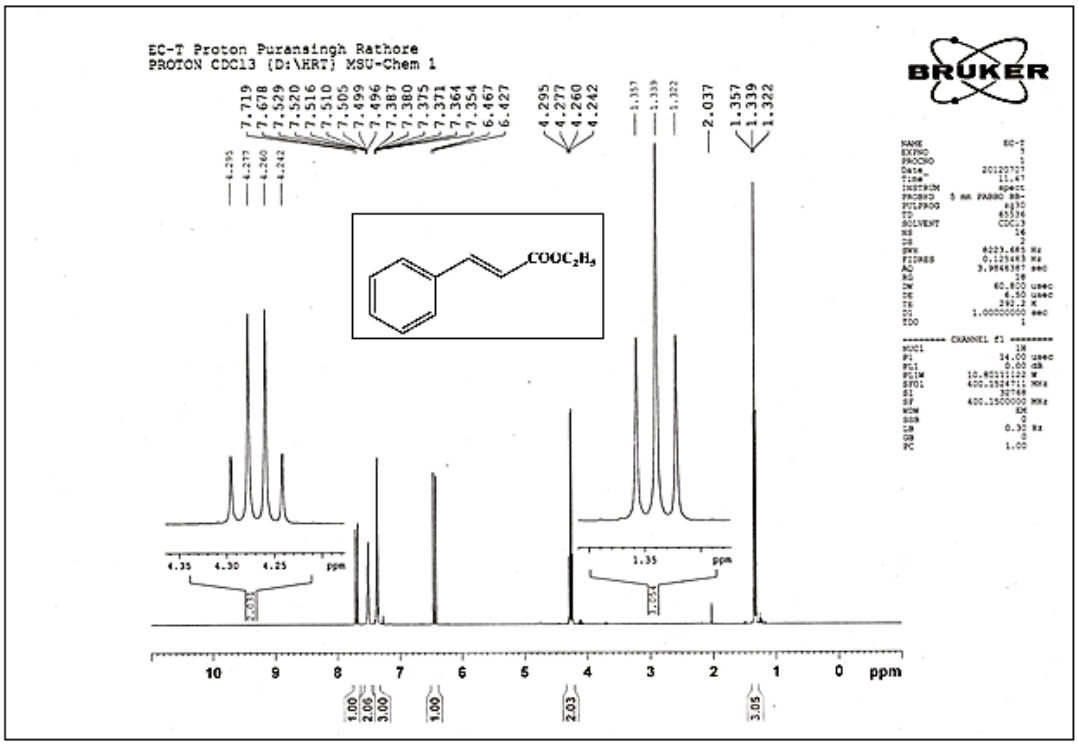

Figure S12 Proton NMR (400 MHz,$CDCl_3$) spectrum of ethyl cinnamate (Table 2.6, entry 13)

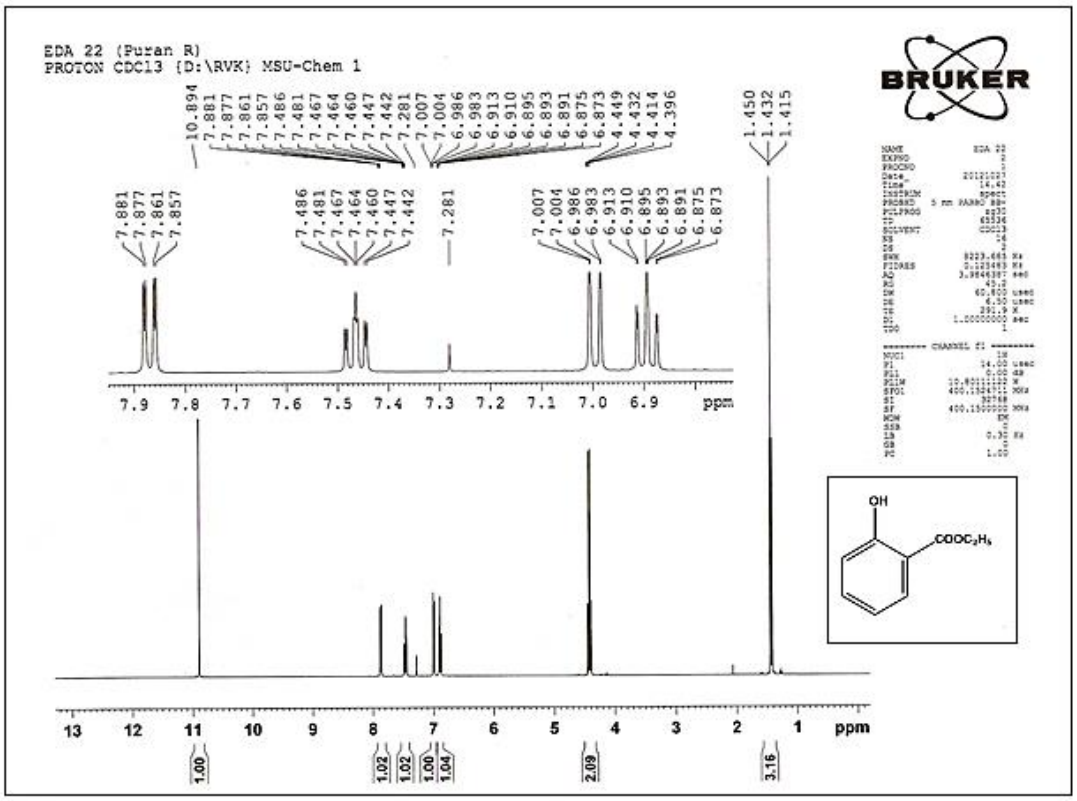

Figure S13 Proton NMR (400 MHz,$CDCl_3$) spectrum of ethyl 2-hydroxybenzoate (Table 2.6, entry 14)

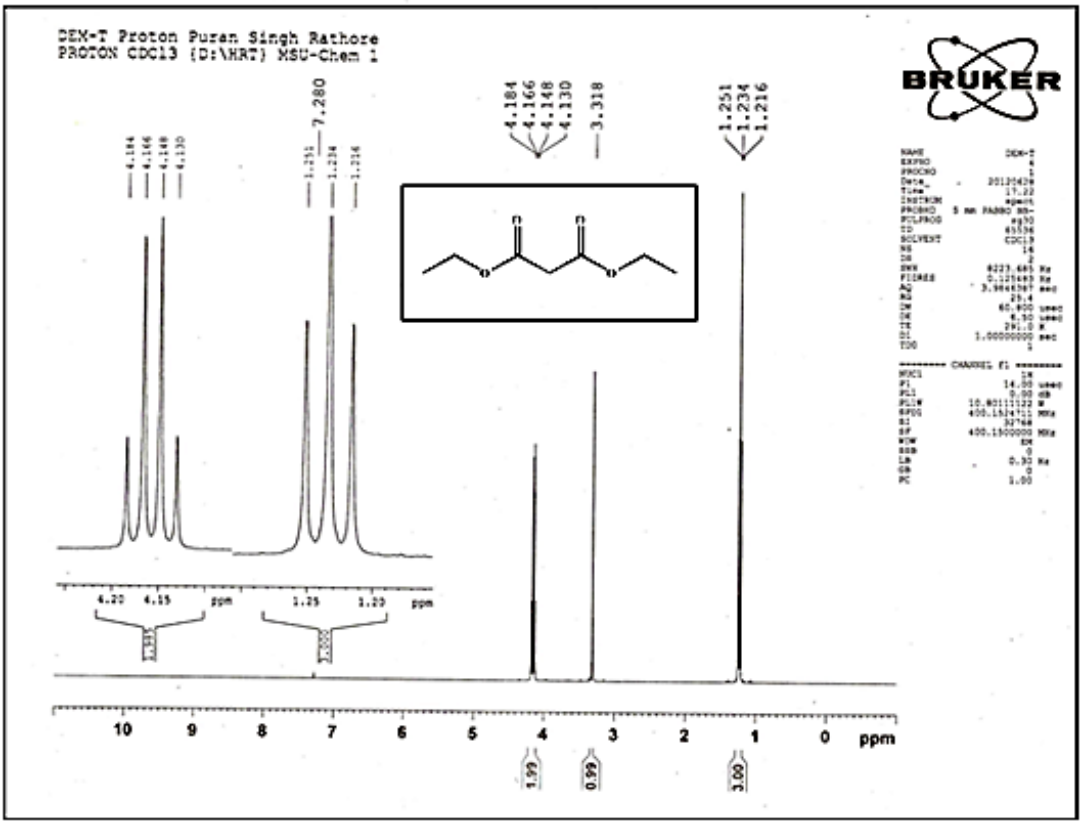

Figure S14 Proton NMR (400 MHz,$CDCl_3$) spectrum of diethyl malonate (Table 2.6, entry 15)

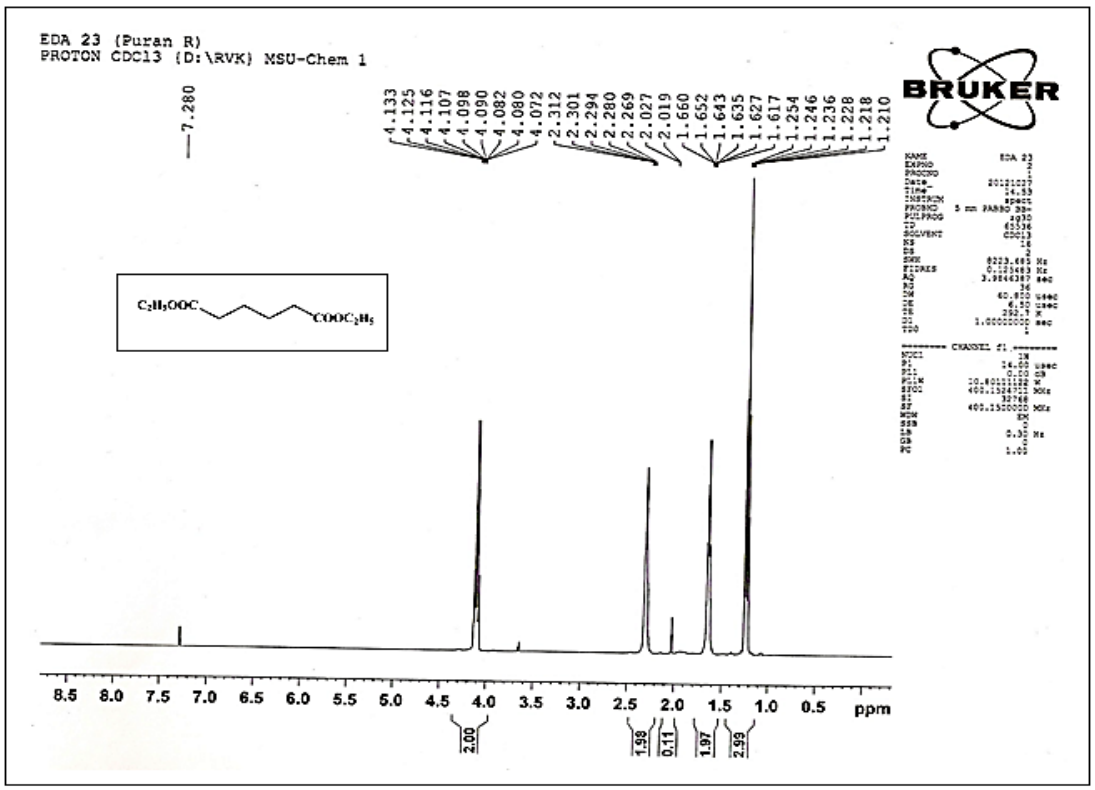

Figure S15 Proton NMR (400 MHz,$CDCl_3$) spectrum of diethyl adipate (Table 2.6, entry 16)

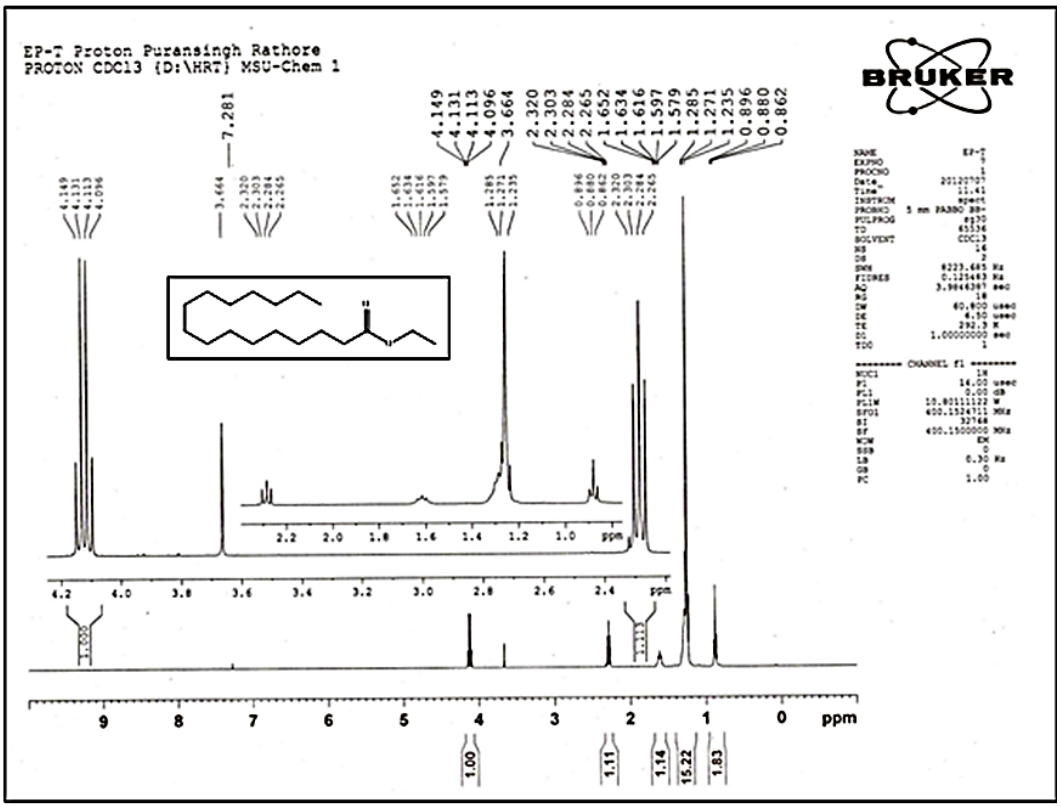

Figure S16 Proton NMR (400 MHz,$CDCl_3$) spectrum of ethyl palmitate (Table 2.6, entry 17)

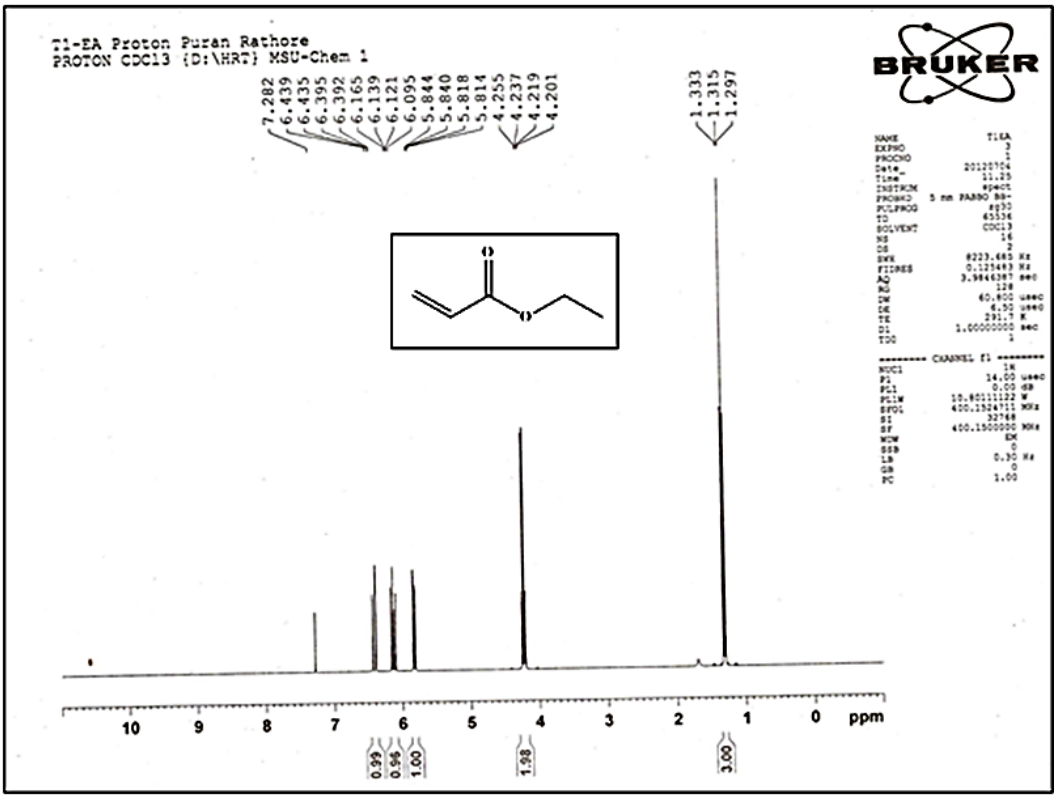

Figure S17 Proton NMR (400 MHz,$CDCl_3$) spectrum of ethyl acrylate (Table 2.6, entry 18)

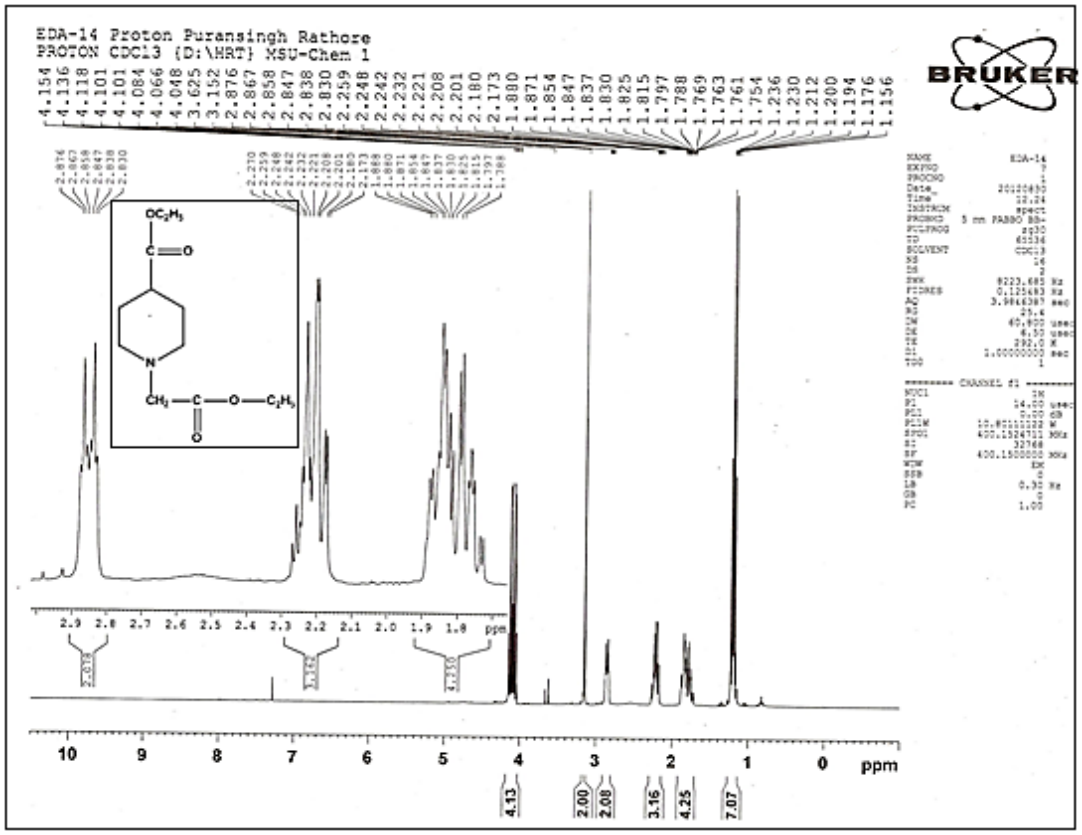

Figure S18 Proton NMR (400 MHz, $CDCl_3$) spectrum of ethyl 1-(2-ethoxy-2-oxoethyl) piperidine-4-carboxylate (Table 2.6, entry 19)

Chapter–2

Part–2

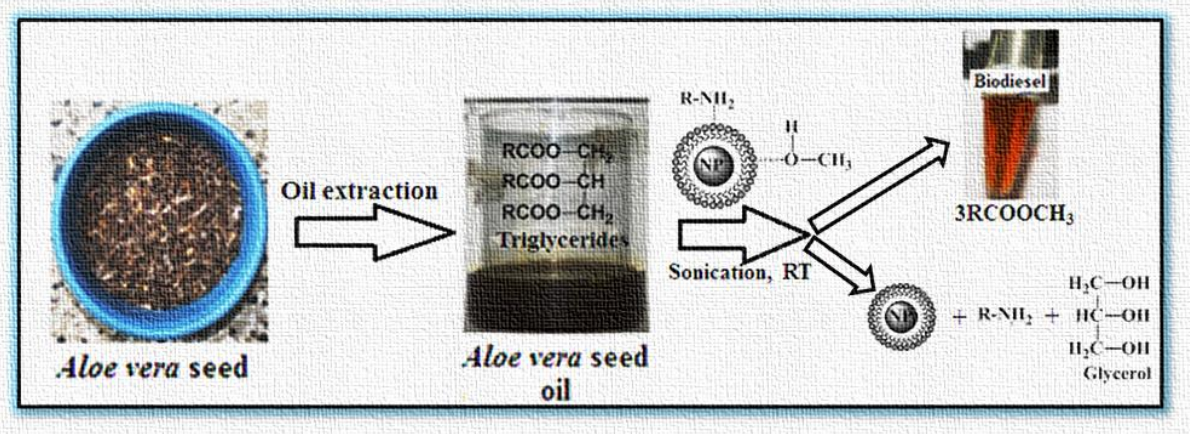

Catalytic application of Nickel Nanoparticles in transesterification of *Aloe vera* seed oil and other oils

Published in Energy & Fuels, 2013, 27, 2776

2.2.1 Introduction

Biodiesel prepared by transesterification of vegetable oil with methanol, is alternative fuel that can be used directly in any existing unmodified diesel engine. Because of properties similar to diesel fuel, biodiesel can be blended at any ratio with diesel fuel. Among the various vegetable oil sources, non-edible oils are suitable for biodiesel production as edible oils are already in demand and too much expensive than diesel fuel. Among the non-edible oil sources, *Jatropha curcas*[1] and *Derris indica* are some of the species identified as potential biodiesel source suitable for tropical and subtropical regions of the world.[2] However, a species already having a high potential market can give an extra edge to its selection. *Aloe vera* is one such species which has been exploited for medicinal, neutraceutical and cosmetic purposes. Today, mostly the *Aloe* gel from the center of the leaves is processed. It primarily consists of polysaccharides to which also many medical properties have been attributed. However, the potential of *Aloe vera* seed oil (AVSO) has not yet been worked out from biodiesel prospective. We have investigated the fatty acid composition of a number of oil species in the past.[3a,b] In the present study, the potential of AVSO was investigated for the production of biodiesel.

The use of strong base like KOH and mineral acids leads to wastage of water and large scale effluent generation.[4] Hence extensive research has been carried out for the development of suitable catalyst for biodiesel production. Solid catalysts like ZnAl hydrotalcite,[5] sulfated zirconia,[6] KF/ZnO,[7] hydrous zirconia supported 12-tungstonphosphoric acid,[8] Zinc dodecatungstophosphate ($Zn_{1.2}H_{0.6}PW_{12}O_{40}$; ZnPW) nanotubes[9], and acid catalyst[10] possess some shortcomings including high cost and easy deactivation. Solid organic bases have also been used as catalyst for the production of biodiesel by Schuchardt *et al.*[11] But the recovery process of catalyst was tedious and expensive. Instead it is advantageous to use some low boiling amines which also have shown good catalytic activity and recovery process is simpler.[12,13] However the vigorous conditions reported previously for these catalysts are not commercially and economically feasible. Since our group has been actively engaged in the synthesis and applications of metal nanoparticles,[14a-d] we decided to develop an easy method of nanoparticles assisted organic amine catalysed synthesis of methyl esters.

Currently metal nanoparticles (NPs) are used widely in many reactions[15] with the advantages like higher specific surface, lower mass transfer resistance, easy separation and less fouling. The high efficiency of a NPs system relies mainly on the approach to the metal core and the structure of the surface. Although a number of organic reactions have been catalyzed, the use of NPs in transesterification reaction has not been extensively reported. In an effort to identify catalyst characteristics that would be ideal for biodiesel synthesis, this study compared the catalytic activity of some organic amines in presence of nickel nanoparticles (NiNPs) with conventional catalyst KOH. Initially triacetin was used as the model system to simplify the analysis and to accelerate the screening speed for suitable amine-NPs catalytic system. Consequently the optimized conditions were used for the synthesis of biodiesel from some recognized oils[16a-e,17] and finally applied on AVSO. The products of the new catalyst system were also compared against the conventional KOH catalyzed reactions.

The synthesis of biodiesel from AVSO using nanocatalytic system that works at room temperature (RT) is reported for the first time.

2.2.2 Experimental section

Triacetin, KOH, H_2SO_4, triethylamine (TEA), ethylenediamine (EDA), diethylamine (DEA), methanol, petroleum ether and chloroform etc. were purchased from Merck, Mumbai, India. Tulsion T-45 BD (Ion exchange resin) was purchased from Thermax Limited, Pune, India. All the solutions were prepared using double-distilled and demineralized water.

2.2.2.1 *Aloe Vera* Seeds collection and oil extraction

Aloe Vera seeds were collected from various parts of Gujarat (Saurashtra and Kutch region) during the favorable season between February to March. All the seeds collected were already matured and dried. The seeds were separated from the fruit. Each plant has 15-20 fruits on the spike and each fruit contains on an average 4-8 seeds which are extremely light weight. The oil from the seeds was extracted using petroleum ether as a solvent in soxhlet apparatus.

2.2.2.2 Transesterification reaction

The molar ratio of methanol and triacetin was taken as 20:1. In a typical reaction methanol (10 ml), amines (6 wt % of substrate) and NiNPs (150mg) were sonicated at room temperature (25-30ºC) for 30 minutes in a round bottom flask (RBF) followed by addition of the substrate triacetin (1 g,). All the reactions were carried out at RT initially. In cases where the reaction did not proceed to completion the mixture was gradually heated to reflux (at 70 °C) with an aim to achieve maximum conversion. Reaction monitoring was done by thin-layer chromatography (TLC). After the completion of reaction the NPs were separated by centrifuge. The yield and purity of final products of the triacetin reaction were analyzed by high performance liquid chromatography (HPLC)

The transesterification of AVSO and other oils was carried out in a similar manner. After the maximum conversion of the reaction the NPs were separated from the reaction mixture by centrifuging along with the glycerol phase. The organic amine and unreacted methanol were removed by distillation to get the final product. About 6-7 ml of the methanol could be recovered by distillation at 75– 80 ^{o}C. Isolated NiNPs were washed by water to remove glycerol followed by petroleum ether to remove wax. Finally after an acetone wash they were dried at 60 ºC under vacuum and used for the next reaction.

The transesterification by KOH (3 wt%) was carried out by conventional method and the product was obtained by following usual work up process. After transesterification, the glycerol byproduct was separated from the resulting biodiesel in a separatory funnel. The excess methanol was removed using a rotary evaporator under reduced pressure. The methyl ester was acidified with dil. H_2SO_4 to neutralize the excess residual KOH and extracted with chloroform. This was followed by water washings with warm distilled water (50 °C) in a separatory funnel, until the pH of the aqueous phase was around 7. The chloroform was removed by evaporation and product dried over anhydrous Na_2SO_4. Further, purification of methyl esters was done by passing through an ion-exchange resin (Tulsion T-45 BD) column (1.5x20 cm^2) that retained the impurities such as residual water, ions and glycerol. The product thus purified was compared with standards using Gas chromatography (GC). Calibration of GC was done by using methyl linoleate, methyl palmitate, methyl stearate, methyl

oleate, 1-oleoyl-rac-glycerol, di-oleoyl-glycerol and tri-olein purchased from Sigma. n-Pentadecane was used as the internal standard. The area of GC peaks for individual fatty acid methyl esters obtained from KOH process were calculated and their cumulative content was assumed to be the maximum yield (100%) corresponding to maximum conversion of AVSO. The methyl esters yield in NP catalysed experiments was expressed in terms of the percentage of methyl esters produced (as analyzed by GC) as per the calibration method reported by Zieba et al[18] for methanolysis of castor oil. Mixtures were prepared with known amounts of AVSO methyl ester (obtained from KOH process), AVSO and methanol in proportions corresponding to various conversions of triglycerides, from 5 to 100%. From the GC peak areas obtained corresponding to various conversions, calibration plot was obtained. This plot was used for calculation of yield of methyl esters obtained using EDA-NiNPs system as catalyst and expressed in terms of the percentage of methyl esters produced.

2.2.2.3 Characterizations methods

AVSO composition was determined by Gas Chromatography-Liquid Chromatography (GC-LC), Two samples were taken for the analysis of the fatty acid composition. The methyl esters of extracted oil were prepared in accordance with the Bureau of Indian Standards (BIS, 548, part III).[19] ANUCON-GLC chromatograph with a flame ionization detector (FID) was employed for the analysis using nitrogen as the carrier gas. The column used was 30 M 9 0.53 mm I.D. 5.0 lm DB-1 Type MXT-1 capillary column. The column oven temperature was programmed from 80 to 280 °C (at the rate of 10 °C min^{-1}) with injector and detector temperatures at 250 and 280 °C, respectively. The total run time was 40 min. Identification of each component was made by comparing its retention time with that of a Sigma-Aldrich standard fatty acids mixture. FFA content was determined by a standard titrimetry method.[20]

Transesterification reactions were monitored by TLC (silica gel 60 F_{254}, Merck, Mumbai, India). The solvent system consisted of hexane/ethyl acetate (1:1 vv^{-1}) for triacetin, hexane/ethyl acetate/acetic acid (95:5:1 vv^{-1}) for AVSO reaction and (90:10:1 vv^{-1}) for other oils.[17] The spots were detected in iodine chamber. The products of triacetin reaction (methyl acetate and intermediates) were analyzed by HPLC (Agilent 2000) with a C18 XDB column and diode array detector. The mobile

phase was methanol–water (50:50) and was tested at 205 nm with a flow rate of 1.0 mL/min and a column temperature of 35 °C.

Other oils like Jatropha (*Jatropha curcas),* Jyotishmati *(Celastrus paniculatus),* Bacuachi (*P*soralea coryfolia), Saragava (*M*oringa oleifera), Mahuva (*Madhuca indica*) and Salvadora (*Salvadora oleifera)* were obtained from a local store.

The methyl esters obtained from transesterification of oils were confirmed by gas chromatography on Perkin Elmer clarus 500 GC with the flame-ionization detector. The capillary column (70% phenyl polysilphenylenesiloxane) used had a length of 30 m with an internal diameter of 0.25 mm. Nitrogen was used as the carrier gas at a constant flow rate. The column oven temperature was programmed from 150 to 250 °C (at the rate of 10 °C min^{-1}) with injector and detector temperatures at 240 and 250 °C, respectively. Finally, the product methyl esters were also analyzed by FTIR (Perkin Elmer RX1 model) and ^{1}H NMR (BRUKER 400 MHz). The Kinematic viscosity measurements were carried out using Scott Gerate AVS 350b capillary viscometer.[21] The viscosity obtained in centipoise was converted to centistokes. The density and specific gravity were measured by means of Pycnometer.

2.2.3 Results and Discussion

2.2.3.1 Properties, composition of AVSO

The percentage of seed oil in *Aloe vera* varied between 20-22 wt%. The fatty acids compositions are described in **Table 2.8**. The unsaturated fatty acids were approximately 85.59% (linoleic up to 69.63% and oleic acid 15.96%). The saturated fatty acid accounted for approximately 14% of the total contents. The dominant saturated acid being Palmitic acid (10.6%). The oil properties are quite similar to that of Sunflower oil.[22] The oil property of AVSO has been depicted in **Table 2.9**. The presence of higher oil with linoleic (73.73%) and oleic acid accounting for 90% unsaturated fatty acid content gives the AVSO the unique property of low melting point and low viscosity. Thus methyl esters formed by the oil will also have low melting point between -19.8 to -35.0 °C.[23]

Table 2.8 Fatty acid composition of AVSO

Fatty acid	wt. %
Palmitic(16:0)	10.6%
Stearic(18:0)	2.44%
Oleic(18:1)	15.96%
Eicosadienoic(20:2)	1.37%
Linoleic(18:2)	69.63%

Table 2.9 Properties of AVSO

Saponification Value	187.2(mg/gm)
Iodine Value	118.4(gm/100gm)
Unsaponifiable Matter (USM)	2.65%
Acid value	39.92 mg KOH /g
Kinematic viscosity(mm2/s)	27.8 Cst (40^0C)
Free fatty acid (FFA)	21.50%

2.2.3.2 Transesterification of triacetin

Transesterification of triacetin was carried out first with KOH at RT. TLC monitoring of the reaction showed stepwise transesterification of each ester group of triacetin, indicating the formation of diacetin followed by monoacetin. At the end of the reaction (after 3h.) all the spots on TLC disappeared due to complete conversion of triacetin into the product methyl acetate and byproduct glycerol which did not appear on TLC. The complete conversion of triacetin to methyl acetate was confirmed by HPLC against standard samples (data not shown).

In order to assess the efficiency of amines as base catalyst instead of KOH the reaction was carried out using each of the three amines without any support. Similar results were observed for all the three amines but the reaction times were much longer (**Table 2.10**). In case of EDA and DEA the reaction took 8h and 10h respectively at RT. While in case of TEA, complete conversion could be obtained only after refluxing for 8h. The order of the catalytic activity EDA>DEA>TEA is due to the

decrease in basicity from primary to tertiary amine and increase in steric hindrance. Similar results were reported by Wang *et al*,[12] for the transesterification of crude rapeseed oil in supercritical methanol (>300°C temperature).

In order to enhance the rate of transesterification at RT, NiNPs were used along with the amines. Significant enhancement in reaction was observed in case of DEA and EDA catalyzed reaction which are complete within 6h and 3h respectively (**Table 2.10**, entries-7 & 10). On the other hand, TEA and KOH catalyzed reactions were less affected by NiNPs. For establishment of optimum conditions a preliminary study was carried out using EDA as the catalyst. After several experiments with different concentrations of EDA, methanol and various quantities of NiNPs, the optimum conditions for transesterification were established.

Table 2.10 Transesterification of triacetin

S.No.	Amines	NPs	Reaction Temperature °C	Reaction time in hrs.	Yield (±2%)
1	KOH	-	RT	3	97
2	-	-	reflux	48	none
3	-	Ni	,,	,,	,,
4	TEA	-	,,	8	93
5	,,	Ni	,,	7.30	,,
6	DEA	-	RT	10	94
7	,,	Ni	,,	6	95
8	,,	,,	reflux	4	,,
9	EDA	-	RT	8	97
10	,,	Ni	,,	3	,,
11	,,	,,	reflux	1	,,
12	,,	Cu[a]	RT	3	,,

(a) Ref.14d

The precise mechanism of this transesterification process is not very clear to us. The reactions in absence of NPs were observed to be quite slow. To understand the role of metal, the reaction under optimized conditions was also carried out with starch capped

copper nanoparticles (CuNPs)[14d] instead of NiNPs to yield similar results (**Table 2.10**, entry-12). The higher efficiency of metal NPs under mild conditions seems due to their higher dispersion in solvent so that the reactant reaches the catalytic site by diffusion. Possibly, the role of metal NPs is to provide surface binding sites for the reactant (methanol) and milder catalyst (amine) during sonication. This facilitates the generation of nucleophile, the methoxide ion, with the help of a weak base,[24] like EDA which then attacks triacetin as shown in **Scheme 2.5**. Further, it is possible that hydrogen-bonding between hydroxyl groups of capping agent starch and methanol also assists the generation of methoxide ion on the surface of NiNPs.[25] The FT-IR spectrum (**Figure 2.7a and b**) of the recovered NiNPs provided the evidence for surface-functionalization of NiNPs with EDA. The FT-IR spectrum of the NiNPs recovered after the first cycle of transesterification showed peaks at 3354 cm^{-1} and 1611 cm^{-1} which can be assigned to the N-H stretching and bending respectively. The peaks at 2979 and 2883 cm^{-1} are assigned to the C-H stretching vibrations and the one at 1482 cm^{-1} is due to C-H bending of alkanes. Thus the metal core, capping agent and amine do not act independently but concomitantly to make the amine-NiNPs system an effective catalyst.

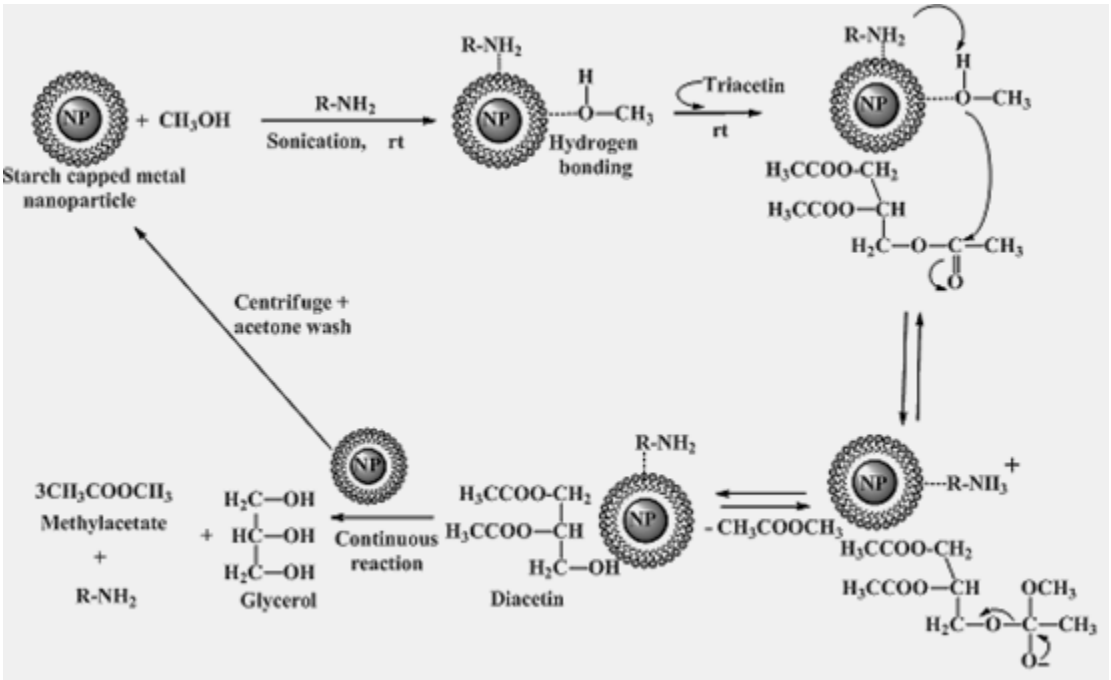

Scheme 2.5 A proposed reaction mechanism for NiNPs supported organic amine catalyzed transesterification systems

EDA gives highest catalytic activity because of greater basicity, followed by DEA. TEA was probably was too weak to generate nucleophile while KOH was strong enough for generation of nucleophile in absence of NiNPs. At reflux temperature of the methanol, good to high conversion were obtained in case of DEA and EDA and the reaction was complete within 4h and 1h respectively (**Table 2.10**, entries 8 & 11). This shows that as the reaction temperature increases, reaction time decreases.

Sequence of addition of reactants was also observed to be important. If substrate triacetin is added before amine, the reaction slows down probably due to preferential adsorption of triacetin which blocks the active site of NiNPs. Hence it is advantageous that amine and methanol come in contact with NiNPs before triacetin. A similar observation has been reported by Liu *et al*.[26] for hydrotalcite based catalyst.

The above results clearly indicated that organic amines could effectively catalyze transesterification of triacetin with methanol. Among the three amines, EDA shows the best catalytic activity at RT which was further enhanced in the presence NiNPs. Encouraged by these results, we decided to explore the potential of this catalytic system (EDA-NiNPs) for transesterification of some recognized seed oils to obtain biodiesel.

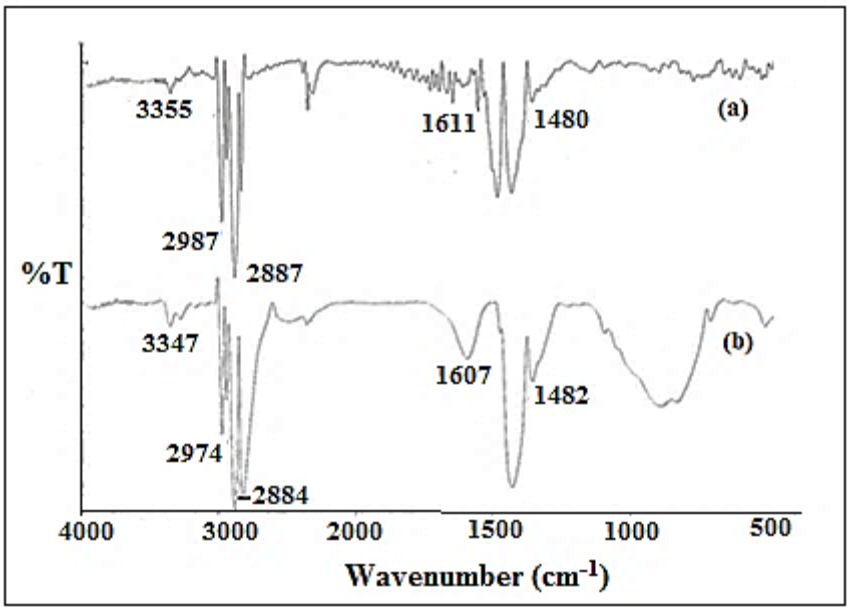

Figure 2.7 FT-IR spectra of (a) NiNPs recovered after 1st run showing traces of bound EDA (b) EDA alone

2.2.3.3 Transesterification of seed oils

The results indicate in **Table 2.11**, that the transesterification proceeds to completion in 3-4h except for Saragava (*M*oringa oleifera) oil where the KOH process itself took 12h to maximum even under reflux conditions. The products obtained from both the processes are identical and the yields were comparable as can be seen from the chromatographic and spectroscopic evidences.

Next the catalytic system was applied to transesterification of AVSO (**Table 2.12**). It is evident that EDA-NiNPs system works efficiently for this reaction at RT as well as under reflux condition and the results are comparable with KOH process (**Table 2.12**). Interestingly, DEA and TEA catalyzed reactions get initiated, but do not proceed to completion even after 8h of reflux in presence of NiNPs. These results suggest the importance of basicity of the amine catalyst and also signify the role of NPs. The importance of addition sequence of raw materials was similar to triacetin reaction. The products obtained from both the process are identical as can be seen from the chromatographic and spectroscopic evidences: GC, TLC (supporting information), IR (**Figure 2.8**), and ^{1}HNMR (**Figure 2.9**).

Table 2.11 Transesterification of some recognized oils with EDA-NiNPs system at RT

Name of oil	Time (h)	Conversion (%)
Mahuva (*Bassa latifolia*)	4	96
Jyotishmati *(Celastrus paniculatus)*	4	95
Jatropha *(jatropha curcas)*	3	96.2
Bacuchi (*Psoralea coryfolia*)	4	92
Saragava (*Moringa oleifera*)	20*	84
Salvadora (*Salvadora oleifera)*	4	90

*Transesterification of this oil by KOH method took 12 h. of reflux for maximum conversion

Table 2.12 Transesterification of AVSO

Entry	Amines	NPs	Reaction Temperature (°C)	Reaction time(h)	Yield (%±1)
1	KOH	-	reflux	1.0	95.0
2	,,	-	RT	3.0	,,
3	TEA/EDA/DEA	-	reflux	8.0	03.3
4	TEA	Ni	,,	,,	04.6
5	DEA	,,	,,	,,	15.5
6	EDA	,,	,,	1.25	94.0
7	,,	,,	RT	4.0	95.0

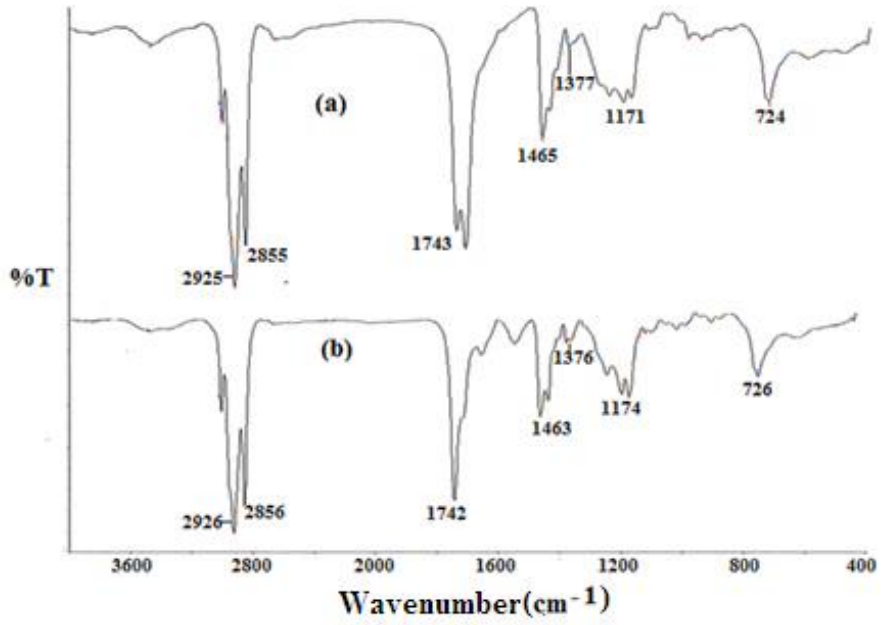

Figure 2.8 The FT-IR spectra of Methyl esters of AVSO catalysed by (a) KOH and (b) EDA-NiNPs

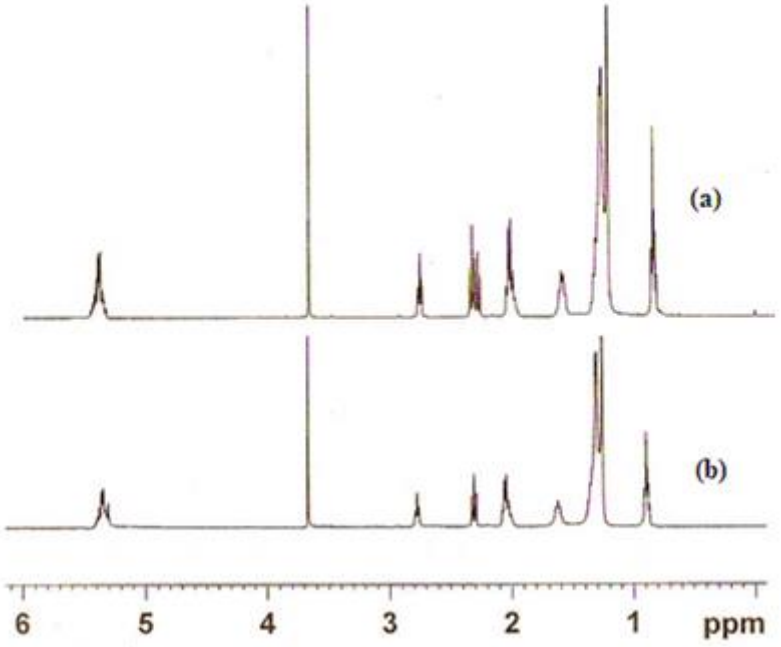

Figure 2.9 ^{1}H NMR spectra of methyl ester of AVSO catalysed (a) by KOH and (b) EDA-NiNPs

Use of organic amines does not produce soap and emulsion and thus can avoid washing procedures. However, in absence of NPs, the reaction time, temperature, pressure and methanol to oil molar ratio were relatively high in the organic amine-catalysed systems.[27,12,13] Since the reactions herein are carried out under ambient conditions, the organic amines can also be easily recovered by distillation,[28,13] while the NPs can also be recycled. The catalytic activity of the present system is comparable to that of KOH (**Table 2.10**, entry-1).

2.2.3.4 Recycling of NiNPs

One of the advantages of using NPs as catalyst is that they can be easily recovered by centrifugation and recycled. It was observed that the catalyst could be reused directly without further purification for five consecutive runs. However the reaction time increased in each successive recycling experiment (**Table 2.13**) reaching from 3h to 4h in the case of triacetin and 4h to 5h in AVSO finally. This may be because the catalytic activity of NiNPs decreases with the number of runs which may be due to various reasons. The possibility of surface oxidation of the NPs is less as evident from the XRD analysis of NiNPs after 5th run (**Figure 2.10**) which does not show any peak due to NiO at 37 deg. This can be attributed to the presence of starch coating which

makes the NPs stable to water and air and maintains their metallic state.[29,30] Another reason could be the surface modification due to deposition of matter during reaction.[31] A decrease in activity for similar reasons has been observed for NiNPs by Alonso *et al*[32] Nevertheless, the reaction does proceed to completion at the same temperature at the end of five cycles giving the same yield.

Table 2.13 Recycling experiments with NiNPs at RT

Triacetin			AVSO		
Run	Time (h)	Yield (%±2)	Run	Time (h)	Yield (%±1)
1	3.0	97	1	4.0	95
2	,,	,,	2	,,	,,
3	3.15	,,	3	4.30	93
4	3.30	,,	4	4.45	94
5	4.0	,,	5	5.0	93

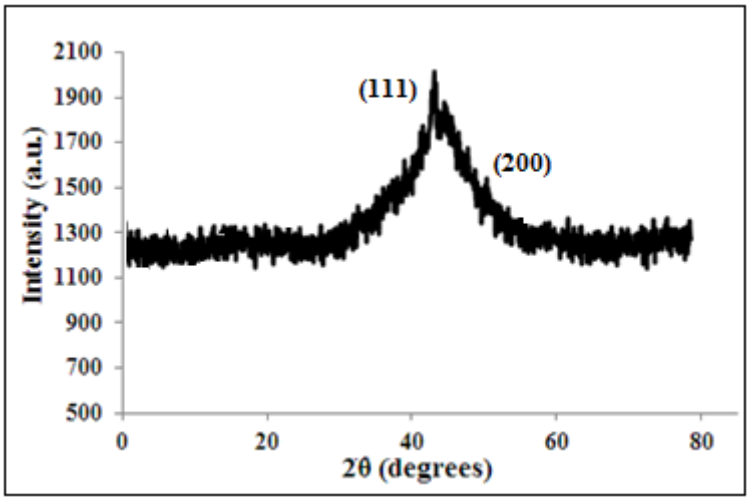

Figure 2.10 XRD pattern of NiNPs recovered after 5th run

2.2.3.5 Characterization of methyl esters of AVSO

The formation of methyl esters from AVSO by both processes was identical as confirmed by GC, TLC, FT- IR spectra (**Figure 2.8**) and ^{1}H NMR (**Figure 2.9**). FT-IR revealed a strong band at 1377 cm^{-1} corresponding to the methyl group. The

presence of ester group was confirmed by the band at 1742 cm^{-1}. The band at 2925–2926 cm^{-1} is characteristic of C–H stretching. The band at 726 cm^{-1} is due to the presence of more than three consecutive $–CH_2$ groups as in case of methyl esters.

The percentage of free fatty acids (FFA) is another critical variable which affects the acid value in transesterification process.[33] For biodiesel preparation the oil should have acid no. < 1mg of KOH / g. While in our case the acid value was close to 39 mg of KOH/g of oil owing to the high FFA content of 21.50% (**Table 2.8**). However, after transesterification the acid no. of the methyl esters reduced to 0.33 mg of KOH / g. alkali which is close to the ASTM standards. It is likely that esterification of FFA have occurred in case of EDA-NiNPs catalyzed process. On the other hand, for KOH process before transesterification, the FFA had to be esterified by reported process.[16b] This also supports the fact that the catalyst might be effective in esterification reaction. However, a detailed investigation needs to be undertaken in order to establish this observation. The NMR spectra do not show evidence of any acidic protons or protons due to formation of byproducts like amide after transesterification (**Figure 2.8**).

A comparison of the properties of AVSO methyl esters with ASTM standards showed (**Table 2.14**) significant similarity with regard to Kinematic viscosity, Density and specific gravity. The scientific study on its stability and its further understanding with respect to biodiesel specification are still in progress. The cetane value is expected to be high because of the fatty acids like linoleic and oleic acid constituting > 80 % of the total AVSO. Thus AVSO can be viewed as a potential source for biodiesel production.

Table 2.14 Properties of AVSO methyl esters obtained by EDA-NiNPs catalysis

Fuel properties	Biodiesel (ASTM D 975)	AVSO methyl esters
Acid value (mg KOH / g)	0.8	0.33
Kinematic viscosity Cst (40 ^{0}C)	4 -6	4
Density Kg / m^3 (30 ^{0}C)	733	856
Specific gravity (30 ^{0}C)	0.880	0.860
Boiling point	-	135 ^{0}C

2.2.4 Conclusion

A simple ecofriendly approach was adopted to prepare methyl esters by using organic amines instead of conventional inorganic catalysts. Ethylene diamine assisted by starch capped Ni nanoparticles proved to be efficient catalysts for room temperature conversion of some recognised seed oils as well as AVSO to methyl esters. The properties of methyl esters thus obtained from AVSO matched well with the ASTM standards for biodiesel.

2.2.5 References

1. J. Liu, C. Liu, G. Zhou, S. Shen and L. Rong, *Green Chem.*, 2012, **14**, 2499.
2. K. Openshaw, *Biomass and Bioenergy*, 2000, **19**, 1.
3. a) B. H. Patel, S. Thakore and P. S. Nagar, *J. Am. Oil Chem. Soc.*, 2009, **86**, 497; b) B. H. Patel, S.Thakore, P. S. Nagar and M. Daniel, *J. lipid sci. technol*., 2011, **43**, 54.
4. S. K. Naomi, H. Hiroki, K. Homare, T. Takuji, F. Takuya and Y.Toshikuni, *Bioresour. Technol.*, 2007, **98**, 416.
5. A. A. Kiss, A. C. Dimian and G. Rothenberg, *Adv. Synth. Catal.*, 2006, **348**, 75.
6. W. L. Xie and X. M. Huang, *Catal. Lett*, 2006, **107**, 53.
7. M. G. Kulkarni, R. Gopinath, L. C. Meher and A. K. Dalai, *Green Chem*., 2006, **8**, 1056.
8. S. Saka and D. Kusdiana, Fuel, 2001, **80**, 225.
9. J. Li, X. Wang, W. Zhu and F. Cao, *ChemSusChem*, 2009, **2**, 177.
10. W-Y. Lou, Q. Guo, W-J. Chen, M-H. Zong, H. Wu and T. J. Smith, *ChemSusChem*, 2012, **5**, 1533.
11. U. Schuchardt, R. Sercheli and R. M. Vargas, *J. Braz. Chem. Soc.*, 1998, **9**, 199.
12. L. Y. Wang, Z. Y. Tang, W. Xu and J. C. Yang, *Catal. Commun.*, 2007, **8**, 1511.
13. L. Zhang, W. Guo, D. Liu, J. Yao, L. Ji, N. Xu and M. Min, *Energy Fuels*, 2008, **22**, 1353.
14. a) M. Valodkar, A. Bhadoria, J. Pohnerkar, M. Mohan and S. Thakore, *Carbohydr. Res.*, 2010, **345**, 1767; b) M. Valodkar, R. N. Jadeja, M. C. Thounaojam, R. V. Devkar and S. Thakore, *Mater. Chem. Phys*., 2011, **128**, 83; c) M. Valodkar, P. S. Nagar, R. N. Jadeja, M. C. Thounaojam, R. V. Devkar and S. Thakore, *Colloids Surf A*, 2011, **384**, 337; d) M. Valodkar, P. S. Rathore, R. N. Jadeja, M. Thounaojam, R. V. Devkar and S. Thakore, *J. Hazard. Mater.*, 2012, **201– 202**, 244.
15. B. C. Ranu, R. Dey, T. Chatterjee and S. Ahammed, *ChemSusChemi*, 2012, **5**, 22.
16. a) M. M. Azam, A. Waris and N. M. Nahar, *Biomass and Bioenergy*, 2005, **29**, 293; b) S. V. Ghadge and H. Raheman, *Biomass Bioenergy*, 2005, **28**, 601; c)

U. Rashid, F. Anwar, B. R. Moser and G. Knothe, *Bioresour. Technol.*, 2008, **99**, 8175; d) G. Kafuku, M. K. Lamb, J. Kansedob, K. T. Leeb and M. Mbarawa, *Fuel Processing Technology*, 2010, **91**, 1525; e) A. Ejigu, A. Asfaw, N. Asfaw and P. Licence, *Green Chem.*, 2010, **12**, 316.

17. S. Shah, S. Sharma and M. N. Gupta, *Energy Fuels*, 2004, **18**, 154.
18. A. Zieba, L. Matachowski, E. Lalik and A. Drelinkiewicz, *Catal Lett*, 2009**,** **127**,183.
19. BIS:548, part-III, analysis of gas liquid chromate graphy, (Bureau of Indian Standards(*BIS*),new Delhi)1964.
20. American Standards for Testing of Materials (*ASTM*) 2003, D 189–01, D 240–02, D 4052–96, D 445–03, D 482–74, D 5555–95, D 6751–02, D 93–02a, D 95–990, D 97–02.
21. C. Y. Lin and S. A. Lin, *Fuels*, 2007, **86**, 210.
22. C. E. Goering, A. W. Schwab, M. J. Daugherty and E. H. Pryde, *Trans. ASAE* ,1982, **25**, 1472.
23. W. Formo, Physical properties of fats and fatty acids. Bailey's Indiustrial oil and Fats Products, Vol 1, 4th Edtion. John Wiley & Sons, New York 1979, p.193.
24. S. Banerjee, J. Das and S. Santra, *Tetrahedron Lett*., 2009, **50**, 124.
25. Y. Liu, E. Lotero, J. G. Goodwin Jr. and X. Mo, *Appl. Catal. A: Gen*, 2007, **331**, 138.
26. C. O. Dalaigh, S. A. Corr, Y. Gun'ko and S. J. Connon, *Angew. Chem. Int. Ed*., 2007, **46**, 4329.
27. F. Ataya, M. A. Dube and M. Ternan, *Ind. Eng. Chem. Res*., 2006, **45**, 5411.
28. J. Sun, J. X. Ju, L. Ji, L. X. Zhang and N. P. Xu, *Ind. Eng. Chem. Res.*, 2008, **47**, 1398.
29. J. M. Yan, X. B. Zhang, S. Han, H. Shioyama and Q. Xu, *Inorg. Chem*., 2009, **48**, 7389.
30. M. Valodkar, S. Modi, A. Pal and S. Thakore, *Mater. Res. Bull*., 2011, **46**, 384.
31. J. J. Spivey, G. W. Roberts, B. H. Davies (Eds.), 2001, Catalyst Deactivation, Elsevier, Amsterdam.
32. F. Alonso, P. Riente and M. Yus, *Tetrahedron*, 2009, **65**, 10637.
33. F. Ma and M. A. Hanna, *Bioresour. Technol.*, 1999, **70**, 1.

(Spectral Data)

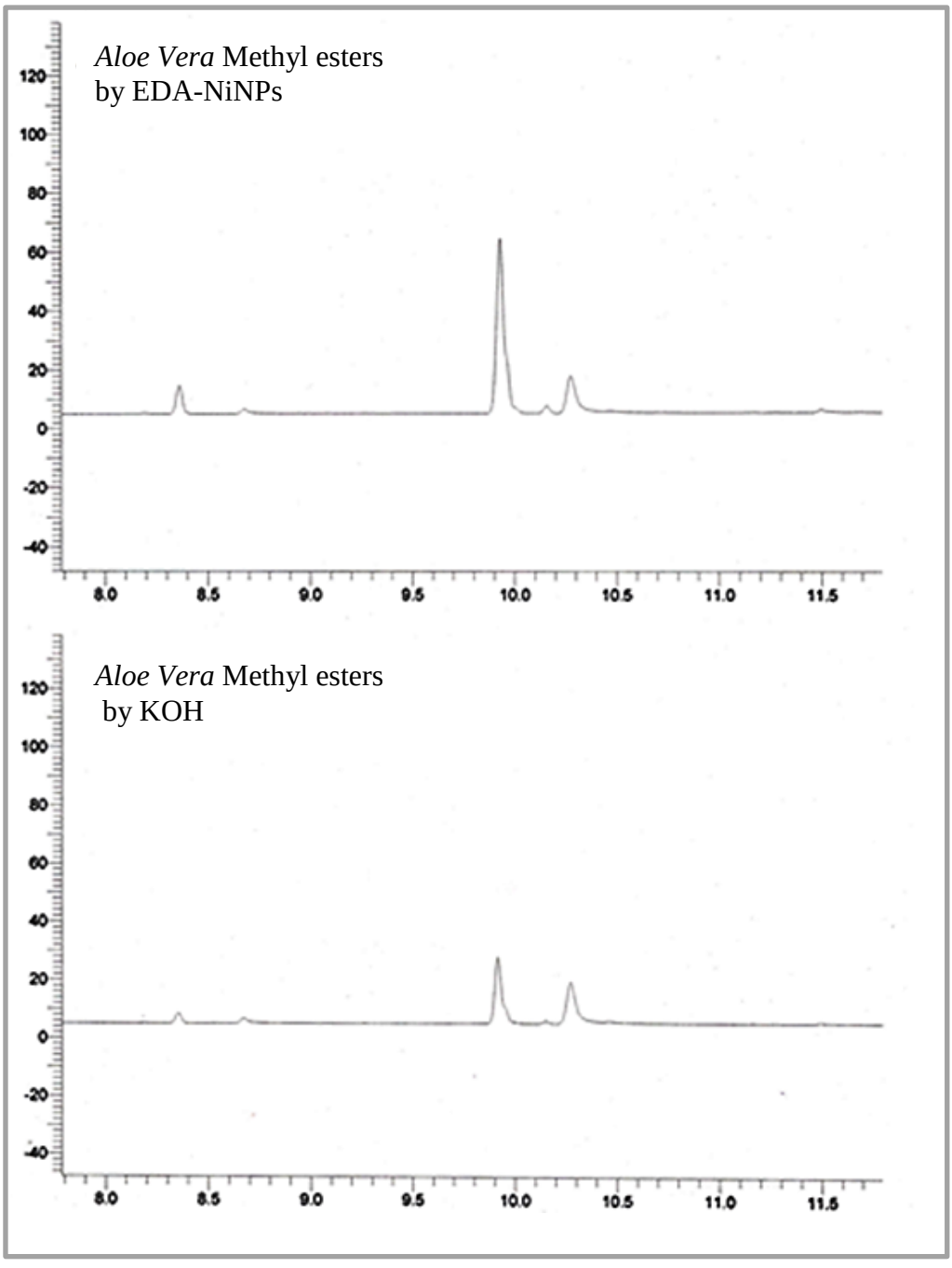

Figure S1 Comparative GC spectra of the methyl esters of *AVSO* obtained by EDA-NiNPs system or KOH as catalysts.

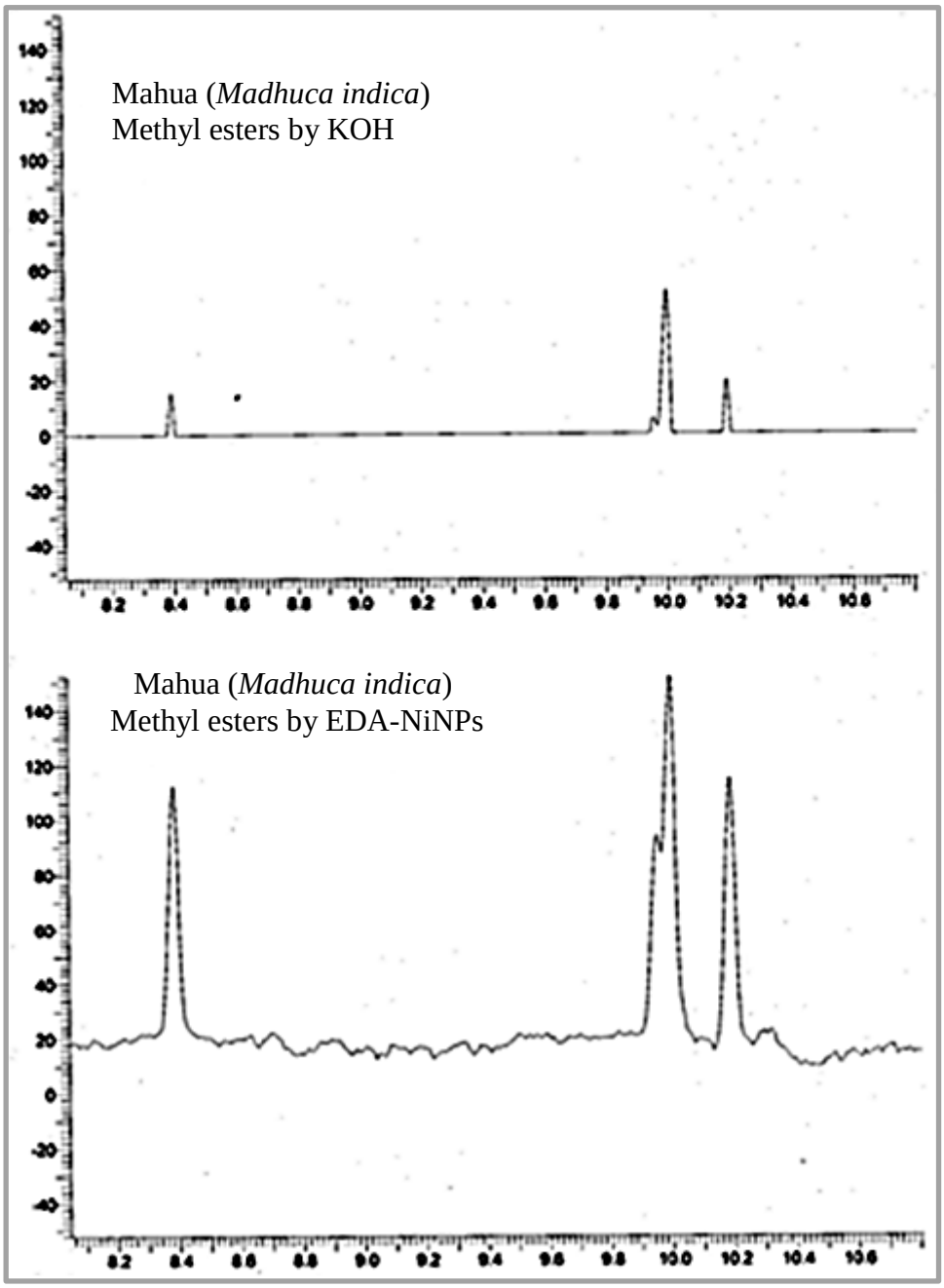

Figure S2 Comparative GC spectra of the methyl esters of *Mahua* oil obtained by EDA- NiNPs system or KOH as catalysts.

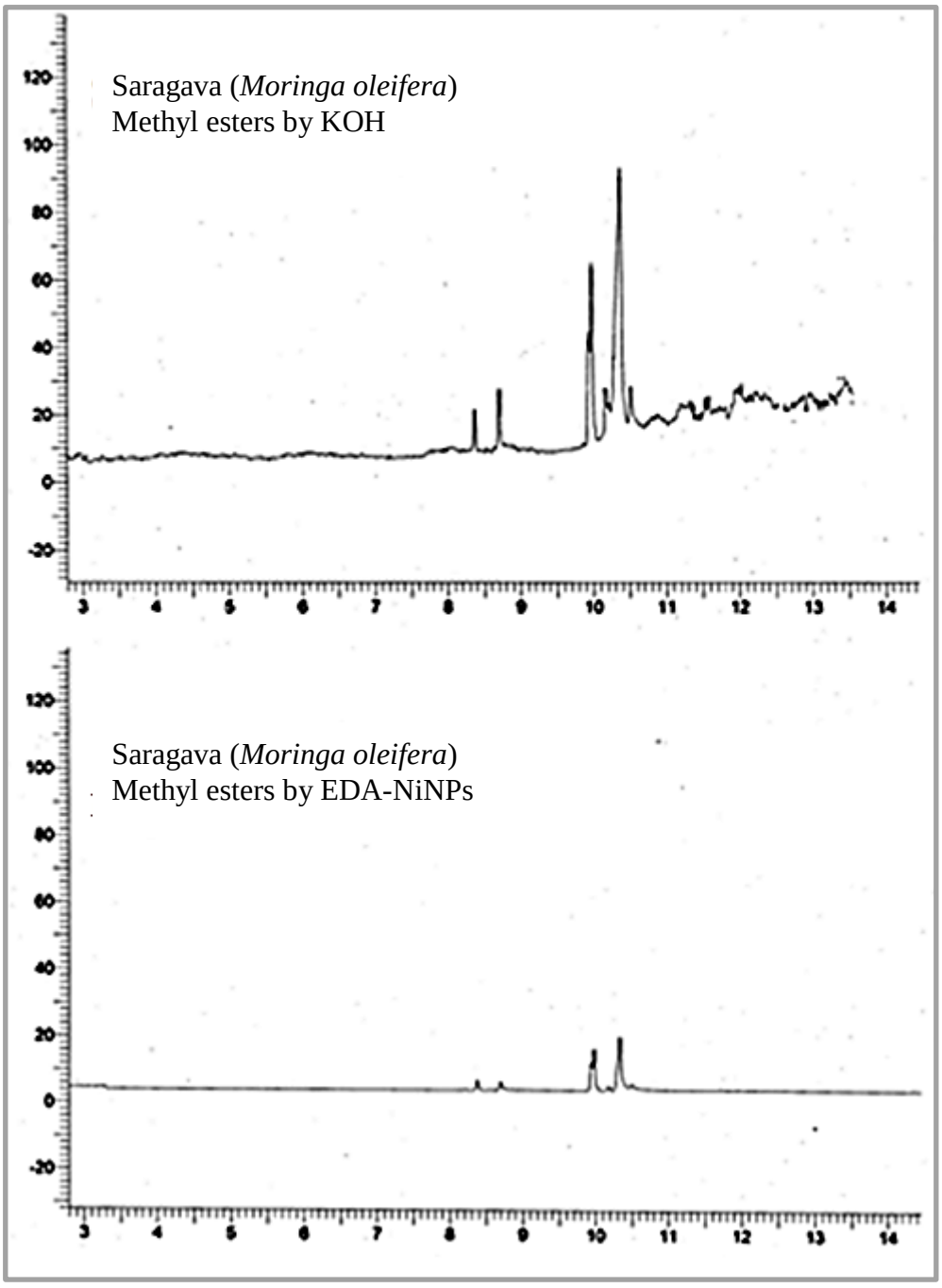

Figure S3 Comparative GC spectra of the methyl esters of *Saragava* oil obtained by EDA- NiNPs system or KOH as catalysts.

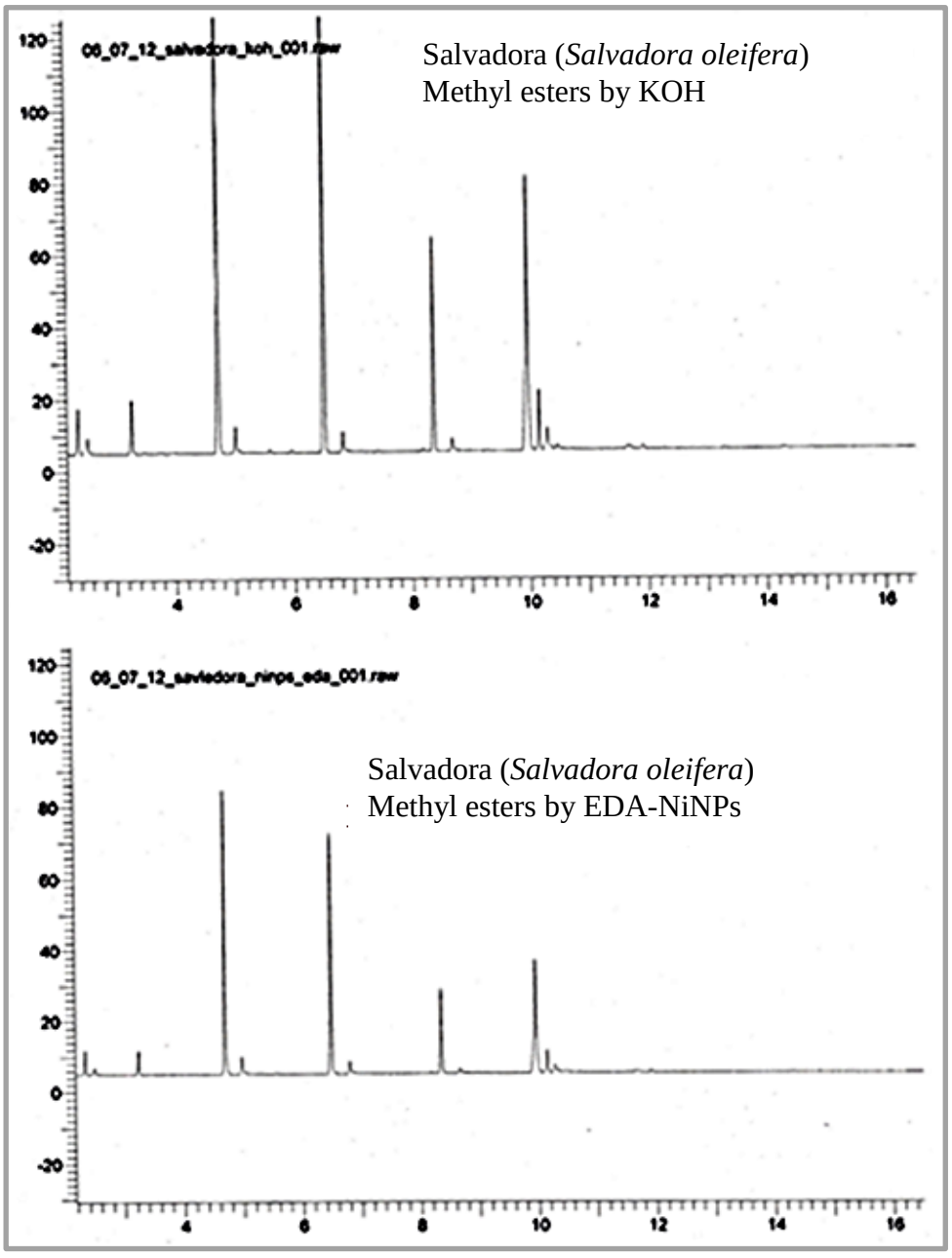

Figure S4 Comparative GC spectra of the methyl esters of *Salvadora* oil obtained by EDA- NiNPs system or KOH as catalysts.

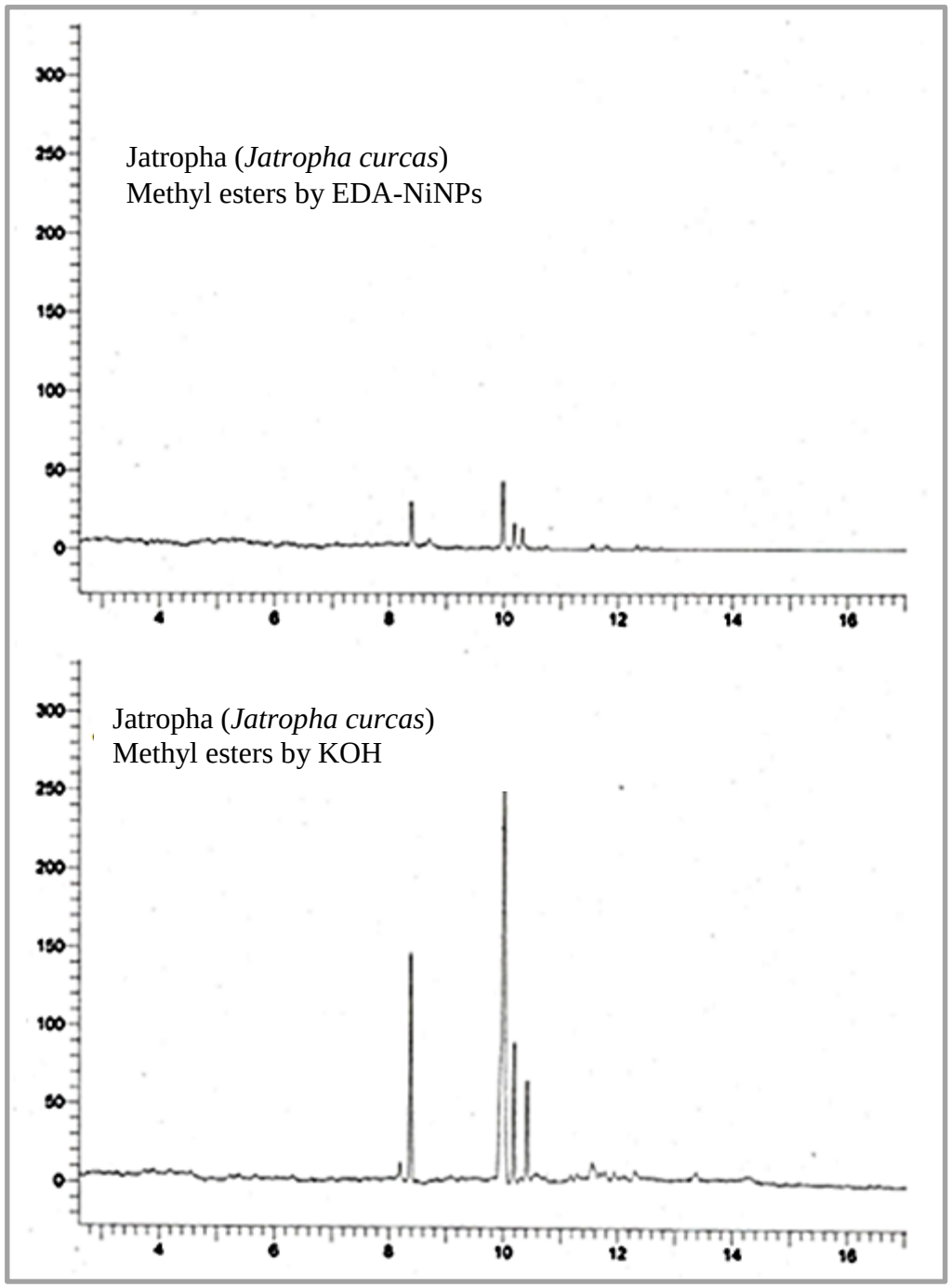

Figure S5 Comparative GC spectra of the methyl esters of *jatropha* oil obtained by EDA- NiNPs system or KOH as catalysts.

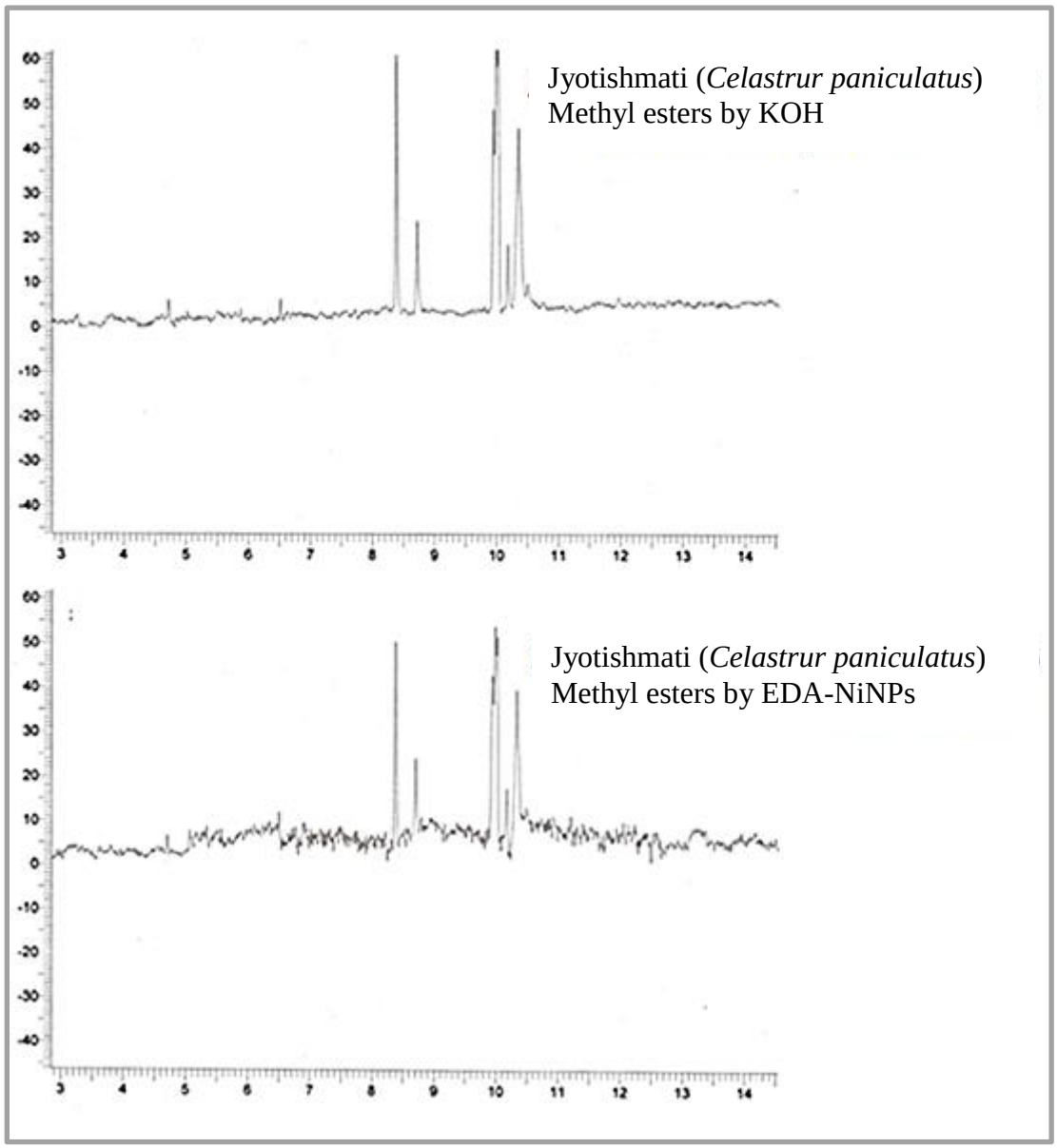

Figure S6 Comparative GC spectra of the methyl esters of *jyotishmati* oil obtained by EDA- NiNPs system or KOH as catalysts.

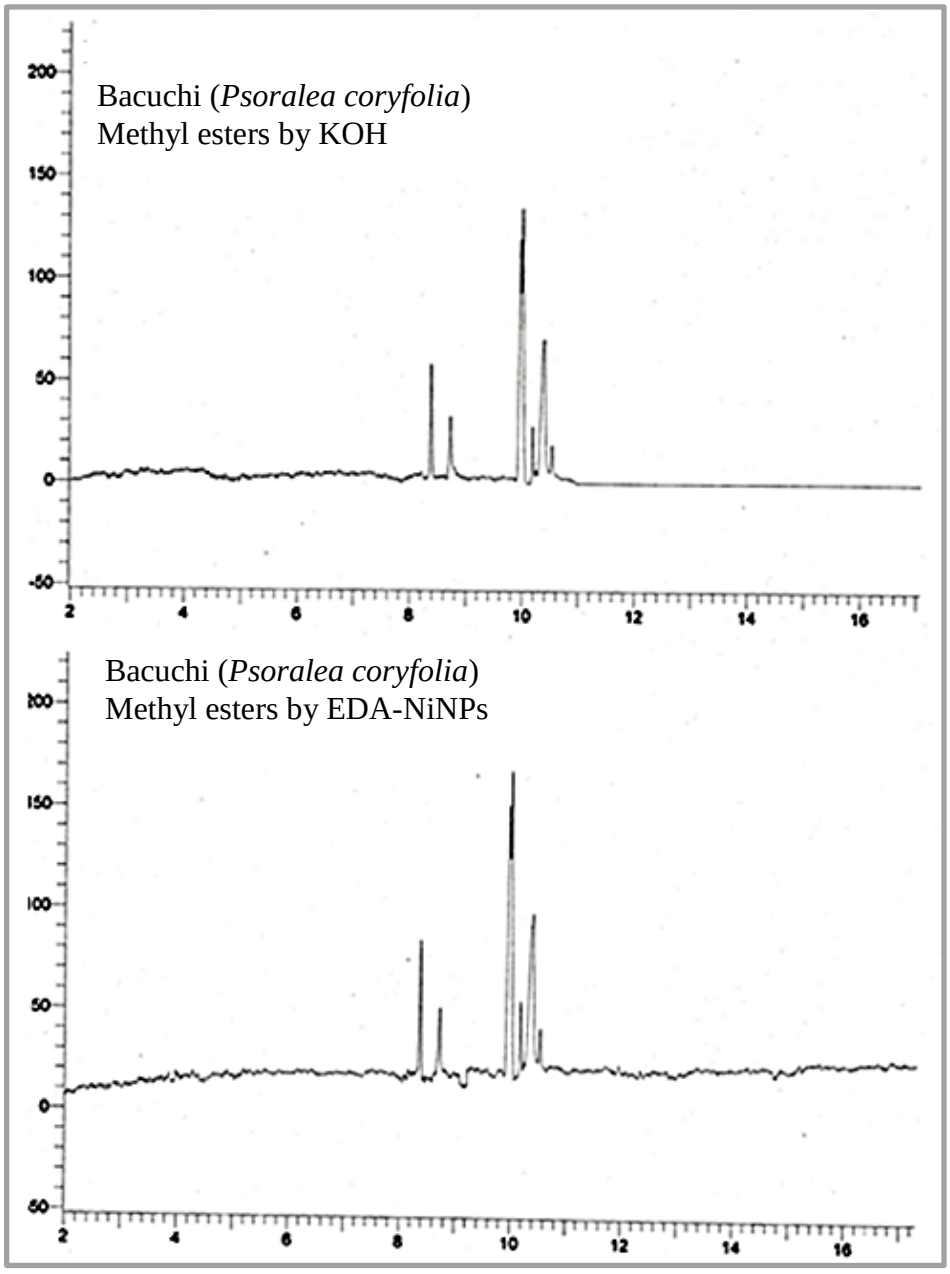

Figure S7 Comparative GC spectra of the methyl esters of *Bacuchi* oil obtained by EDA- NiNPs system or KOH as catalysts.

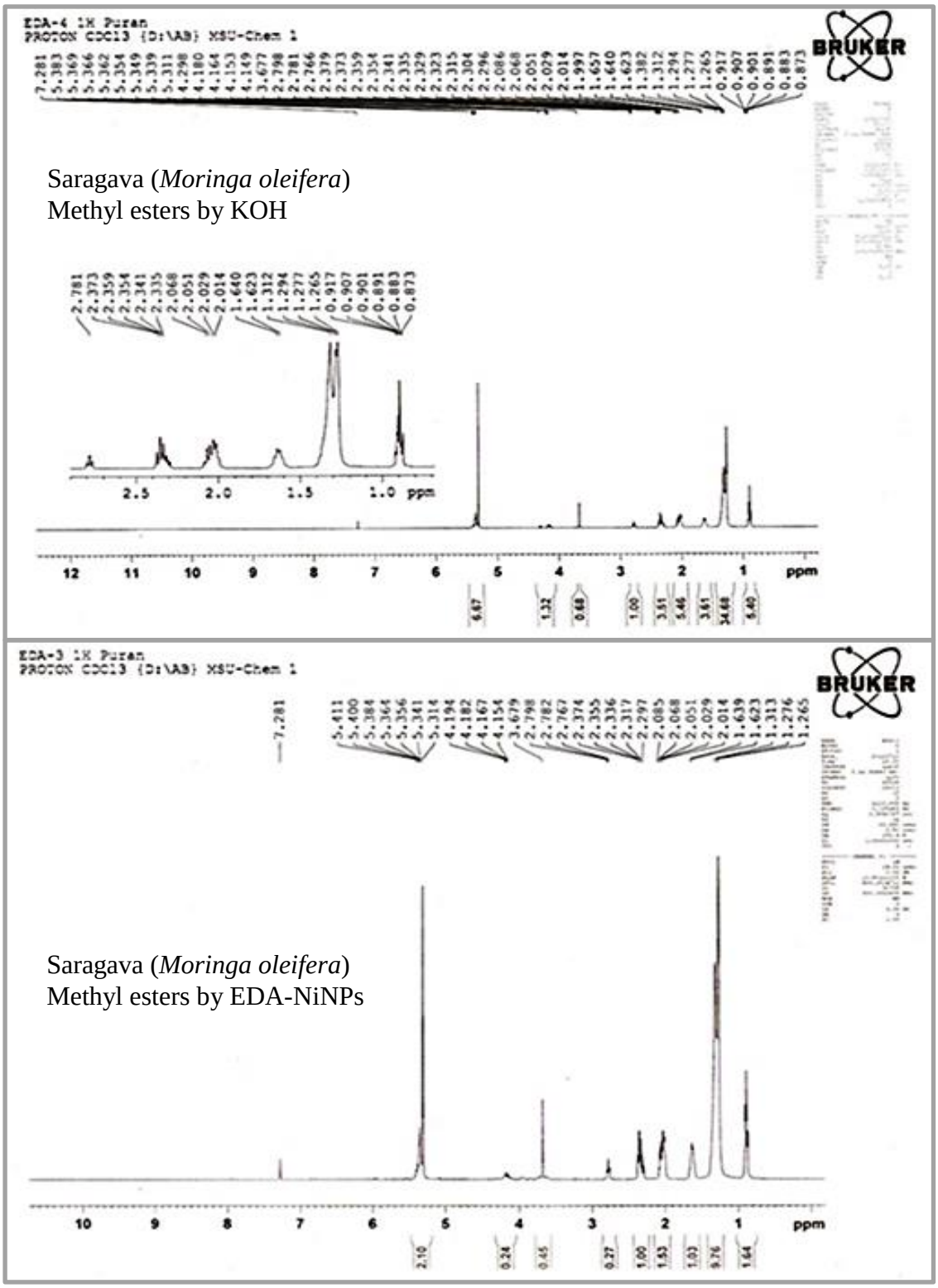

Figure S8 Comparative [1]H spectra of the methyl esters of *Saragava* oil obtained by EDA- NiNPs system or KOH as catalysts.

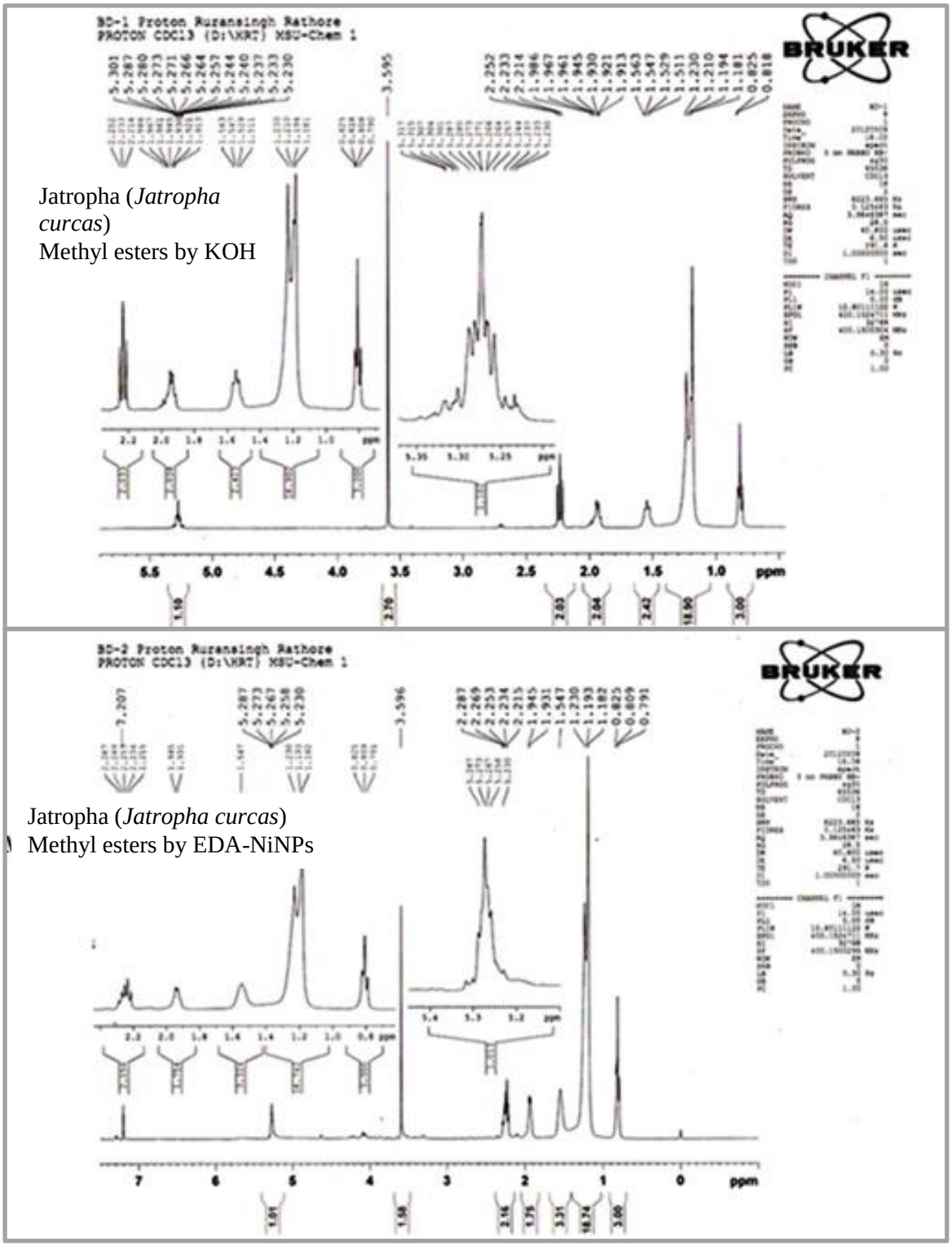

Figure S9 Comparative ^{1}H spectra of the methyl esters of *Jatropha* oil obtained by EDA- NiNPs system or KOH as catalysts.

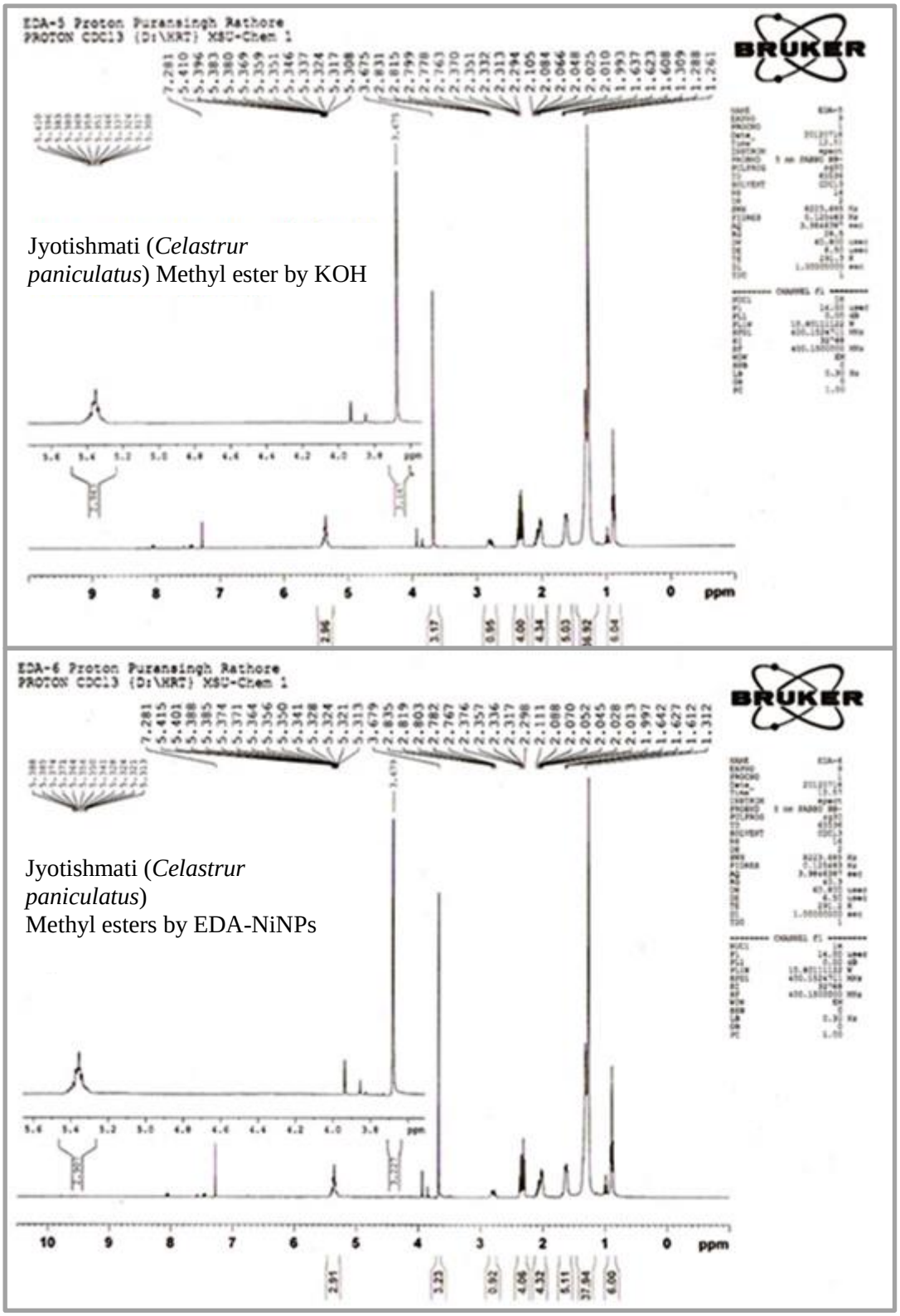

Figure S10 Comparative ^{1}H spectra of the methyl esters of *Jyotishmati* oil obtained by EDA- NiNPs system or KOH as catalysts.

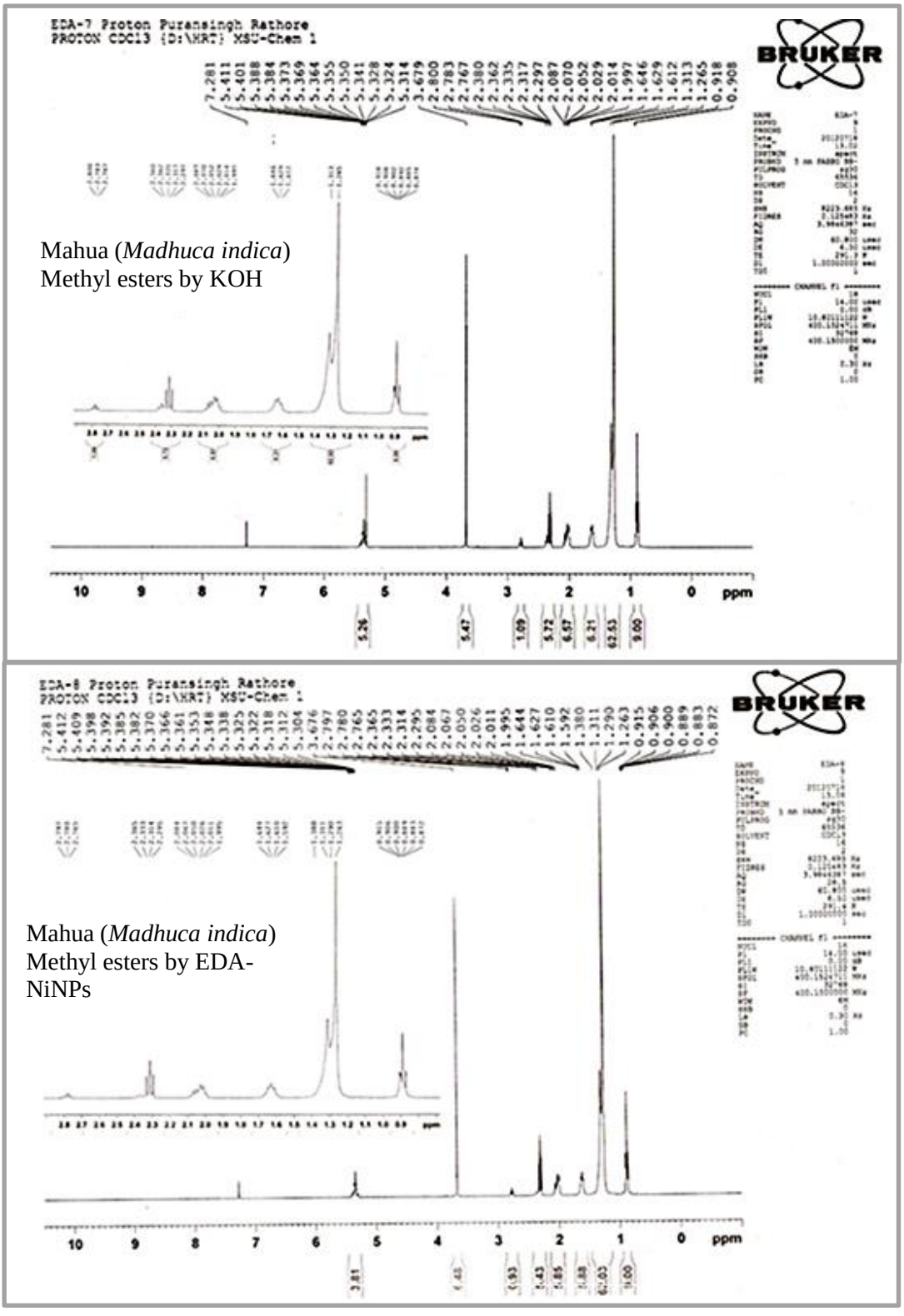

Figure S11 Comparative ^{1}H spectra of the methyl esters of *Mahua* oil obtained by EDA- NiNPs system or KOH as catalysts.

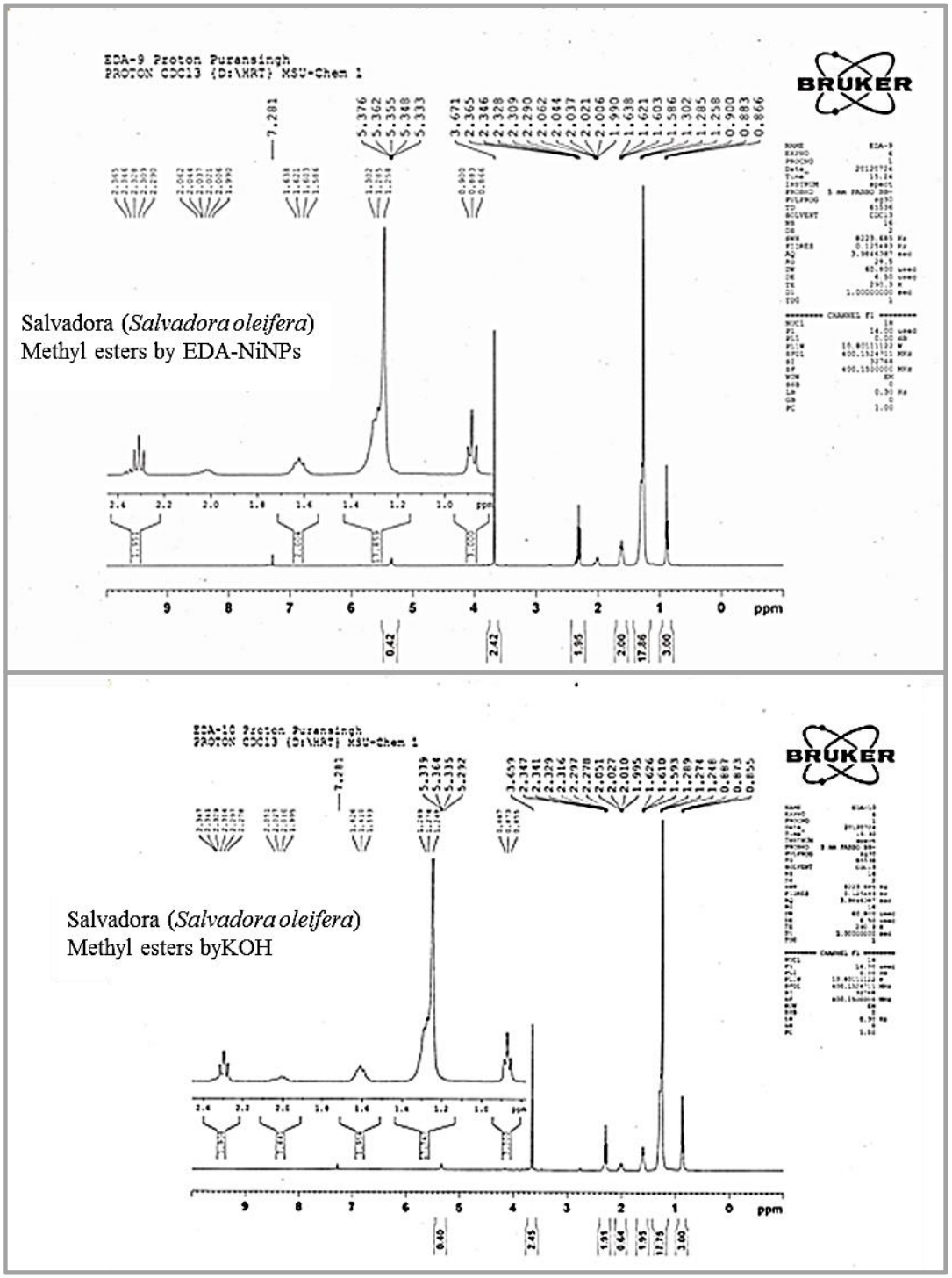

Figure S12 Comparative ^{1}H spectra of the methyl esters of *Salvadora* oil obtained by EDA- NiNPs system or KOH as catalysts.

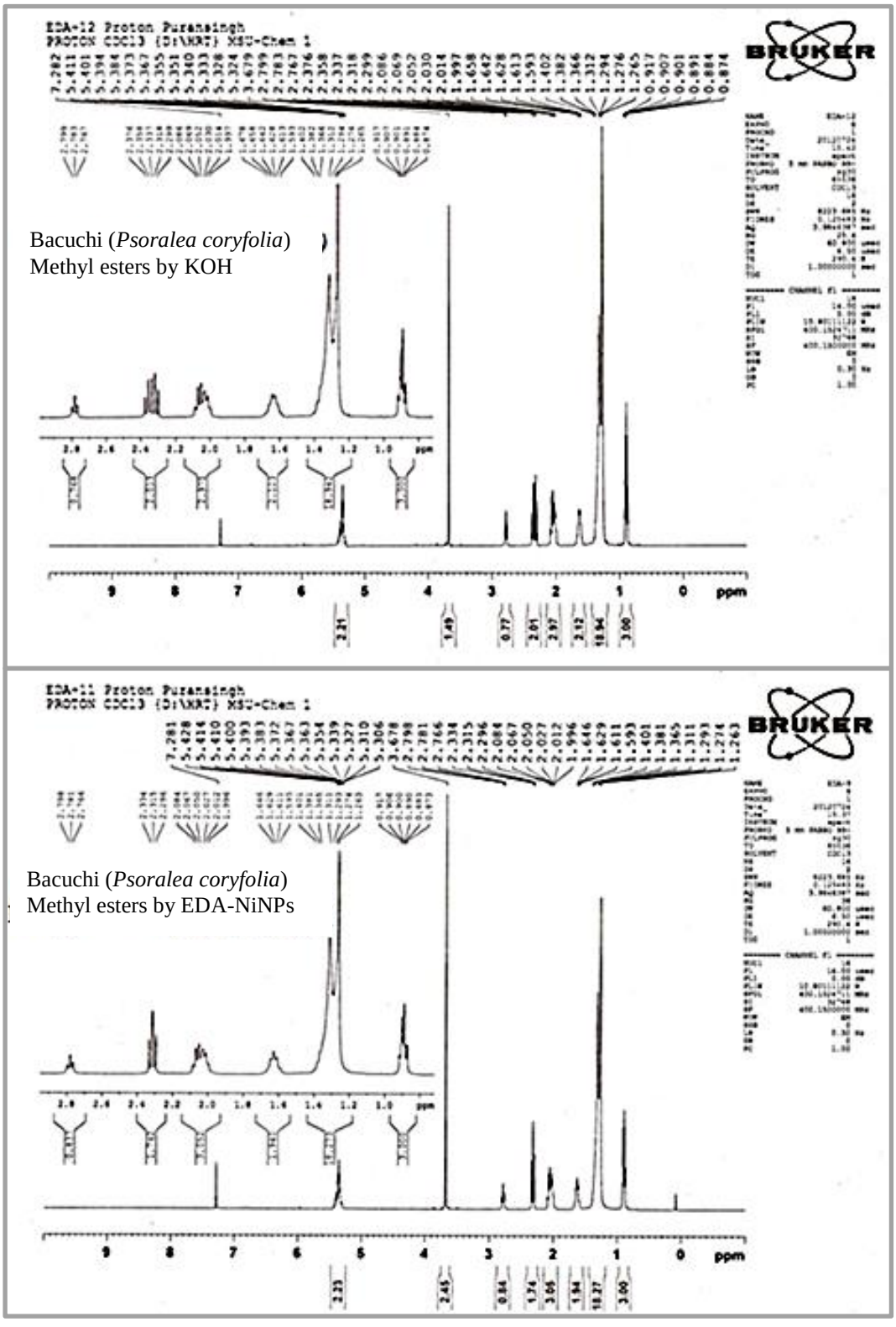

Figure S13 Comparative ^{1}H spectra of the methyl esters of *Bacuchi* oil obtained by EDA- NiNPs system or KOH as catalysts.

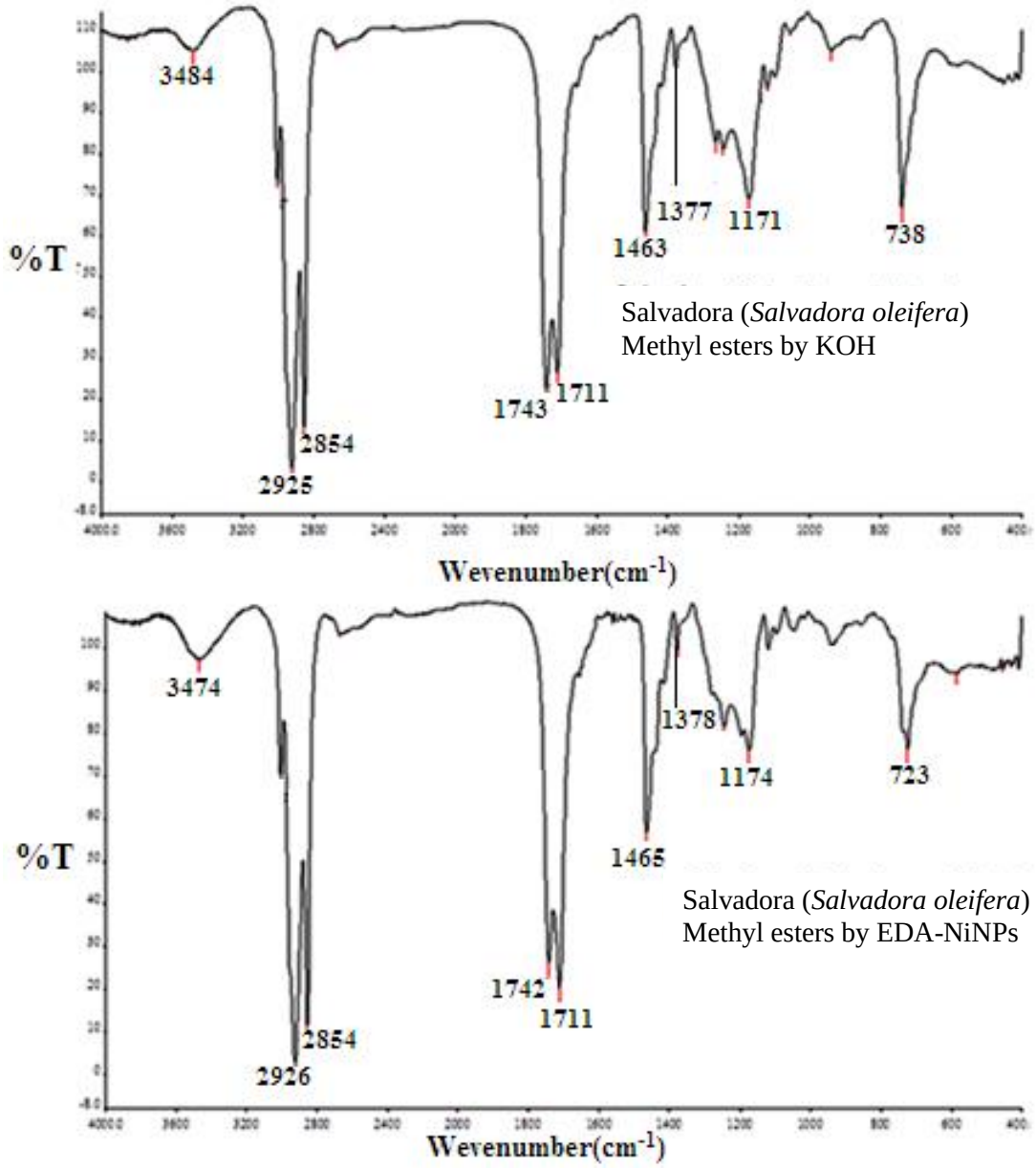

Figure S14 Comparative FT-IR spectra of the methyl esters of *Salvadora* oil obtained by EDA- NiNPs system or KOH as catalysts.

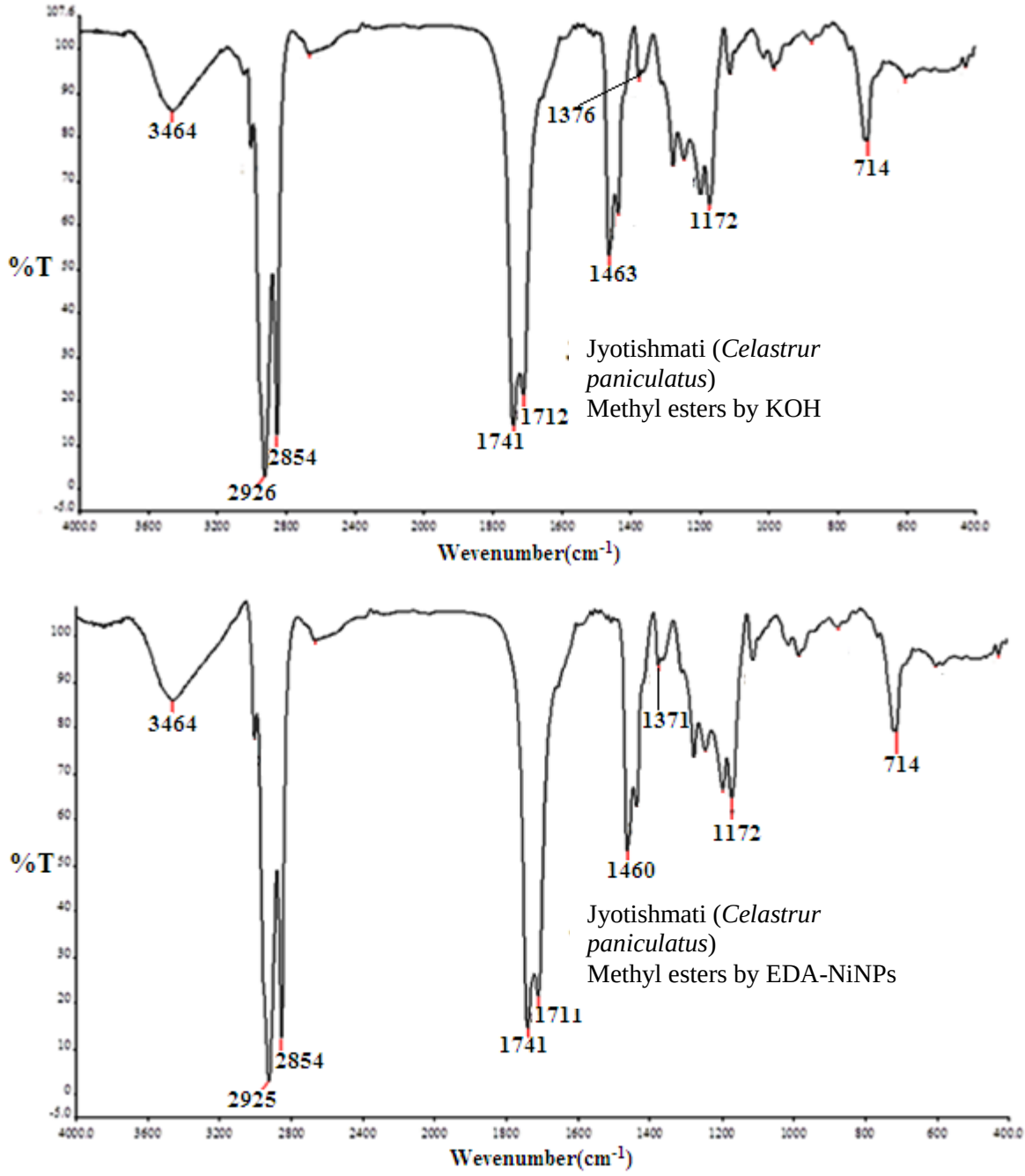

Figure S15 Comparative FT-IR spectra of the methyl esters of *Jyotishmati* oil obtained by EDA- NiNPs system or KOH as catalysts.

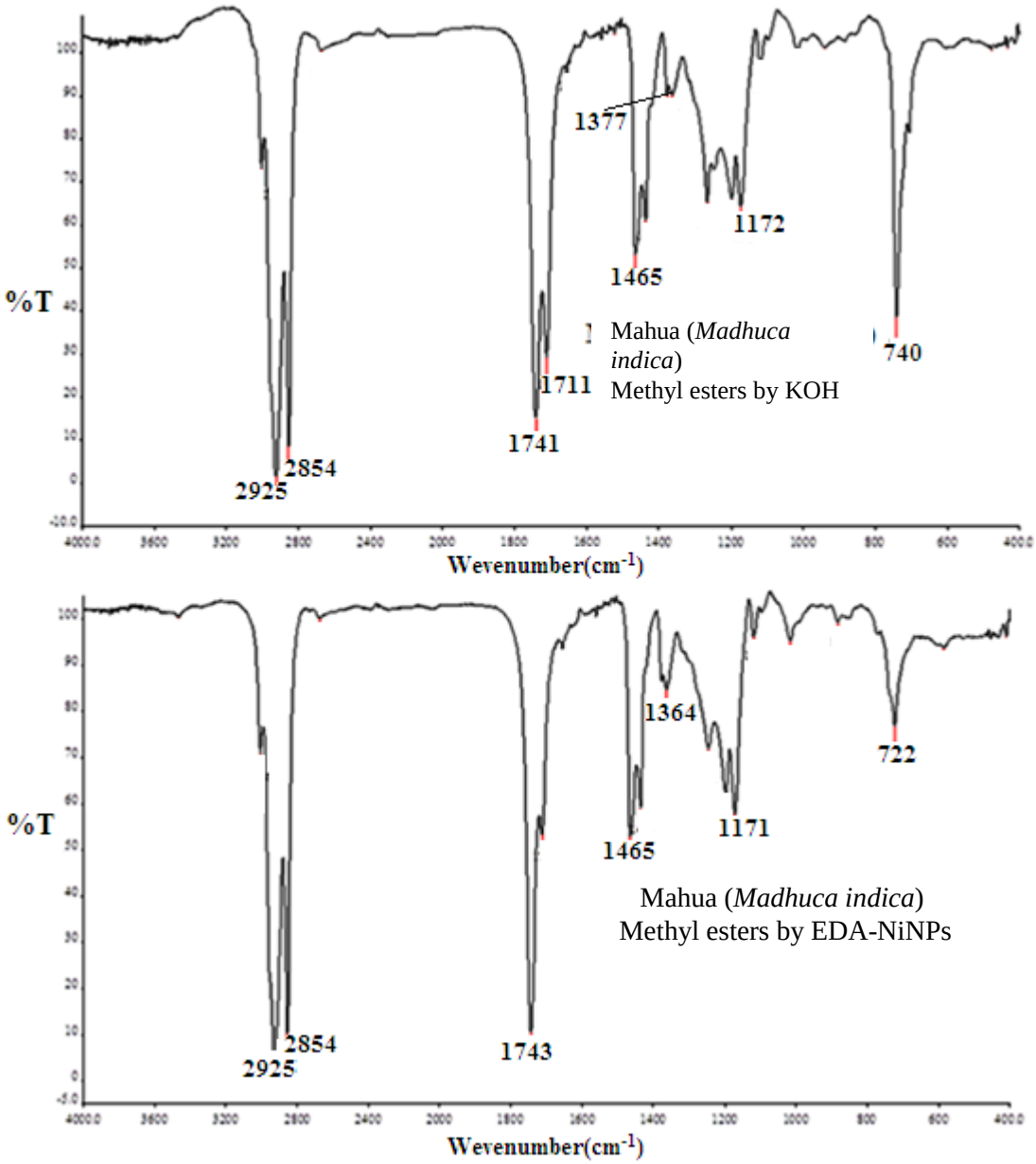

Figure S16 Comparative FT-IR spectra of the methyl esters of *Mahua* oil obtained by EDA- NiNPs system or KOH as catalysts.

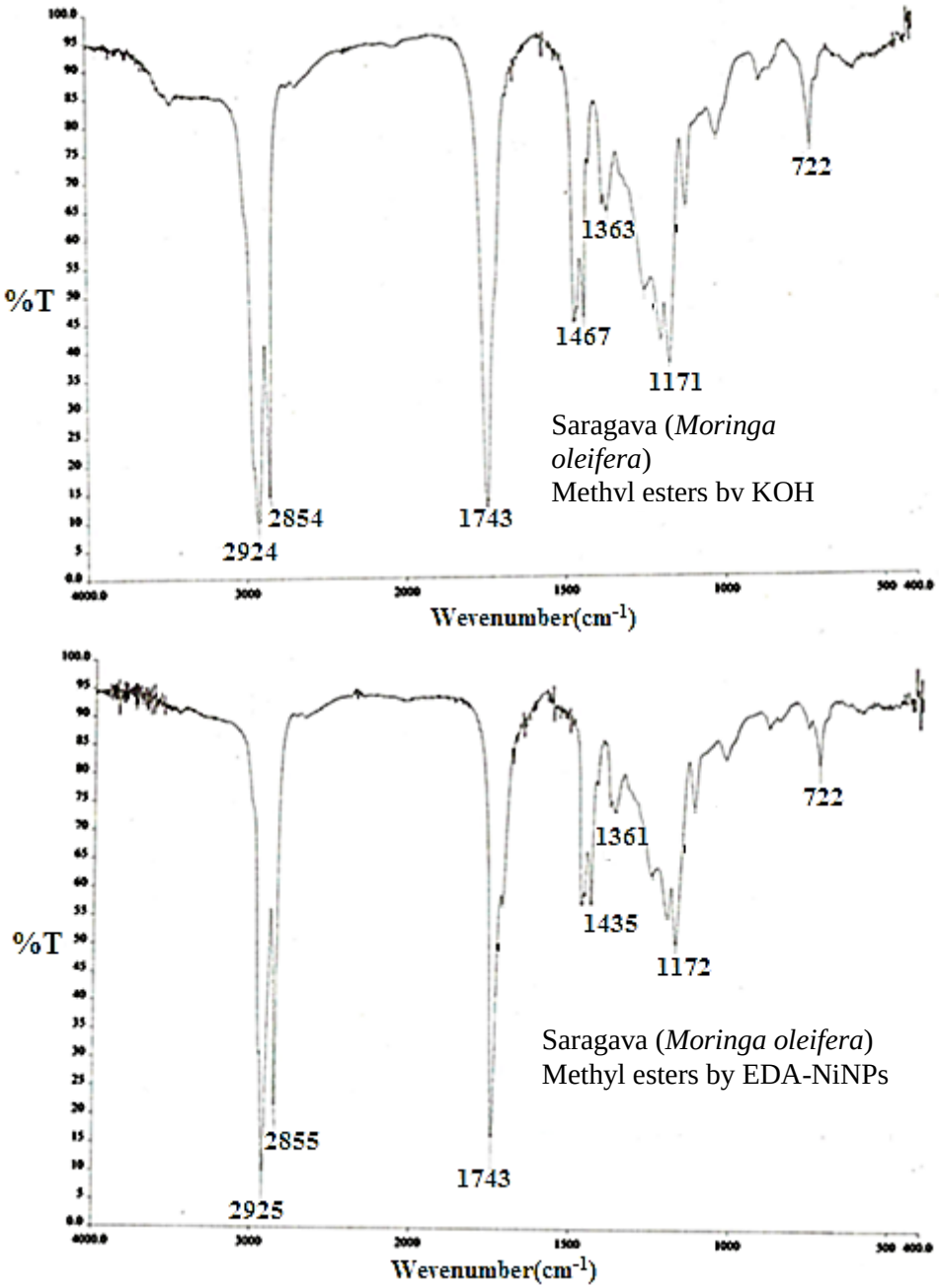

Figure S17 Comparative FT-IR spectra of the methyl esters of *Saragava* oil obtained by EDA- NiNPs system or KOH as catalysts.

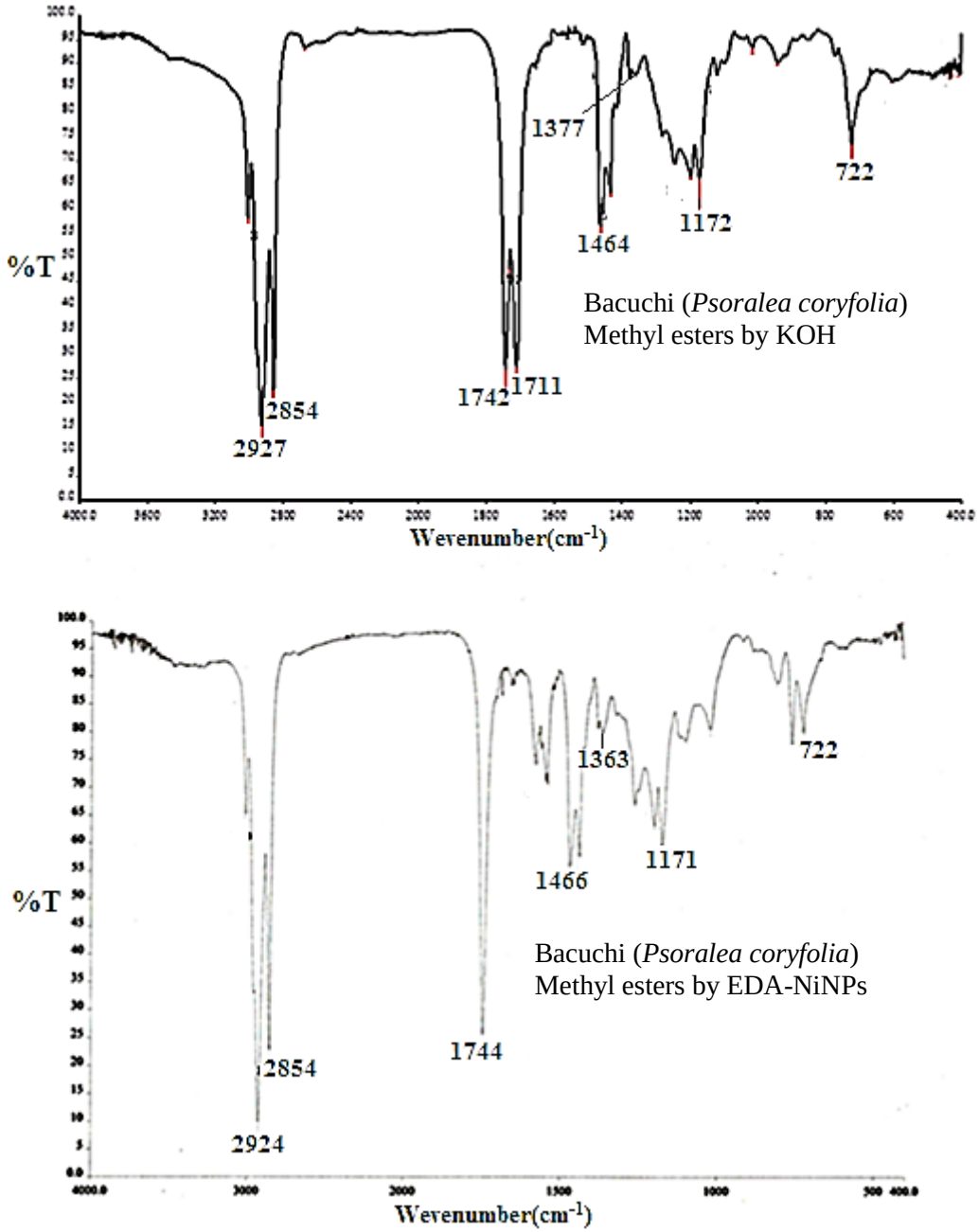

Figure S18 Comparative FT-IR spectra of the methyl esters of *Bacuchi* oil obtained by EDA- NiNPs system or KOH as catalysts.

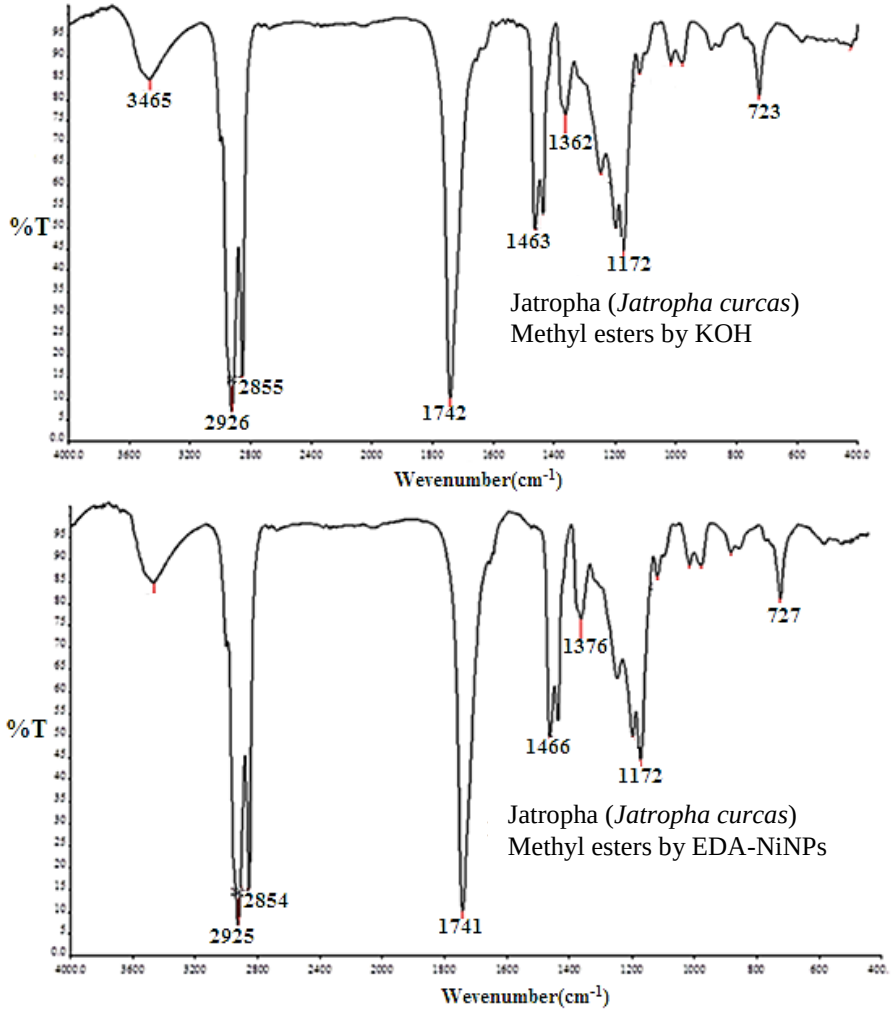

Figure S19 Comparative FT-IR spectra of the methyl esters of *Jatropha* oil obtained by EDA- NiNPs system or KOH as catalysts.

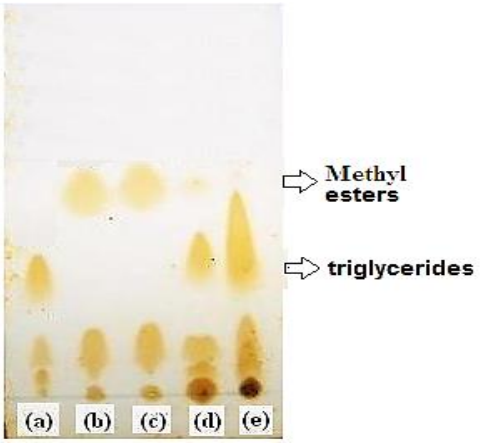

Figure S20 TLC analysis of (a) AVSO and biodiesel from AVSO obtained by different catalysts (b) KOH, (c) EDA + NiNPs, (d) DEA + NiNPs and (e) TEA + NiNPs.

Chapter–2

Part–3

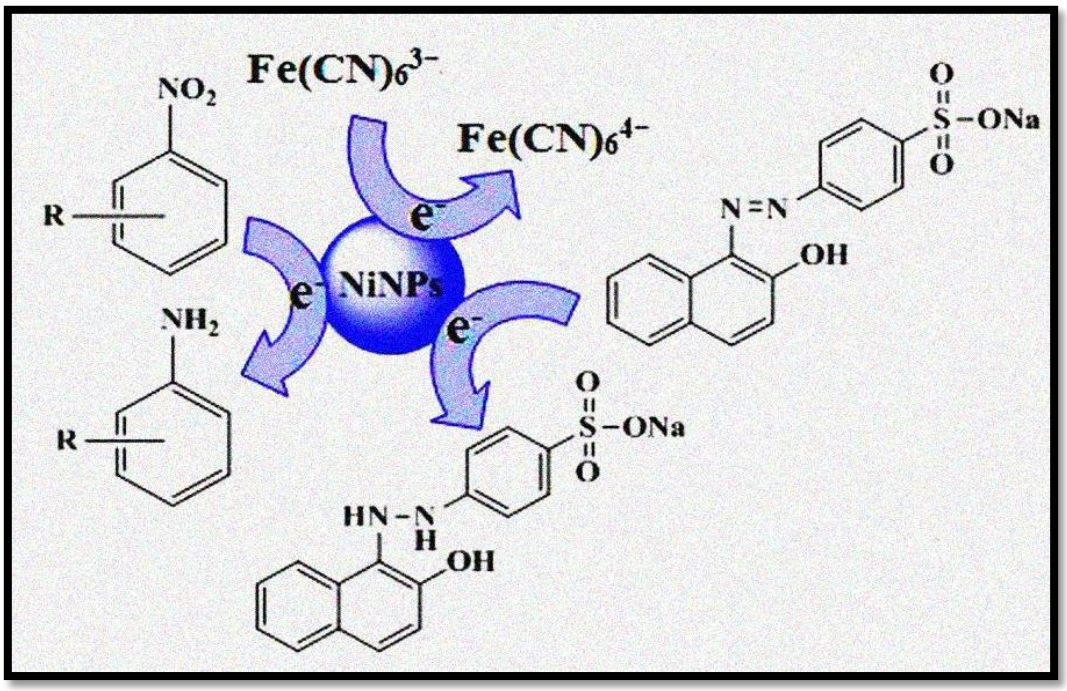

Catalytic applications of Nickel Nanoparticles in electron transfer reactions

Published in *Catalytic Letter, 2014, 144, 439*

2.3.1 Introduction

Nickel nanoparticles are used in various electron transfer reaction including other reaction like chemoselective oxidative coupling of thiols,[1] reduction of carbon-carbon multiple bonds,[2-3] imine reduction,[4] hydrodehalogenation of organic halides,[5] reduction of sulfonates and aromatic compounds,[6] homocoupling of aryl iodides,[7] Wittig-type olefination,[8] α-alkylation of methyl ketones with primary alcohols,[9] reduction of aldehydes and ketones,[10-11] and supports for hydrogen adsorption.[12-13]

The reduction of aromatic nitro compounds to the corresponding amines is important in synthetic chemistry because aromatic amines are frequent intermediates in the production of pharmaceuticals, agrochemicals, polymers, dyes, and other fine chemicals.[14] A variety of procedures and reducing agents are available for this purpose.[15] In literature a few procedures involving noble metal NPs such as Pd, Pt, Ag, Au, as well as Cu, and Ni NPs have been demonstrated for the reduction of nitro group.[15-17] The main limitations of earlier reported work were the necessity of high H_2 pressures, organic solvents and high temperatures. Further, the selection of metal and its support, the hydrogen source and operational simplicity, which are the important parameters for effective conversions, are restricted. However, an alternative efficient, simple, chemoselective, green and cost-effective procedure is highly appreciated.

The role of metal nanoparticles is very important in redox reactions and can be explained in terms of electrochemical potentials.[18] The considerable catalytic activity for the NiNPs can be probably attributed to the following two factors: (1) larger surface than a bulk metal to simultaneously accommodate both the oxidation and reduction half reactions and (2) NiNPs could provide a much higher activity than a bulk metal due to the size effect. In other words, the superior catalytic activity of the NiNPs is a result of two effects: good electrical connection and small sizes related to their bulk part.

In the past our group has focused on biological and catalytic applications of metallic NPs of Ag, Cu and Ni.[19-21] The present work highlights the use of NiNPs as catalyst for three different kinds of reactions. (1) Selective hydrogenation of aromatic nitro compounds at room temperature (RT) in aqueous medium, (2) Microwave (MW) assisted azo dyes reduction by ascorbic acid (AA) and (3) Electron transfer reaction between potassium ferricyanide (PFC) and sodium thiosulfate (STS).

2.3.2 Experimental

2.3.2.1 Materials and methods

para-Nitroaniline (PNA), other aromatic nitro compounds, potassium ferricyanide (PFC), sodium thiosulfate (STS), ascorbic acid (AA) and azo dyes were all purchased from Merck Mumbai, India. All the solutions were prepared using double-distilled and demineralized water. Characterisation of starch capped NiNPs has been discussed in our previous chapter.

NiNPs catalyzed hydrogenation, decolourization of dye and redox reactions were monitored on PerkinElmer Lambda 35 UV–vis spectrophotometer by corresponding λ-max. Hydrogenation reaction monitoring was also done by thin-layer chromatography (TLC, Using ninhydrin as staining reagent) and gas chromatography (GC). All products of the reduction of nitroarenes are commercially available and were identified by comparing their physical and spectral data (m.p., TLC (silica gel 60 F254, Merck, Mumbai, India), GC (Perkin Elmer clarus 500 GC) and ^{1}H NMR (BRUKER 400 MHz) with those of authentic samples or reported data (data not shown). For decolourizationof azo dyes microwave (MW) oven operated at the 100% power of 1350W and frequency 2450 MHz.

2.3.2.2 Catalytic Reduction of *p*-Nitroaniline and other aromatic nitro compounds

In a typical reaction PNA (0.0036mole) was used as a starting material, $NaBH_4$ (0.0260mole) as a source of hydrogen, water (6 mL) as solvent and NiNPs 50mg (10wt % of PNA, 0.85mmol) as catalyst. All the components were mixed together in 50mL round bottom flask and the reaction was carried out at room temperature (RT, 25-30 °C) under stirring for 90min.

The product was isolated by extraction in dichloromethane and evaporation of solvent followed by column chromatography (10:90, ethyl acetate in hexane v/v) over basic alumina furnished PPDA. The spectroscopic data of this compound are in good agreement with those reported. The reaction was also carried out in absence of NiNPs for comparison.

Reduction of other nitro aromatics was carried out in a similar manner. The products purified by short-path basic alumina chromatography (0-40% ethyl acetate in hexane v/v) were analyzed by ^{1}HNMR (data not given).

2.3.2.3 Decolourizationof azo dye

Experiments were carried out by using four different kinds of azo dyes. The dyes used were Orange II (OR-II), Methyl Red (MR), Methyl Orange (MO), Erichrome Black-T (EBT) and mixture of dyes (MD). Each microwave (MW) assisted reduction experiments were carried out by taking 6mg of NiNPs (0.102mmol) into 50 mL stoppered borosilicate Erlenmeyer flasks together with 5mL of an aqueous solution with 6.5×10^{-4} mol L^{-1} of azo dyes and 3×10^{-3} mol L^{-1} ascorbic acid (AA). Analogous experiments were performed without AA, NiNPs and alternatively without MW irradiation (at RT, 25-30ºC). The decolourization of each dye was measured by its absorbance at λ_{max} using UV–vis spectrophotometer. Reduction of a mixture of dyes was also attempted in a similar manner.

2.3.2.4 Redox reaction

The reaction mixture containing as synthesized NiNPs (5mg, 0.085mmol), 1mL of 0.001mole potassium ferricyanide (PFC) and 1mL of 0.1mole sodium thiosulfate (STS) was placed in a quartz cell with 1 cm^3 path length. The reaction was monitored by UV-vis spectroscopy in the presence and absence of NiNPs at 25±2 ^{0}C temperature.

All experiments have been repeated three times and the reproducibility confirmed. The recyclability of the NPs was also surveyed. The NPs were recovered by centrifugation, washed with acetone, dried at 60 ºC under vacuum and used for the next reaction.

2.3.3 Results and discussion

2.3.3.1 Catalytic Reduction of *p*-Nitroaniline and other aromatic nitro compounds

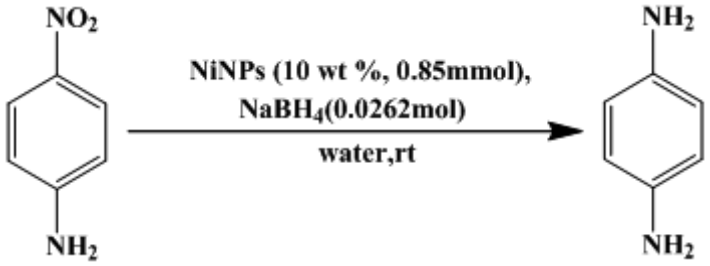

Scheme 2.6 Schematic representation of the performance of NiNPs as catalysts in the reduction of PNA to PPDA by $NaBH_4$ in water

Table 2.15 Optimization of reaction conditions for hydrogenation of *p*-Nitroaniline

Sr. No.	Catalyst(mg)	$NaBH_4$(mole)	Temperature(°C)	Time (h\min)	%Yield[b] (±2)
1	None	none	25-30 to reflux	24h	-
2	50	,,	,,	,,	-
3	None	0.0260	,,	,,	< 5
4	50	< 0.005	,,	,,	<10
5	,,	0.007	,,	,,	31±5
6	,,	0.0132	25-30	180min	95±3
7[a]	**,,**	**0.0260**	**,,**	**90min**	**,,**
8	,,	,,	50-60	60min	,,
9	,,	,,	70-80	15min	,,
10	10	,,	25-30	300min	,,
11	20	,,	,,	,,	,,
12	30	,,	,,	,,	,,
13	40	,,	,,	180min	,,
14	≥ 50	,,	,,	90 min	,,

Reaction conditions: *p*-Nitroaniline-0.0036 mole, solvent (water)-6 mL, a-optimized reaction condition and b- Isolated yield.

Metal nanocatalyst can catalyze the reduction of nitro compounds by acting as an electronic relay system to overcome the kinetic barrier, in which the electrons donated by BH_4^- can be transferred to the acceptor nitro groups.[22] In the present case hydrogenation of PNA as a model system was used to study the efficiency of the NiNPs as catalyst in aqueous medium (**Scheme 2.6**). The results of the conversion of PNA to PPDA are illustrated in **Table 2.15**. It is seen from the table (entries 1-3) that the presence of a catalyst along with $NaBH_4$ is required for hydrogenation of PNA. The optimum reaction conditions for PNA reaction are given in **Table 2.15** (entry 7), which yields 95±2 % of product at RT after 90min and selectivity was 100%.

This reaction was monitored by UV-vis spectrophotometer (**Figure 2.11**), where the product and reactant show different absorption bands at 307nm and 381nm, respectively. As shown in **Figure 2.11**, when the reaction conditions mentioned in **Table 2.15** (entry-7) was used, the reaction proceeded faster within 90min and the λ_{max} shifted from 381nm to 307nm. Whereas, in the absence of NiNPs, the peak at 381nm corresponding to PNA did not disappear even after 24h of reflux.

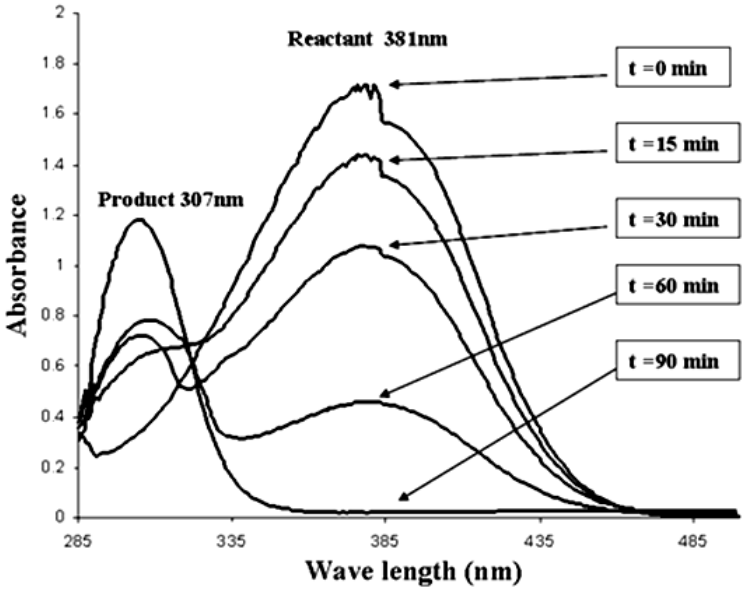

Figure 2.11 UV-vis spectra indicating the change of *p*-Nitroaniline to *p*-Phenylenediamine in presence of NiNPs

Furthermore, experiments were performed using a different mole ratio of $NaBH_4$ in standard reaction. On using $NaBH_4$ less than 0.005mole, reaction yield was less than

10% even after 24h of reflux (**Table 2.15**, entry 4). When we increased moles of $NaBH_4$ from 0.005 to 0.007, the yield increased to 31±5% (table-1, entry 5), whereas using 0.0132 mole of $NaBH_4$ resulted into a remarkable yield (95±2%) at 35°C within 180min (**Table 2.15**, entry 6). However, lowering the amount of $NaBH_4$ caused an increase in the reaction time and hence an adequate quantity of $NaBH_4$ was used in optimum reaction condition. Good to high yields were obtained at 80ºC temperature and the reaction was completed within 15min. This shows that as the reaction temperature increases, reaction time decreases (**Table 2.15**, entries 8, 9).

Variation in quantity of NPs (**Table 2.15**, entries 10 to 14) under optimum reaction conditions showed that even 10mg was sufficient for catalyzing the reaction at RT but took 300min for maximum conversion (**Table 2.15**, entry 10). On the other hand with 40mg the reaction time decreased to 180min (**Table 2.15**, entry 13). Beyond 50mg the reaction time and yield did not change (**Table 2.15**, entry 14).

Under the optimized conditions, we investigated the scope of converting various aromatic nitro compounds to aromatic amines by using NiNPs, $NaBH_4$ and water (**Scheme 2.7**). NiNPs was applied for all substrates and they almost gave same yield in similar reaction time (**Table 2.16**). The results were satisfactory for various aromatic nitro substrates with different functional groups (**Table 2.16**). Further, this catalytic system works efficiently in aqueous system and therefore no hazardous solvent was required. This reaction has been investigated in the presence of other protic solvents such as methanol, ethanol, and ethylene glycol; however, none of them gave satisfactory results. In an aqueous system $NaBH_4$ gives sodium metaborate ($NaBO_2$)[28] which is the only waste generated during the reaction. However sodium metaborate can be recycled using magnesium hydride (MgH_2) or magnesium silicide (Mg_2Si) by annealing (350–750° C) under high H_2 pressure (0.1–7 MPa) for 2–4h.[28] This opens up new possibilities for eco-friendly synthesis of aromatic amines.

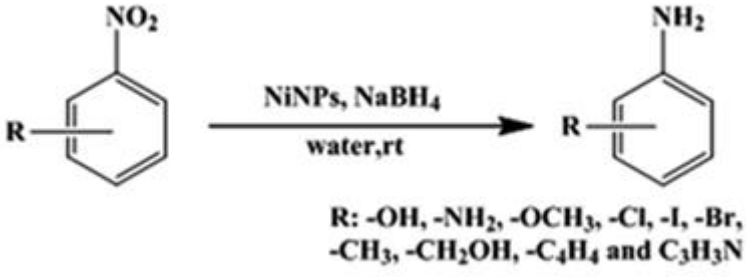

Scheme 2.16 General scheme for reduction of various Nitro aromatics

Table 2.16 Selective reduction of Nitro aromatics to aromatic amines in water with NiNPs at RT

S. No	Substrate	Product	Time (min)	Yield[a] (%±3)	Selectivity (%)
1	*o*-Nitrophenol	*o*-Aminophenol	80	90	100
2	*p*-Nitrophenol	*p*-Aminophenol	80	95	,,
3	*m*-Nitrophenol	*m*-Aminophenol	100	95	,,
4	*o*-Nitrotoluene	*o*-Toulidine	120	85	,,
5	*p*-Nitrotoluene	*p*-Toulidine	120	90	,,
6	*m*-Nitrotoluene	*m*-Toulidine	100	90	,,
7	*p*-Nitrobenzyl alcohol	*p*-Aminobenzyl alcohol	120	92	,,
8	*m*-Nitrobenzyl alcohol	*m*-Aminobenzyl alcohol	120	91	,,
9	*o*-Nitrobenzyl alcohol	*o*-Aminobenzyl alcohol	130	94	,,
10	4-Chloro-3-nitro aniline	4-Chlorobenzene-1,3-diamine	150	90	,,
11	4-Chloro-2-nitro aniline	4-Chlorobenzene-1,2-diamine	140	90	,,
12	Nitrobenzene	Aniline	180	95	,,
13	*o*-Nitroaniline	*o*-Phenylenediamine	90	95	,,
14	*m*-Nitroaniline	*m*-Phenylenediamine	95	94	,,
15	*p*-Nitroaniline	*p*-Phenylenediamine	90	95	,,
16	*o*-Chloronitobenzene	*o*-Chloroaniline	100	95	,,
17	*m*-Chloronitobenzene	*m*-Chloroaniline	100	94	,,
18	*p*-Chloronitobenzene	*p*-Chloroaniline	90	95	,,
19	*o*-Bromonitobenzene	*o*-Bromoaniline	110	96	,,
20	*m*-Bromonitobenzene	*m*-Bromoaniline	110	95	,,
21	1-Methoxy-3-nitrobenzene	3-Methoxyaniline	80	96	,,
22	1-Methoxy-2-nitrobenzene	2-Methoxyaniline	80	97	,,
23	1-Iodo-4-nitrobenzene	4-Iodoaniline	100	94	,,
24	6-Nitroquinoline	Quinolin-6-amine	130	90	,,

25	1-Nitronaphthalene	1-Naphthylamine	140	91	,,
26	2-Nitronaphthalene	2-Naphthylamine	160	90	,,
27	3-Nitroquinoline	Quinolin-3-amine	180	92	,,

Reaction conditions: Substrate-0.0036 mole, catalyst-10 wt% (0.85mmol) of Substrate, sodium borohydride-0.0260 mole and solvent (water)-6 mL, a-Isolated yield after Colum chromatography and reactions were carried at RT.

2.3.3.2 Decolourization of azo dyes

Degradation of dyes, especially azo dyes which contribute to about 70% of all used dyes, is difficult due to their complex structure and synthetic nature.[23] The most commonly used method is adsorption which causes the high operational cost because regeneration is generally not so effective.[24] The use of noble metal NPs like Pd,[25] Au, [26] Ni,[27] and Ag[28] in dye decolourization or reduction has been reported. This is the first report on the MW (Microwave) assisted decolourization reaction of azo dye by NiNPs. As a representative case, the catalytic activity of NiNPs was first investigated in the decolourization of Orange II (OR-II) in MW, a kind of azo dye with –N=N– bonds. UV–vis spectra in **Figure 2.12** shows that before the addition of NiNPs, there was the maximum absorption band centred at 483nm, which could be assigned to the conjugated system formed by the –N=N– bonds of OR-II. The colour of the dye is attributed to this maximum absorption band, which could be used to monitor the decolourization reaction. Ascorbic acid alone could not induce complete decolourization of the dye in MW. But when irradiated in presence of NiNPs ascorbic acid led to complete decolourization of the dye. The absorption band at 483nm decreased and disappeared, which could be ascribed to the loss of conjugation of –N=N– bonds due to electron transfer through surface of NiNPs (**Scheme 2.8**). As discussed by Pande and co-workers,[29] when the size of bulk metals goes to the nanoscale, electron transfer is efficient, in addition to large surface area. Thus the electron transfer between the dye and ascorbic acid occurs before rapid diffusion pulls them apart.[30]

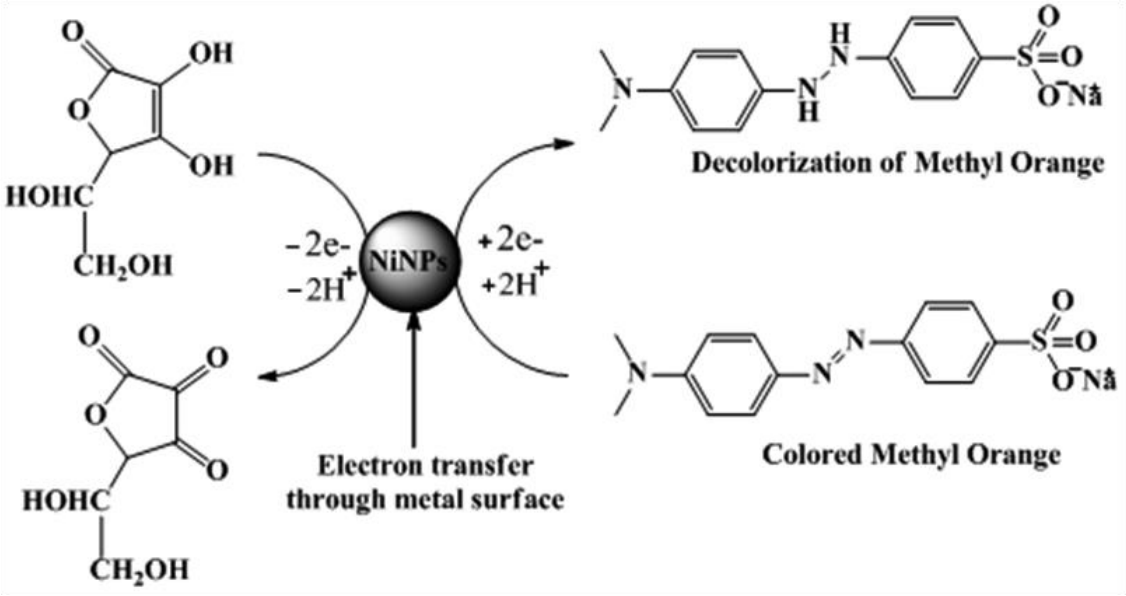

Scheme 2.8 Schematic representation of the performance of NiNPs as catalysts in the electron transfer reaction between ascorbic acid and MO for decolourization of dye.

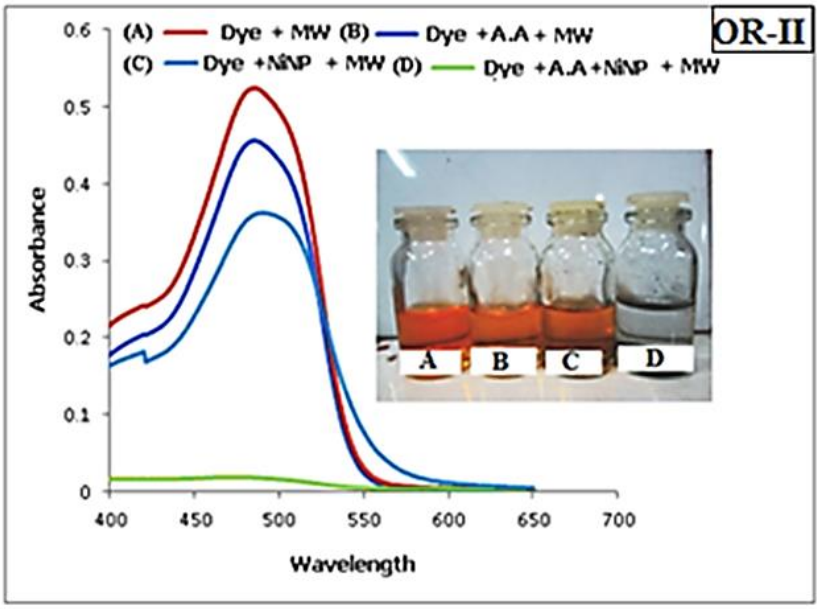

Figure 2.12 UV-vis spectra related to experiments on decolourization of OR-II dye under different conditions. Inset shows related digital photograph

Although the role of starch is only to cap the NiNPs and prevent its oxidation[21] its role as adsorbent needs to be assessed in the present case since starch is highly active towards adsorption of dye molecules.[31] To rule out the possibility of adsorption, a control experiment was performed with only starch. No significant decrease in the

absorbance was observed indicating that the decolourization is not simply due to dye adsorption onto the support. Also under MW condition adsorption will not occur due to the high kinetic energy of dye molecules.

Table 2.17 Name, corresponding λ_{max}(nm), decolourization time and structure of dyes.

Name of dyes[a]	λ_{max}(nm)	Decolourization time (sec)	Structure of dye
Orange-II (OR-II)	483	120	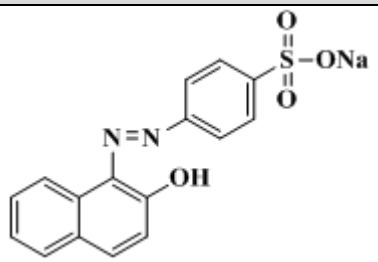
Methyl orange (MO)	465	220	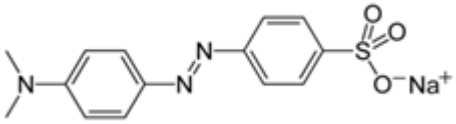
Methyl red (MR)	427	195	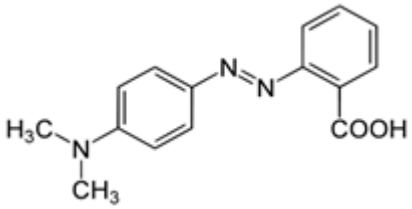
Erichrome black-T (EBT)	540	190	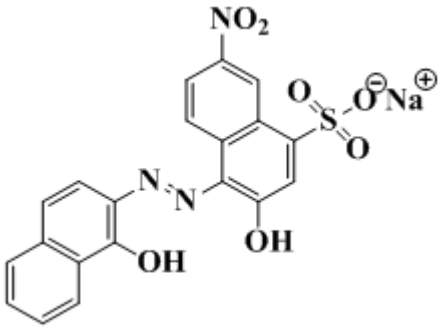
Mixture of dyes (MD)	456	190	-

a-Reaction conditions: NiNPs-6mg (0.102mmol), aqueous solution of azo dyes-2.5mL (6.5×10^{-4} mol L^{-1}) and ascorbic acid-2.5 mL (3×10^{-3} mol L^{-1}) and MW.

Similarly, in the study of decolourization of other azo dyes with AA, it was noted that the absorption peak at corresponding wavelength (λ_{max}) (**Table 2.17**) of all azo dyes

significantly decreases indicating that NiNPs catalyzes the decolourization of azo dyes.

The experiment was also successful with a mixture of dyes (**Figure 2.13**). In all experiment decolourization occurred within 2 to 4 min (**Table 2.17**). The process is extremely slow at RT (**Figure 2.13**) irrespective of the presence of NP while it was feasible in a very short time on MW irradiation.

This suggests that both NiNPs and MW play an important role in the decolourization of dye.

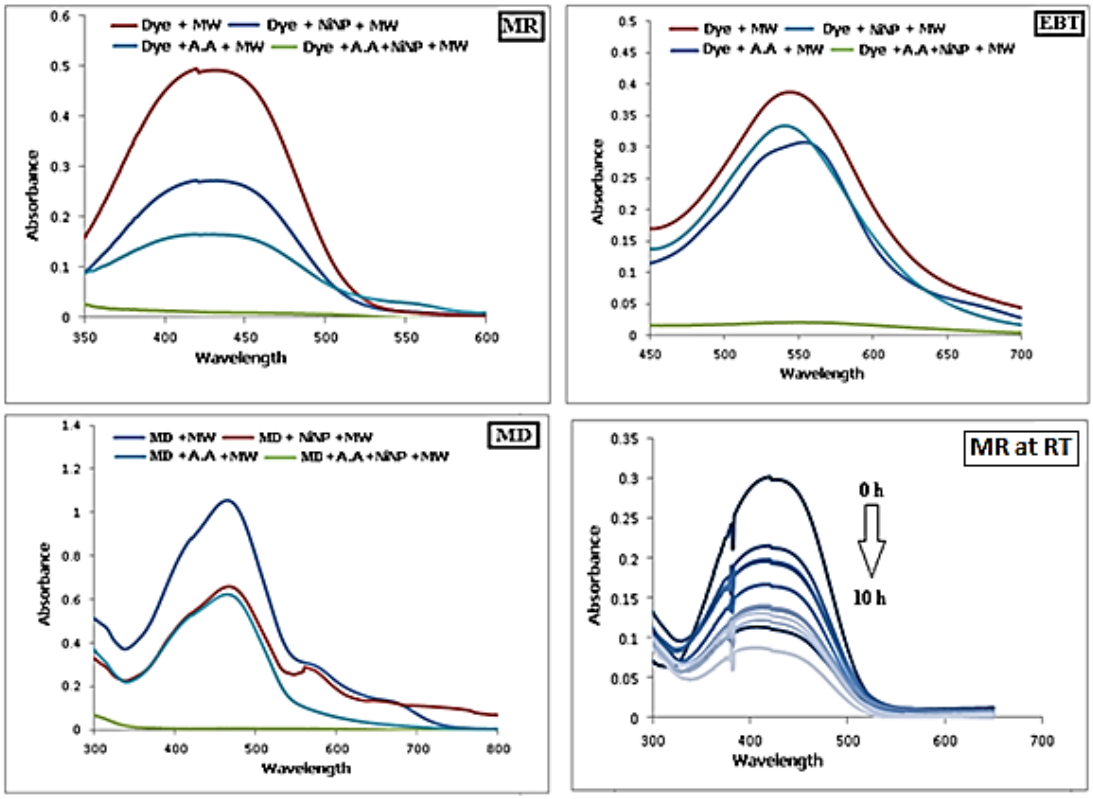

Figure 2.13 UV-vis spectra indicating the decolourization of MR, EBT and MD dyes in the presence of NiNPs; UV-vis spectra indicating the decolourization of MR dye at room temperature (MR-RT) in the presence of NiNPs.

2.3.3.3 Redox reaction between potassium ferricyanide and sodium thiosulfate

It has been reported that the electron transfer reaction between $Fe(CN)_6^{-3}$ and $S_2O_3^{-2}$ is catalyzed by noble metal like Pt.[32-33] The redox reaction proceeds by electron transfer through the surface of the PtNPs, where they act as highly dispersed electrodes. We attempted this reaction for the first time in presence of NiNPs which are economically more viable.

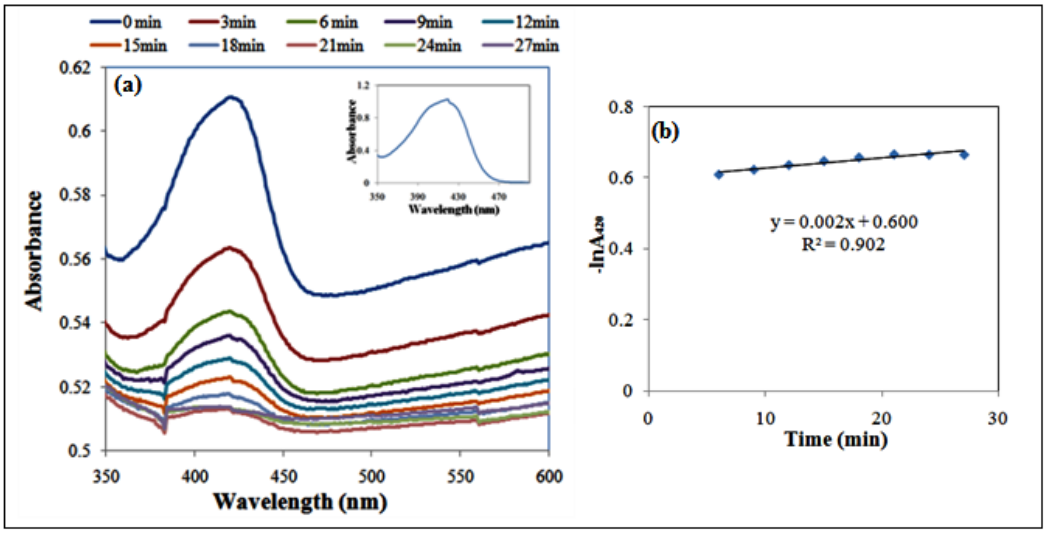

Figure 2.14 (a) UV-vis spectra indicating change of $Fe(CN)_6^{-3}$ concentration during the reaction between $Fe(CN)_6^{-3}$ and $S_2O_3^{-2}$ at 25±2 °C in the presence of NiNPs, and the inset shows the UV-vis spectra of an uncatalyzed reaction in the absence of NiNPs **(b)** Pseudo-first-order plot of $-\ln A_{420}$ against time for the determination of the rate of reaction between $Fe(CN)_6^{-3}$ and $S_2O_3^{-2}$ using NiNPs.

The characteristic absorption of $Fe(CN)_6^{-3}$ was observed at 420nm. When reaction takes place between $Fe(CN)_6^{-3}$ and $S_2O_3^{-2}$ intensity of corresponding peak (420nm) decreased with time. In both reactions absorption was measured at 3min time intervals. In presence of NiNPs (**Figure 2.14a**) there was a continuous decrease in absorbance at 420nm with respect to time and after 27min, peak completely disappeared. Whereas, in absence of NiNPs reaction proceeds very slowly and takes 6h for its completion (**Figure 2.14a**, inset). On the other hand, using PtNPs with the same concentration the reaction remained incomplete even after 40min.[32-33] Therefore, it can be said that in presence of NiNPs redox reactions proceeds faster

owing to efficient electron transfer due to the larger surface area of NiNPs. The pseudo first-order plot of $-\ln A_{420}$ against time showed a linear relationship with a correlation coefficient of 0.9027 (**Figure 2.14b**). The rate constant value of the reaction, in the presence of the NiNPs, obtained from the slope of the straight line, was observed to be 0.0028 min^{-1}. These results were comparable with the results obtained using PtNPs.[33]

2.3.3.4 Recycling of NiNPs

The recyclability of the NPs was also surveyed in optimum condition for all three reactions (**Tables 2.18 to 2.20**). It was observed that the catalyst could be reused directly without further purification for seven consecutive runs in case of PNA to PPDA (**Table 2.18**). Upto three cycles there was no loss in activity. After that the reaction time increased in each successive recycling experiment reaching from 90min to 180min finally after the 7^{th} experiment. This may be due to gradual loss of the catalytic activity of NiNPs with the number of runs for various reasons mentioned in our previous work.[21] Similarly in case of decolourization of azo dye (**Table 2.19**) and redox reaction between PFC and STS (**Table 2.20**) was observed that the catalyst could be reused directly without further purification for five consecutive runs in both cases although reaction time increases.

Table 2.18 Recycling experiments of hydrogenation of *p*-Nitroaniline at RT in optimum condition

Cycle	Reaction time (min)	% Yield (Isolated, ±3)	Selectivity (%)
1	90	95	100
2	90	95	100
3	90	94	100
4	110	94	100
5	120	95	100
6	140	95	100
7	180	94	100

Table 2.19 Recycling experiments of decolourization of OR-II azo dye by NiNPs in MW.

Cycle	1	2	3	4	5
Time (Sec)	120	125	140	160	200

Table 2.20 Recycling experiments of redox reaction between PFC and STS by NiNPs

Cycle	1	2	3	4	5
Time (min)	27	28	30	30	42

2.3.4 Conclusions

Nickel nanoparticles exhibited an excellent catalytic activity for room temperature reduction of aromatic nitro compounds in aqueous medium. The catalyst used here is economic and ecofriendly as it requires neither higher temperature nor harsh acid or bases, and produces higher yields with excellent chemoselectivity in reduction of nitro aromatics substrates. NiNPs also helped in speeding up decolourization of azo dyes and changed the order of a redox reaction. Recycling experiments demonstrated that the catalyst can be reused for successive runs.

2.3.5 References

1. F. Alonso and M. Yus, *Tetrahedron Lett*, 1996, **37**, 6925.
2. F. Alonso, I. Osante and M. Yus, *Tetrahedron*, 2007, **63**, 93.
3. Y. Moglie, F. Alonso, C. Vitale, M. Yus and G. Radivoy, *Tetrahedron* , 2006, **62**, 2812.
4. F. Alonso, G. Radivoy and Y. Moglie, *Tetrahedron*, 1999, **55**, 4441.
5. G. Radivoy, F. Alonso and Y. Moglie, *Tetrahedron*, 1999, **55**, 14479.
6. F. Alonso, P. Riente and M. Yus, *Arkivoc*, 2008, **4**, 8.
7. F. Alonso, P. Riente and M. Yus, *Acc Chem Res*, 2011, **44**, 379.
8. F. Alonso, P. Riente and M. Yus, *Eur J Org Chem*, 2008, **29**, 4908.
9. F. Alonso, P. Riente and M. Yus, *Tetrahedron*, 2008, **64**, 1847.
10. F. Alonso, P. Riente and M. Yus, *Tetrahedron Lett*, 2008, **49**, 1939.
11. A. Dhakshinamoorty and K. Pitchumani, *Tetrahedron Lett*, 2008, **49**, 1818.
12. L. Zank and J. Zielinski, *Appl Catal A: Gen*, 2008, **334**, 268.
13. R. S. Downing, P. J. Kunkeler and H. V. Bekkum, *Catal Today*, 1997, **37**, 121.
14. A. Saha and B. Ranu, *J Org Chem*, 2008, **73**, 6867 and references therein.
15. A. Corma and P. Serna, *Science*, 2006, **313**, 332.
16. N. Sahiner, S. Butun and P. Ilgin, *Coll Surf A***,** 2011, **386**, 16.
17. P. L. Freund and M. Spiro, *J Phys Chem B*, 1985, **89**, 1074.
18. M. Valodkar, P. S. Rathore, R. N. Jadeja, M. Thounaojam, R. V. Devkar and S. Thakore, *J Hazard Mater*, 2012, **201-202**, 244.
19. M. Valodkar, S. Modi, A. Pal and S. Thakore, *Mater Res Bull*, 2011, **46**, 384.
20. P. S. Rathore, J. Advani, S. Rathore and S. Thakore, *J Mol Catal A: Chem*, 2013, **377**, 129.
21. X. Huang, X. Liao and B. Shi, *Green Chem*, 2011, **13**, 2801.
22. Y. Kojima and T. Haga, *Int J Hydrogen En*, 2003, **28**, 989.
23. R. Maas and S. Chaudhari, *Process Biochem*, 2005, **40**, 699.
24. G. M. Walker and L. R. Weatherley, *Water Research***,** 1999, **33**, 1895.
25. L. Xu, X-C. Wu and J-J. Zhu, *Nanotechnology*, 2008, **19**, 305603.
26. T. S. Rezende, G. R. S. Andrade, L. S. Barreto, N. B. CostaJr, I. F. Gimenez and L. E. Almeida, *Mater Lett***,** 2010, **64**, 882.
27. F. Alonso, G. Radivoy and Y. Moglie, *Tetrahedron*, 2000, **56**, 8673.

28. V. S. Lebedeva, A. G. Vitukhnovskya, A. Yoshidac, N. Kometanic and Y. Yonezawac, *Coll Surf A***,** 2008, **326**, 204.
29. S. Pande, S. K. Ghosh, S. Nath, S. Praharaj, S. Jana and S. J. Panigrahi, *Colloid Interface Sci*, 2006, **299**, 421.
30. S. Kundu, S. K. Ghosh, M. Mandal and T. Pal, *New J Chem*, 2003, **27**, 656.
31. V. Janaki, K. Vijayaraghavan, B-T. Oh, K-J. Lee, K. Muthucheli, A. K. Ramasamy and S. Kamala- Kannan, *Carbohydr Polym*, 2012, **90**, 1437.
32. W. Yang, Y. Ma, J. Tang and X. Yang, *Colloid Surf A,* 2007, **302**, 628.
33. A. Pal, S. Shah, D. Chakraborty and S. Devi, *Aust J Chem*, 2008, **61**, 833.